U.PORTO

MESTRADO
TOXICOLOGIA E CONTAMINAÇÃO AMBIENTAIS

Bioactivity screening of marine cyanobacteria for the isolation of novel compounds for obesity related co-morbidities

Natália Gonçalves da Silva

M
2018

U.PORTO

Natália Gonçalves da Silva. Bioactivity screening of marine cyanobacteria for the isolation of novel compounds for obesity related co-morbidities

M.ICBAS **2018**

Bioactivity screening of marine cyanobacteria for the isolation of novel compounds for obesity related co-morbidities

Natália Gonçalves da Silva

SEDE ADMINISTRATIVA **INSTITUTO DE CIÊNCIAS BIOMÉDICAS ABEL SALAZAR**
FACULDADE DE CIÊNCIAS

Natália Gonçalves da Silva

Bioactivity screening of marine cyanobacteria for the isolation of novel compounds for obesity related co-morbidities

Dissertation for the master degree in Environmental Toxicology and Contamination submitted to the Abel Salazar Biomedical Sciences Institute from the Porto University.

Supervisor: Doctor Ralph Urbatzka
Category: Postdoctoral researcher
Affiliation: CIIMAR, Interdisciplinary Centre of Marine and Environmental Research

Co-supervisor: Doctor Mariana Reis
Category: Postdoctoral researcher
Affiliation: CIIMAR, Interdisciplinary Centre of Marine and Environmental Research

Co-supervisor: Prof. Vítor Vasconcelos
Category: Full Professor
Affiliation: Sciences Faculty of Porto University
Category: President of the Board
Affiliation: CIIMAR, Interdisciplinary Centre of Marine and Environmental Research

Acknowledgments

My sincere appreciations go to my supervisor Dr. Ralph Urbatzka, and co-supervisor Dr. Mariana Reis, for all their patience during this year. I am extremely grateful for their impeccable guidance, continuous support, and teachings that allowed me to go forward in each step. For all the careful readings of the thesis and endless availability to discuss it, always towards a better version. Thank you very much for your demanding on me which allowed my growth over this year.

Also, my sincere acknowledgement to Professor Doctor Vitor Vasconcelos for accepting me in the laboratory to perform my master's thesis and as well the support to complete this work.

Likewise, my sincere thanks for all the people of the LEGE team for their help, advise, chit-chat and laugh moments. Thank you for the good working environment that made every day easier.

To Professor Doctor Olga Lage from the Sciences Faculty of the Porto University for the help to troubleshoot some problems during this project, providing access to the microscope room, necessary to complete this project.

Special thanks to all my friends who have always been there for me, good and bad times, and follow me throughout this journey. Without you I would not have reach so far.

A huge and special thanks to my parents, for everything. Without you none of this would be possible.

To the project EnhanceMicroAlgae - High added-value industrial opportunities for microalgae in the Atlantic Area - EAPA_338/2016 - of the Interreg Atlantic Area Program funded by the European Regional Development Fund.

To the project BLUEHUMAN - BLUE biotechnology as a road for innovation on HUMAN's health aiming smart growth in Atlantic Area- EAPA_151/2016 - of the Interreg Atlantic Area Program funded by the European Regional Development Fund.

To the European ERA-NET Marine Biotechnology project CYANOBESITY (ERA-MBT/0001/2015) for support this research work, financed by national funds through FCT (Foundation for Science and Technology, Portugal).

Related publications: poster communication

Silva N, Reis M, Vasconcelos V and Urbatzka R (2018). Isolation of novel compounds from marine cyanobacteria for obesity related co-morbidities. *Frontiers Marine Science Conference Abstract: IMMR'18 | International Meeting on Marine Research 2018*, 5th-6th July, Peniche, Portugal.

Abstract

Obesity is a complex metabolic disease that became one of the major public health concerns in our societies. This condition increases the risk of developing several chronic diseases, including diabetes (T2DM), cardiovascular diseases, among others. Complementary strategies are necessary for the treatment of obesity, including pharmacological treatments. Currently, research has focused on natural product discovery for health treatments, as an alternative to the ongoing drugs on market. Natural compounds have shown promising anti-obesity properties and the microorganism cyanobacteria are regarded as a prolific source of biologically active natural compounds. For example, the cyanobacteria *Arthrospira* sp., previously named *Spirulina*, has shown the potential to exhibit therapeutic properties with human health benefit.

In this work, a bioassay-guided isolation strategy was used to explore the potential of secondary metabolites from marine cyanobacteria from LEGE CC with beneficial activities towards obesity. Therefore, different strains of cyanobacteria were cultured and harvested. The freeze-dried biomass were exhaustively extracted using first methanol and then dichloromethane. The resultant organic extract was submitted to VLC, and then either to flash chromatography, normal phase SPE, preparative TLC and normal or reverse-phase HPLC to generate fractions, which were tested against zebrafish Nile Red fat metabolism assay. The chemical nature of the fractions were followed by spectroscopic techniques (NMR).

The strongest effects were identified in sub-fractions E18179 D-E6E4 and D-E6E6, from strain *Synechocystis salina* LEGE 06099. These reduced the neutral lipids in the zebrafish larvae in 74.61 ± 6.07% and 67.8 ± 9.1%, respectively, with statically significant difference from control. The NMR proton profile of the last sub-fractions suggested that the responsible compounds could be chlorophyll derivatives. Additionally, in sub-fraction E17161 E4C11A from strain *Nodosilinea* sp. LEGE 06001 the structure of compound **(1)** was isolated and characterized through 1D and 2D NMR spectroscopy and LR-ESI mass spectrometry. This compound was identified as a novel molecule, being very similar to hydroxy-pheophytin but with a farnesyl group instead of phytyl group. It reduced the neutral lipids in the zebrafish larvae in 51.67 ± 15.59%, with statically significant difference from control at 20 $\mu g.ml^{-1}$ and had an IC_{50} value of 18.64 µM.

In the future, the molecular mechanism of the novel compound should be evaluated as well as its suitability as dietary supplement, which may be beneficial for the treatment of obesity or obesity-related co-morbidities.

Resumo

A obesidade é uma complexa doença metabólica que se tornou uma das principais preocupações de saúde pública. Esta doença aumenta o risco de desenvolvimento de outras doenças crónicas, como diabetes (DMT2), doenças cardiovasculares, entre outras. Estratégias complementárias são necessárias para o seu tratamento, incluindo tratamentos farmacológicos. Atualmente, como alternativa aos fármacos no mercado, a pesquisa foca-se na descoberta de produtos de origem natural para o tratamento de doenças. Compostos naturais têm mostrado promissoras propriedades anti-obesidade sendo as cianobactérias consideradas uma fonte prolifica de compostos naturais com atividade biológica. Por exemplo, a cianobactéria *Arthrospira* sp., anteriormente denominada *Spirulina*, possui o potencial de exibir propriedades terapêuticas com benefício para a saúde humana.

Neste trabalho, foi usada uma estratégia de isolamento guiada por bioensaios, de forma a explorar o potencial das cianobactérias marinhas da LEGE CC de produzirem metabolitos secundários com atividade benéfica relativamente à obesidade. Para tal, houve culturas de diferentes estirpes de cianobactérias com posterior recolha da biomassa. A biomassa congelada foi exaustivamente extraída, usando primeiro metanol e depois diclorometano. O extrato orgânico obtido foi submetido a uma CLV, e posteriormente a cromatografia de flash, EFS em fase normal, CCD preparativa, e CLAE em fase normal ou reversa, de forma a originar frações que foram testadas no bioensaio de metabolismo lipídico com peixe-zebra corados com Vermelho Nile. A natureza química destas frações foi seguida por técnicas espectroscópicas (RMN).

Os efeitos mais fortes foram identificados nas sub-frações E18179 D-E6E4 e D-E6E6, da estirpe *Synechocystis salina* LEGE 06099. Estas reduziram os lípidos neutros nas larvas do peixe zebra em 74.61 ± 6.07% e 67.8 ± 9.1%, respetivamente, com diferenças estatisticamente significativas em relação ao controlo. O perfile de protões RMN das sub-frações D-E6E4 e D-E6E6 sugeriram que os compostos responsáveis possam ser derivados de clorofila. Adicionalmente, o composto **(1)** da sub-fração E17161 E4C11A, da estirpe *Nodosilinea* sp. LEGE 06001, foi isolado e caracterizado através de espectroscopia 1D e 2D de RMN e BR-ESI espectrometria de massa. Foi identificado como sendo similar à hidroxi-feofitina, mas com grupo farnesil em vez de grupo fitil. Na concentração 20 $\mu g.ml^{1}$ foi capaz de reduzir os lípidos neutros nas larvas de peixe-zebra em 51.67 ± 15.59%, com diferença estatisticamente significativa em relação ao controlo, e com valor de IC_{50} de 18.64 µM.

No futuro, os mecanismos moleculares do novo composto devem ser avaliados, bem como a sua adequabilidade como suplemento dietético para o tratamento das comorbidades relacionadas à obesidade.

Table of contents

Tables Index

Figures Index

Abbreviations list

α-MSH	Alpha melanocyte stimulating hormone
AGE	Advanced glycation end-products
AMD	AMD: Age-related macular degeneration
BBE	BBE: Blue biotechnology and ecotoxicology
^{13}C NMR	Carbon-13 nuclear magnetic resonance
C18	eighteen carbon chain bonded to silica particles
CCR2	C-C chemokine receptor type 2
CD4/CD8	Cluster of differentiation 4 or 8
$CDCl_3$	Chloroform deuterated solvent
CH_2Cl_2	Dichloromethane
CLS	Crown-like structure
CoA	Coenzyme A
COSY	Correlation spectroscopy
DEPT	Distortionless enhancement by polarization transfer
DMSO	Dimethyl sulfoxide
DMSO-d6	Dimethyl sulfoxide deuterated solvent
ECM	Extracellular matrix
ESI-MS	Electrospray ionization-mass spectrometry
EMA	European medicinal agency
EtOAc	Ethyl acetate
FDA	Food and drug administration
GLP-1	Glucagon-like peptide 1
^{1}H NMR	Proton nuclear magnetic resonance
HIF-1	Hypoxia inducible factor 1
HIV	Human immunodeficiency virus
HMBC	Heteronuclear multiple bond correlation spectroscopy
H_2O	Water
HPLC	High-performance liquid chromatography
HSQC	Heteronuclear single quantum coherence spectroscopy

IC_{50}	Half maximal inhibitory concentration
LC-MS	Liquid chromatography mass spectrometry
LEGE CC	Cyanobacteria culture collection LEGE – CIIMAR
MCP-1	Monocyte chemoattractant protein-1
MeCN	Acetonitrile
MeOH	Methanol
MEP	Methylerythritol phosphate
MIF	Macrophage migration inhibitory factor
MMP2/MMP9	Matrix metalloproteinase 2 or 9
NMR	Nuclear magnetic resonance
NRPS	Non-ribosomal peptide synthetase
PDA	Photodiode array
PKS	Polyketide synthase
PMA	Phosphomolybdic acid
PPARγ	Peroxisome proliferator-activated receptor
PTU	Phenylthiourea
REV	Resveratrol
ROESY	Rotating-frame overhauser spectroscopy
RP-HPLC	Reverse-phase high-performance liquid chromatography
Si	Silica
SiO_2	Silicon dioxide
SPE	Solid-phase extraction
TG	Triglycerides
TGFβ	Transforming growth factor beta
TLC	Thin-layer chromatography
TOCSY	Total correlation spectroscopy
TRPV1	Transient receptor potential cation channel subfamily V member 1
VLC	Vacuum liquid chromatography
WHO	World health organization

Appendixes

1. Introduction

The introduction will focus mainly on two subjects, the problematic of obesity worldwide and the potential of microorganisms, in particular cyanobacteria, to produce natural compounds that may help to overcome this chronic disease.

1.1. General overview on obesity

Obesity has nowadays become a major public concern worldwide and is regarded as one of the leading causes of disability and death affecting, not only adults, but also children and teenagers (Frühbeck *et al*., 2013). In 2016, 1.9 billion (39%) of the adults worldwide were overweight, a number that since 1980 has more than doubled, according to the most recent report of the World Health Organization (WHO, 2014; Vandevijvere *et al*., 2015). In 2015 the overweight or obese population in Portugal was about two-thirds (67.7%) of the resident population. Moreover, when compared over the past decade the prevalence of obese people doubled and was transversal to all age groups. Comparing with other European countries, the prevalence estimated in Portugal is one of the highest, along with the prevalence reported for England (Gaio *et al.*, 2018).

Obesity can be defined as a complex metabolic disease characterized by an abnormal or excessive fat accumulation in adipocytes. These cells are important regulators of the whole body metabolism and homeostasis by producing hormones such as adiponectin, which regulates the glucose and lipids metabolism, or as leptin that regulates food intake and energy uptake (Castro *et al*., 2016; WHO, 2014). Adipose tissue on mammals is composed of two distinct types of cells: white adipocytes are the main responsible for energy storage and brown adipocytes allow the maintenance of the body temperature through thermogenesis. The adipose tissue has many essential roles in thermogenesis, lactation, immune responses, endocrine regulation, energy supply, among others (Castro *et al*., 2016). Therefore, the abnormal fat accumulation can represent a serious health risk. A negative influence of this condition is associated to many chronic diseases, including diabetes (T2DM, Type 2 Diabetes Mellitus), dyslipidaemia, hypertension, cardiovascular diseases, musculoskeletal disorders, sleep apnea, some types of cancer (breast and ovarian), or even reproductive performance (Castro *et al*., 2016; Daneschvar *et al*., 2016; Kang and Park, 2012; Rodgers *et al*., 2012).

Obesity has in the majority of cases no single cause or cure, and quite frequently the resolution can be very problematic, since a significative percentage of the global population may not only need a strategic change on lifestyle adjustment, including dietary and physical

activity changes, to overcome long-term obesity (Rodgers *et al*., 2012; Kang and Park, 2012; WHO, 2014). Nevertheless, urgent actions from governments, food industry and even society across the globe are necessary to overcome this disease. Nowadays, obesity represents a significant public health issue with a large economic burden. Namely, the global impact is estimated to be US $2.0 trillion or 2.8% of the global gross domestic product (Tremmel *et al.,* 2017). Obesity is responsible for a large fraction of costs to health care system since englobes all diseases associated with this chronic condition. However, not only affects public founding, but also society as families, with lower productivity at work, lost work days and permanent disability (Tremmel *et al.,* 2017). If the prevalence on the current trend of overweight or obese people continues so does the costs attributable to treatment of obesity and obesity related-comorbidities.

1.1.1. Adipose tissue remodelling in pathophysiology of obesity

Adipose tissue undergoes a continuously dynamic remodelling process that maintains tissue health and allow adaptation to alterations in nutrients supply. This process in obese states is pathologically accelerated to an almost unlimited capacity of tissue expansion, by either hyperplasia or hypertrophy. The expansion can lead to several effects, including reducing angiogenic remodelling (hypoxia), extracellular matrix (ECM) overproduction, immune cell infiltration and subsequent inflammatory responses, characterizing adipose tissue dysfunction. Thereby, obesity may turn an adaptive strategy into a metabolic associated syndrome, the so called obesity related co-morbidities, reviewed in several articles (Gustafson *et al*., 2013; Lee *et al*., 2010; Sun *et al*., 2011).

Essentially, adipose tissue is comprised of adipocytes and preadipocytes, endothelial cells, pericytes, fibroblasts and immune cells (macrophages and T cells). This immune cells are mediators of remodelling, surrounding dead adipocytes in so-called crown-like structures (CLS), phagocyting lipids and other cellular debris while new adipocytes populate the tissue (Lee *et al*., 2010; Sun *et al*., 2011). Necrosis of adipocytes, driven by hypertrophy and accelerated by obesity, along with chemotactic pathway (MCP-1/CCR2), adipokines such as macrophage migration inhibitory factor (MIF), matrix metalloproteinases (MMP2 and MMP9), leptin and transcription factor HIF-1 are upregulated by hypoxia that consequently induce local fibrosis (Cinti *et al*., 2005; Henninger *et al*., 2014; Hosogai *et al*., 2007; Kanda *et al*., 2006; Weisberg *et al*., 2006; Ye *et al*., 2007). Strikingly, these are the key ultimately stimulus that regulates infiltration of immune cells in adipose tissue, implying tightly interconnected metabolic and inflammatory pathways.

A delicate balance exists of different populations of macrophages necessary to maintain adequate adipocyte function. In the lean state, resident immune cells (denominated M2 anti-inflammatory macrophages, eosinophils and regulatory T cells) promote tissue repair and angiogenesis in the expansion of adipose tissue, however in the obese state, the resident cells are mast cells, CD8 and CD4 T cells, along with the remarkable heterogeneity of macrophages that acts through a transformation designated “phenotypic switching” from M2 to M1 pro-inflammatory macrophages. Thus, obesity provides metabolic signals that mimic bacterial infection, promoting inflammation. The prolongated exposure to inflammatory signals could enhance cardiovascular and metabolic settings of obesity, such as insulin resistance (Kosteli *et al*., 2010; Lumeng *et al*., 2007; Schipper *et al*., 2012).

So, a healthy expansion is characterized by enhancing differentiation into small adipocytes, along with vascularization and minimal induction of ECM and inflammation, while in pathological expansion there is an enlargement of already existing adipocytes, transformation and infiltration of macrophages, hypoxia and massive fibrosis associated with chronic inflammation and systemic insulin resistance.

1.1.2. Treatment strategies for obesity and mechanisms of action of anti-obesity drugs

Complementary strategies are necessary to overcome obesity, beyond all appropriate management actions of obesity complications, which today focus on surgery and/or pharmacological treatment. On one hand, bariatric and metabolic surgery should be considered adequate for morbid obese adults, since surgical complications and the need for reoperation are frequent. These interventions are proven effective for weight loss and improvement of co-morbidities in these situations, and as a result, on quality of life and overall mortality (Kang and Park, 2012). On other hand, pharmacotherapy usually is applied on obese patients to reduce obesity-related health risks and to improve quality of life, either targeting the consumption or absorption of food (Rodgers *et al*., 2012; Yumuk *et al*., 2015). Nonetheless, anti-obesity drugs are considered a complementary treatment, since their long-term success is limited, many adverse side effects occurred, and once the medication is interrupted, a strong possibility exists for weight regain (Kang and Park, 2012).

Depending on the mechanism of action of anti-obesity drugs, they can be divided into four groups: drugs suppressing appetite, drugs increasing insulin sensitivity, drugs targeting sodium/glucose co-transporters and drugs decreasing lipid absorption (Castro *et al*., 2016).

However, the primary issue outlined by the history of anti-obesity drugs is their problematic and dangerous side effects, and so the main regulatory agencies, namely EMA

(European Medicinal Agency) and FDA (Food and Drug Administration), withdrawed its marketing (Daneschvar *et al*., 2016; Kang and Park, 2012; Rodgers *et al*., 2012; Yumuk *et al*., 2015). Until the year 2016, five drugs were approved by FDA, including three of them by EMA (Daneschvar *et al*., 2016). The drugs approved by both agencies are orlistat (Figure 1), the combination of bupropion/naltrexone (Figure 1) and liraglutide (Yumuk *et al*., 2015).

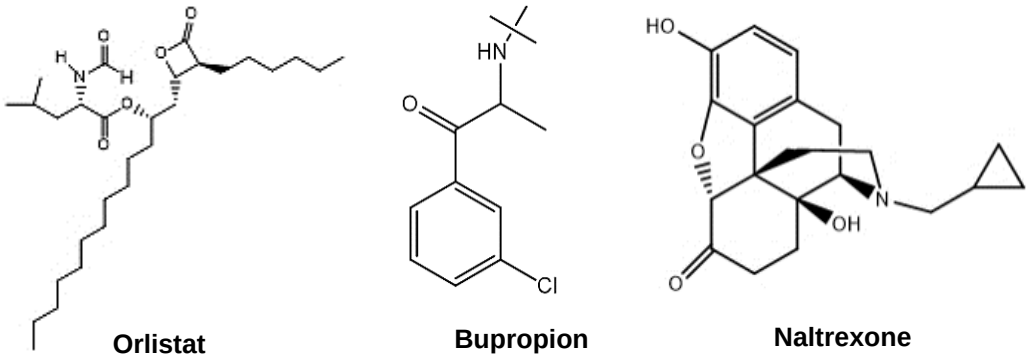

Figure 1 - Chemical structures of compounds approved by both FDA and EMA (Cooke and Bloom, 2006).

The combination of drugs resulted as an efficient solution for those drugs that have been or were close to approval but were not able to consistently achieve a weight loss of more than 10% of total body weight. The combination treatment targets in more than one biological mechanism can culminate in various advantages (Kang and Park, 2012; Rodgers *et al*., 2012).

Orlistat, a synthetic derivative of lipstatin isolated from bacteria *Streptomyces toxytricini,* is a potent and selective gastrointestinal (pancreatic and gastric) lipase inhibitor, and as consequence intestinal digestion and absorption of fat is decreased. Bupropion and naltrexone are synthetic drugs, which mechanism of action is still not entirely understood (Daneschvar *et al*., 2016; Yumuk *et al*., 2015). Nonetheless, it was reported that this combination allows the release of a neuropeptide hormone, melanocyte stimulating hormone (α – MSH), from the hypothalamic areas, which is involved in feeding and body weight control (Yumuk *et al*., 2015). Liraglutide, a derivative of human incretin GLP-1 (glucagon-like peptide-1), acts as an agonist of receptor GLP-1R. As consequence, the glucagon response is reduced, and the appetite supressed, while the insulin response is stimulated (Yumuk *et al*., 2015). Despite all this, these three main medications in similarity with other drugs on market, also present side-effects, but have an acceptable risk to benefit ratio (Kang and Park, 2012; Yumuk *et al*., 2015).

Besides orlistat, other natural products are also being used as template for the discovery and synthesis of new drugs with potential improved pharmacological and pharmacokinetic properties, and also easier to manufacture (Gogineni and Hamann, 2018; Raja *et al*., 2016; Shah *et al*., 2017). One very recent example is metabocin, a synthetic product based on

capsaicin, a compound derived from chili peppers. It was reported that metabocin has anti-obesity properties without producing inflammation or adverse side effects, stimulating the non-accumulation of fat through stimulation of the TRPV1 (transient receptor potential cation channel subfamily V member) receptors. In fact, the animal studies data allowed the progression of this drug to human clinical trials (Baskaran et al., 2018).

However it is necessary to consider that obesity is a complex metabolic disease. For example, (1) the inhibition of adipogenesis, a complex process involving cell proliferation, clonal expansion, cell inhibition or growth arrest and lipid accumulation, or (2) the inhibition of adipocytes proliferation, is regarded as unhealthy, since it may lead to other metabolic diseases as fatty liver disease, type 2 diabetes and atherosclerosis. Similarly, excessive lipolysis may contribute to the development of dyslipidaemia due to high circulating fatty acids levels (Balaji *et al.*, 2016; Yun, 2010).

Because of all this, new, safer and more effective anti-obesity drugs are urgently needed. Novel research and drug development strategies have been increasing in the past few years and focussed either on synthetic or on natural product-based drugs. Natural resources represent a huge bio- and chemodiversity and the chemical space is characterized by a higher structural diversity compared to synthetic compounds. Recent research established that various natural products, including crude extracts and isolated compounds as secondary metabolites from different natural sources, such as plants, cyanobacteria's, fungi or phytoplankton possess anti-obesity activities (Castro *et al*., 2016; Daneschvar *et al*., 2016; Hu *et al*., 2016; Kang and Park, 2012; Noinart *et al*., 2017; Rodgers *et al*., 2012).

1.2. Bioactive natural compounds with anti-obesity activity

Currently, the potential of natural products for treatment of obesity is under exploration as an alternative to the ongoing drugs, due the disapproval with high costs and potentially dangerous side effects of the current anti-obesity drugs available on the market.

Nature, in general, represents a wide reservoir of biologically active compounds, and the reduction of the incidence of chronic diseases, as obesity, was associated to the consumption of marine foods and marine bioactive compounds (Hu *et al*., 2016; Suleria *et al*., 2016).

Natural compounds with anti-obesity activities can be classify based on their molecular mechanisms into five categories: (i) lipase inhibition, which leads to a decreased lipid absorption, (ii) suppression of food intake and, as consequence on energy, (iii) stimulation

of energy expenditure like thermogenesis of the brown adipose tissue by dissipation of excess energy as heat, (iv) inhibition of pre-adipocyte differentiation and proliferation, since adipocyte tissue growth can be due to both hyperplasia and hypertrophy of adipocytes, or (v) regulation of lipid metabolism as decreased lipogenesis (through key enzymes as acetyl CoA carboxylase, carboxylesterase, fatty acid synthase, melanyl CoA, among others), or increased lipolysis by stimulation of triglyceride hydrolysis (Balaji *et al.*, 2016, Hu *et al*., 2016 and Yun, 2010).

These natural anti-obesity compounds are mostly from terrestrial and aquatic plants, seaweed, micro- and macro-fungi, other microorganisms as filamentous bacteria, or other marine macro-vertebrates and invertebrates.

Yoshinone-A a compound composed of c-pyrene and a linear side chain (Figure 2), was isolated from the cyanobacteria *Leptolyngbya sp.*, as a suppressant of the adipocyte differentiation, showing inhibitory activity against 3T3-L1 cells. Although the mechanism of action is not yet well understood, the position of the pyrone ring in the side chain is important to exhibit this activity (Inuzuka *et al*., 2014; Koyama *et al*., 2016). Other γ-pyrone compound is kalkipyrone (Figure 2), that was first isolated from a mixture of cyanobacteria *Moorea producens*, formely known as *Lyngbya majuscule*, later from *Tolypothrix sp.* (Graber and Gerwick, 1998; Koyama *et al.*, 2016).

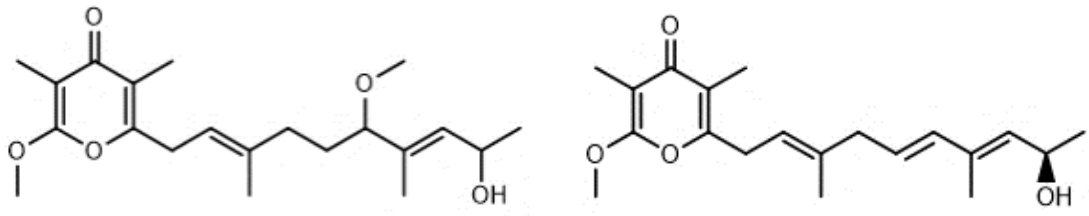

Yoshinone-A **Kalkipyrone**

Figure 2 – Chemical structures of compounds isolated from cyanobacteria: yoshinone-A (Inuzuka et al., 2014) and kalkipyrone (Koyama et al., 2016).

In addition, several studies performed with cyanobacterial extracts as dietary supplements confirmed that holds many beneficial effects, for instance, improved cardiac and hepatic functions (Jang and Choung, 2013; Jarouliya *et al*., 2012; Ku *et al*., 2013; Mascher *et al*., 2006). The administration of the cyanobacteria *Arthrospira* sp., previously named *Spirulina*, in mammals led to the mitigation of obesity symptoms such as reducing hypertension allowing a better regulation of vascular tone, as well as protect against renal failure and promote the growth of intestinal microflora (Liang *et al*., 2004; Mascher *et al*., 2006). Two anti-inflammatory compounds γ-linoleic acid and c-phycocyanin (an antioxidant biliprotein pigment) (Figure 3), and the pigment β-carotene (Figure 4) are major therapeutically important compounds and components of this strain, suspected to lower the body weight, serum and liver triglyceride content, although the authors did not elucidate the

underlying mechanism(s) (Cheong et al., 2010; De Rivera et al., 1993; Iwata et al., 1990; Jarouliya et al., 2012; Torres-Durán et al., 1999).

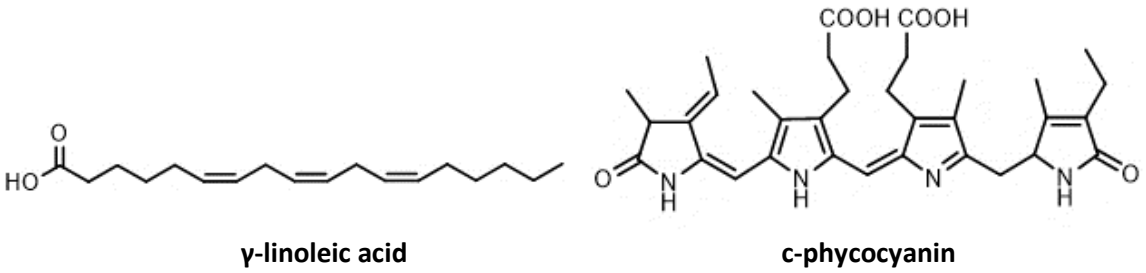

γ-linoleic acid **c-phycocyanin**

Figure 3 - Chemical structures of natural compounds: γ-linoleic acid (Raposo et al., 2013) and c-phycocyanin (Hoseini et al., 2013).

Moreover ethanolic extracts of the algae *Laminaria japonica* help attenuate metabolic complications associated to adipose tissue dysfunction in obesity states, including anti-hyperglycaemic, anti-lipidemic and hepatoprotective activities through decreased activity in lipogenesis as well as the increase in fatty acid oxidation (Jang and Choung, 2013). Also the authors suggested a protective effect against the development of insulin resistance (Jang and Choung, 2013).

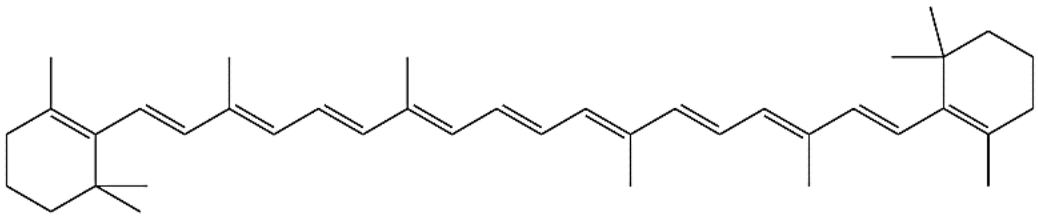

Figure 4 - Chemical structure of compound β-carotene (Kirti et al., 2014).

Many natural compounds with anti-obesity activity were only evaluated *in vitro* and the mechanism of action still was not elucidated. Further research is still necessary to investigate their efficacy in animal experiments, and to decipher their mechanisms of action, potential toxic side-effects and other safety assessments of administration. Additionally, it is necessary to analyse how the actual methodologies can be converted into green methodologies for exploring these microorganisms with lower quantities of time and resources expended (Duarte *et al*., 2014).

1.3. Brief description of the current state of cyanobacteria

Cyanobacteria are an ancient group of gram-negative photosynthetic prokaryotes, both planktonic and benthic, and are worldwide distributed in a broad spectrum of environmental conditions (Brito *et al*., 2015; Sharma *et al*., 2011; Singh *et al*., 2005).

These microorganisms have a high morphological, biochemical and genetic diversity and are classified into five main subsections (Brito *et al*., 2012). Subsections I and II (Chroococcales and Pleurocapsales) represent the unicellular cyanobacteria, while subsections III, IV and V (Oscillatoriales, Nostocales and Stigonematales, respectively), comprise the filamentous strains (Brito *et al*., 2012).

Besides their ecological importance, nowadays cyanobacteria are well known to produce a vast variety of chemically unique secondary metabolites owed to their metabolic plasticity, which can be of interest for us (Leão *et al*., 2012; Sharma *et al*., 2011). The marine natural product research became established as one field of interest more than fifty years ago. Since then there was a rapid rise in popularity of this field with Porifera phylum being selected for the most of investigation (Blunt *et al*., 2015). However, the research popularity of the phylum cyanobacteria has somewhat enhanced since the mid-1990s.

Secondary metabolites that are isolated from marine cyanobacteria are of greater consideration due to their unique structural scaffolds and competency to produce potent and significant biological properties. According to the author Gerwick et al., 2008 until this year, most of the promising secondary metabolites tend to be yielded by filamentous marine cyanobacteria, in which nearly half of the 800 reported compounds come from Oscillatoriales order. More recently, the authors Vijayakumar *et al*., 2016 and Mi *et al*., 2017 confirmed that most of the secondary metabolites are isolated from the order Oscillatoriales and more precisely from the genera *Oscillatoria*, *Lyngbya*, *Moorea* and *Okeania*, in which until the last year, 58% of the natural products were reported from the genus *Oscillatoria* while 35% from *Lyngbya*.

The majority of cyanobacterial secondary metabolites are lipopeptides (40%) which are synthesized by large NRPS or mixed PKS-NRPS enzymatic systems. These metabolites also include amino acids (5.6%), fatty acids (4.2%), macrolides (4.2%) and amides (9%) (Raja *et al*., 2016). Cyanobacteria possess, as well, an array of toxic compounds, commonly denominated cyanotoxins (Machado et al., 2016; Nunnery et al., 2010). Many scientific studies show evidence that support the benefits of cyanobacteria for human health in both human and animal studies. In fact, the lipopeptides compounds, besides of being the most abundant, also tend to be the ones with the highest pharmaceutical and biotechnological interest, particular in the cytotoxicity and antitumor areas (Raja *et al*., 2016). Yet this not

exclude the potential of other minority compounds as vitamins and minerals that possess strong antioxidant properties. Additionally, these metabolites possess a great diversity of therapeutic properties as anti-tumoral, anti-inflammatory, anti-fungal, anti-microbial, anti-viral, anti-parasitic and immunosuppressive (Brito *et al*., 2015; Nunnery *et al*., 2010; Sharma *et al*., 2011; Singh *et al*., 2005; Singh *et al*., 2017). Moreover, it was also reported that can also prevent hypertension, cardiac diseases and chronic neurodegenerative disease, as Alzheimer. These are some of the activities highlighted in reviews published for marine cyanobacteria compounds, which does not mean that are the only ones (Blunt *et al*., 2015; Dixit and Suseela, 2013; Gogineni and Hamann, 2018; Raja *et al*., 2016; Raposo *et al*., 2013; Shah *et al*., 2017).

In short, only a few groups of microorganisms exist that are as chemically prolific as cyanobacteria, and the number is substantially reduced if deemed the great resistance of these microorganisms in various environmental conditions. Additionally, cyanobacteria were recognized as an exceptional source of lead compounds for drug discovery efforts and have a rich potential for pharmaceutical, medicinal and biotechnological development and application, notably marine cyanobacteria, which revealed considerable chemical richness producing structurally unique molecules (Leão *et al*., 2013; Nunnery *et al*., 2010; Tan, 2013).

1.4. Compounds produced by marine strains: *Synechocystis salina*, *Nodosilinea nodulosa* and *Nodosilinea* sp.

In the context of this study, the cyanobacteria studied in bioassay-guided fractionation were not only filamentous and included the picoplanktonic unicellular marine strain *Synechocystis salina* (LEGE 06099) belonging to Chroococcales order and also the picoplanktonic filamentous marine strains *Nodosilinea nodulosa* and *Nodosilinea* sp. (LEGE 06102 and 06001, respectively) belonging to Synechoccales order (Ramos *et al*., 2018a). The cyanobacterial strains that belong to different orders are morphologically and phylogenetically distant but have a geographical co-occurrence in the Portuguese Northern coast (Costa *et al*., 2016; Ramos *et al*., 2018b). In fact, these strains were largely overlooked and have been rarely studied with respect to their potential as producers of interesting bioactive compounds. Nonetheless, recent studies with extracts and fractions revealed possible secondary metabolites with biotechnological potential from these strains or genus of these cyanobacteria, except for *Nodosilinea* sp.

Extracts from strains belonging to *Synechocystis* genus showed toxicity to early life stages of marine invertebrates and capacity to produce the well-known hepatotoxin, microcystin (Barboza *et al*., 2017; Martins *et al*., 2007). Moreover, *S. salina* extracts exhibited antibacterial activity towards human bacterial pathogens and antifungal activity (Sakthivel and Kathiresan, 2012). Furthermore, Modiri *et al*., 2015 reported that strains from *Nodosilinea* genus are not good candidates to biofuel production due to their low lipid and biomass productivities. More recently, fractions of these same strains displayed strong cytotoxic effects against several cancer cell lines, especially HepG2 cell line, and showed to be promising for skin treatments and protection (Alfeus, 2016; Costa *et al*., 2014).

The extracts research were initial screenings that displayed the potential for biotechnological properties, such as anticancer and cosmetic care. In fact, (i) the photoprotective methyl methacrylate, (ii) the cytotoxic nakienones A-C and nakiritol, (iii) the anti-cyanobacterial terpene dehydroabietic acid, (iv) the antimicrobials phytol, fucosterol, noephytadiene, palmitic, palmitoleic and oleic acids, along with (v) the anticancer glycolipids bartolisides A-D and cytotoxic bartoloside A anologs, minor monoglycosylated bartolosides E-K were identified from the *S. salina* strain or genus (Afonso *et al*., 2016; Costa *et al*., 2016; Jain *et al*., 2017; Leão *et al*., 2015; Paul and J, 1999; Plaza *et al.*, 2010). So, to the best of our knowledge, from *Synechocystis* genus, several fatty acids, volatile compounds and pigments were already isolated, while from *Nodosilinea* genus few natural products are known (Plaza *et al.*, 2010). The exceptions are the anti-cyanobacterial terpenes dehydroabietic and abietic acids and the bartolosides A-D that were identified from the *N. nodulosa* strain or genus (Costa *et al*., 2016; Leão *et al*., 2015). Despite in these studies bartolosides A-D did not show strong bioactive properties, their high abundance in these microorganisms suggests that could have a fundamental biological role yet not identified.

1.5. Physiologically relevant small whole animal models

Bioassays are important for the screening of bioactivities of samples derived from natural compounds, extract libraries or fractions. Experimental models become an indispensable tool for studying various human disorders, and different possible approaches exist to assess anti-obesity activity of natural products, for instance by using stable cell lines *in vitro*. However, cells do not represent the complexity of a whole organism and its interplay between different tissues or organs, which is in particular important for obesity as a complex disease. Furthermore, many compounds active in *in vitro* systems, do not translate into effective drugs *in vivo* or present toxicity problems. Since the cellular models have some limitations, efforts are being made to use small whole animal models (Giacomotto and Ségalat, 2010).

In the past few years, Zebrafish (*Danio rerio*), a small freshwater teleost, became an attractive model organism for biomedical research, which presents considerable logistical advantages towards classical vertebrate models as rats or mice (Giacomotto and Ségalat, 2010; Hölttä-Vuori *et al*., 2010; Nguyen *et al.*, 2013; Tabassum *et al.*, 2015). Zebrafish possess high physiological and genetic homology to mammals, well-developed endocrine and neural pathways, high sensitivity to environmental alterations, relatively low cost of maintenance, ease experimental manipulation, high fecundity, availability of both adult and larval models, and culture conditions compatible with high-throughput screening for larvae (Giacomotto and Ségalat, 2010; Hölttä-Vuori *et al*., 2010; Oka *et al.*, 2010; Nguyen *et al.*, 2013; Tabassum *et al.*, 2015). *D. rerio* embryos are optical transparent and develop rapidly in the first 24 to 48 hours externally from their mothers. This competence allows the study of a wide range of biological processes and/or diseases mechanisms on early development stages by the use of fluorescent markers screens in microplates (Giacomotto and Ségalat, 2010; Hölttä-Vuori *et al*., 2010; Tabassum *et al.*, 2015). Because of all these reasons, *D. rerio* is increasingly used to study metabolic and neurobehavioural disorders as a novel complementary model to the rodent models, with easier handle, high predictive validity and cost-efficiency (Nguyen *et al.*, 2013; Oka *et al.*, 2010). Besides, the use of rodent models comprise some disadvantages, such as being more expensive and time-consuming for the purpose of this study, in addition of existing ethical conflicts. Nonetheless, *D. rerio*, as other teleost fish models, have their limitations, including the fact that they are ectothermic organisms and have genome duplication (despite their evolutionary conserved nature) which can affect their metabolic and neuroendocrine regulation (Giacomotto and Ségalat, 2010; Hölttä-Vuori *et al*., 2010; Nguyen *et al.*, 2013).

Despite all, several reports have been published about the use of *D. rerio* in studies of obesity. Strikingly, significant similarities were observed in the lipid metabolism between zebrafish and mammals, which allowed to develop a novel screening assay using Nile Red fluorescence (Jones et al., 2008). This screening tool allows the identification of new active compounds that can be later validated on mammals, and help reduce the list of potential future drugs targets for treating clinical obesity, as an intermediate step between *in vitro* and rodent assays in obesity research (Hölttä-Vuori *et al*., 2010; Jones *et al*., 2008; Oka *et al.*, 2010; Tingaud-Sequeira *et al*., 2011). In our laboratory, the zebrafish Nile Red fat metabolism assay was already successfully applied to identify compounds with lipid reducing activities without any general toxicity from marine fungi and chemically modified plant polyphenols (Noinart et al., 2017; Urbatzka *et al.*, 2018).

1.6. Main objectives

The primary aim of this research work was to discover novel bioactive compounds from different cyanobacterial strains towards obesity or obesity related co-morbidities.

In order to accomplish this aim, the work was focussed on cyanobacterial strains that have showed promising lipid reducing activities in previous screening assays. Selected cyanobacterial strains from the LEGE culture collection were cultured on a large scale in a 100 l plastic bag system or 20 l Nalgene flask, and biomass was continuously collected. After initial extraction and fractionation, a bioassay-guided isolation procedure was performed in order to purify and isolate the responsible natural compounds. The zebrafish Nile Red fat metabolism assay was applied for analysis of bioactivity, and spectroscopic (1D and 2D NMR, Nuclear Magnetic Resonance) and spectrometric (LC-MS, Liquid Chromatography Mass Spectrometry) techniques for structure elucidation.

2. Materials and Methods

2.1. General procedures and material

Solvents used in the chemical chromatographic procedures were both analysis and HPLC grade. For NMR analysis chloroform or dimethyl sulfoxide deuterated solvents (99.8% deuterium) were used.

For all vial fractions the weight was measured with an analytical Sartorius balance with 0,01 mg deviation error. For extraction procedure, a Bandelin Sonorex RK100H sonicator was used.

Fractionation steps can be accomplished by VLC (vacuum liquid chromatography), as well as flash chromatography, using silica gel (0.015 - 0.040 mm or 0.04 - 0.06 mm, Merck, KGaA, Darmstadt, Germany) packed in glass synthware Sigma-Aldrich columns. Similarly, for SPE (solid-phase extraction) Phenomenex prepacked normal-phase Si (silica) Strata cartridges with 55 µm and 70 A, were used, either with 2 g or 5 g. Merck, KGaA, aluminium-backed TLC (thin-layer chromatography) sheets coated with fluorescent indicator F254 and layered with 120-160 µm silica were used to monitor the chromatographic procedures; and preparative TLC (Merck, KGaA) was performed using 20 x 20 glass-backed plates also coated with fluorescent indicator F254 and layered with 210 - 270 µm silica, both with visualization under UV light (λ 254 nm). TLC sheets were also visualized with PMA (phosphomolybdic acid) stain followed by heating.

HPLC (high-performance liquid chromatography) was achieved with reverse stationary phase on a Waters Alliance e2695 instrument coupled with PDA (photodiode array) detector, and the software Empower 2 (chromatography data software) was used for data interpretation. Also, a normal stationary phase was achieved on a Waters 1525 instrument with a Binary HPLC pump. This instrument is coupled with a dual λ absorbance detector. The software Empower 3 was used for data interpretation.

Bioassays were also performed after each chromatographic step. The phase contrast and red fluorescence images were obtained with a Leica DM6000B microscope.

Compounds were characterized by low-resolution LC-MS (liquid chromatography mass spectrometry) Finnigan Surveyor linked to a Mass Spectrometry detector, MS LCQ Fleet Ion Trap equipped with an electrospray ionization source, both from Thermo Finningan (Thermo Scientific, San Jose, Californnia, USA). For data acquisition and analysis, the software Xcalibur version 2 (Thermo Scientific) was used. Nitrogen served as nebulizer gas and auxiliary gas, both in arbitrary units.

Besides this, ^{1}H NMR spectra (Nuclear Magnetic Resonance) were recorded on a Bruker Avance III instrument with 400 MHz frequency, in order to obtain the chemical nature of the fractions. For structural elucidation of pure compounds 1D and 2D NMR experiments were acquired with a Bruker Avance III HD 600 MHz frequency. Both chemical shifts (^{1}H and ^{13}C) are expressed in δ (ppm), referenced to the solvent used and the proton coupling constants *J* in hertz (Hz). Spectra were assigned using appropriate COSY, HSQC, HMBC, TOCSY and ROESY sequences.

2.2. Biological procedures

2.2.1. Cyanobacteria culture and harvest

The BBE (Blue Biotechnology and Ecotoxicology) team has its own culture collection – LEGE CC - with 386 cyanobacterial strains and a database with information about each strain including morphological description, taxonomic-related data, origin and culture conditions (Ramos *et al*., 2018a).

According to previous results from screening assays for bioactive compounds conducted by the BBE team, the strains *Romeria* aff. *gracilis* LEGE 07310, *Romeria* sp. LEGE 06013 and *Cyanobium* sp. LEGE 06097, belonging to Synechococcales order, were pinpointed as promising for production of compounds with lipid-reducing activities. Therefore, these cyanobacterial strains were selected to culture at a large-scale. The final intended volume of each strain was at least 120 l. The culture conditions consisted of a medium known as Z8 which integrates both macro and micronutrients (Table I.1, Appendix I) and 25 $g.l^{-1}$ salt (Kotai, 1972). The standard procedure was to initiate the culture in a new 50 ml culture flask under sterile conditions using a Telstar Bio II Advance laminar flow chamber. Following the culture was transferred to a previously autoclaved glass flask with half litre of deionized water with salt and the correct amount of nutrients (Table I.1, Appendix I). The scale-up procedure included the transfer of a small amount of biomass, normally 400 ml to 2 l, to the new and bigger glass (4 l) or Nalgene flask (20 l). Other and more recent procedure was do the scale-up culture directly in a 100 l plastic bag system, allowing the continuous harvest of half of the culture volume until the desired amount of biomass was obtained. To ensure the proper conditions of the culture, a routine reading of the optical density was performed using a plate reader (Biotek, Synergy HT) with three different absorbance wavelengths, 600, 735 and 750 nm, to measure the abundance of cells in suspension, and to compare with chromophore content in culture. These cultures were

maintained at a temperature of 25 ºC, a photoperiod of 16 h light :8 h dark, and light intensity of 10-30 µmol.m^{-2}.s^{-1}.

The biomass of the strains was harvested by centrifugation with 4700 rpm (7186 g), 4 ºC for 15 min (Thermo Scientific Sorvall Bios 16). Due to the marine nature of the strains a washing step with deionized water was included to remove the salt from the harvested biomass using the conditions mentioned above. The biomass pellet was then frozen at -80 ºC for later freeze-drying in a Telstar LyoQuest. The obtained powder was stored at room temperature until the subsequent extraction. The strains that were extracted and fractionated in this work are different from the ones that were cultured.

The following cyanobacterial strains were selected to start a large-scale culture:

i. *Romeria* aff. *gracilis* LEGE 07310
ii. *Romeria* sp. LEGE 06013
iii. *Cyanobium* sp. LEGE 06097

Additionally, for the organic extraction procedure were chosen the cyanobacterial strains listed below:

i. *Synechocystis salina* LEGE 06099
ii. *Nodosilinea nodulosa* LEGE 06102

Lastly, the cyanobacterial strains selected for the bioassay-guided fractionation were the following:

i. *Nodosilinea* sp. LEGE 06001 (E17161)
ii. *Synechocystis salina* LEGE 06099 (E15074 and E18179)
iii. *Nodosilinea nodulosa* LEGE 06102 (E17165)

2.2.2. Zebrafish Nile Red fat metabolism assay

The original procedure is published in Jones *et al*., 2008, and the assay performed with some modifications optimized by BBE team with the aim of screening for compounds with anti-obesity and obesity related co-morbidities activities. This bioassay has a total duration of six days, including acclimatization of eggs and zebrafish embryos in salt medium with PTU (phenylthiourea) at 28 ºC and selection of viable eggs. This medium was previously prepared with final concentrations of 60 µg.ml^{-1} salt and 200 µM PTU to suppress melanisation. On 3 DPF (days post-fertilization), six to eight replicates of larvae per well were exposed in a 48 well-plate to the cyanobacterial fractions/sub-fractions. The stock concentration of each fraction was 10 mg.ml^{-1} in DMSO (dimethyl sulfoxide) and a dilution

of 1:1000 was performed in the assay plate to achieve the final exposure concentration of 10 µg.ml^{-1}. A positive control REV (resveratrol, 50 µM), and solvent control, DMSO (0.1%) was included on each assay plate. On 4 DPF the medium and compounds get renewed, and possible existing egg shells or mortalities were removed. Furthermore, the stain Nile Red was added with a final concentration of 10 ng.ml^{-1} used for neutral lipid staining. Finally, on 5 DPF, larvae were anesthetized with tricaine (MS-222, 0.03%) and fluorescence was quantified in a fluorescence microscope (Olympus BX-41) with red contrast.

For specific sub-fractions, namely *Nodosilinea* sp. LEGE 06001 E17161 E4B and *Synechocystis salina* LEGE 06099 E18179 D-E3D, the death of all zebrafish larvae replicates was noted either at 24 h or 48 h. Following, 5 or 4 dilutions were realized through successive dilutions at 1:2, obtaining final concentrations ranging from 5 to 0.3125 µg.ml^{-1} and re-tested for bioactivities.

Additionally, sub-fraction E17161 E4C11A was tested with 7 different final concentrations, ranging from 20 to 0.3125 µg.ml^{-1}, also through dilution (1:2) series, in order to determine IC_{50} values.

2.2.3. Data analysis

The quantification of fluorescence intensity from images obtained from Zebrafish Nile Red fat metabolism assay was realized through the program Image J. The data were analysed for statistical differences with the program GraphPad Prism 7. The Gaussian distribution was tested by D´Agostinho-Pearson, Shapiro-Wilk and Kolmogorov-Smirnov normality test (P value < 0.05). The difference between the solvent control group (DMSO) and all other fractions was analysed by One-Way ANOVA with Dunnett posthoc test (P value < 0.05) if the data had parametric distribution, and Kruskal-Wallis with Dunn´s posthoc test (P value < 0.05) if the distribution was non-parametric. The data were represented as box-whisker plots with values in 5-95 percentiles, and fractions with significance differences were indicated by the symbol * .

Additionally, to determine IC_{50} values for bioactivity level was used data from dose-response curves. Mean intensity fluorescence data were normalized to the mean value of the solvent control (100%) and to mean value of the 50 µM resveratrol positive control (0%), and concentrations of the compound were log-transformed. A non-linear regression was applied with a variable slope and least square fitting to obtain the dose-response curves.

2.3. Chemical procedures

2.3.1. Organic extraction

The dry biomass of *Synechocystis salina* LEGE 06099 (31.46 g) and of *Nodosilinea nodulosa* LEGE 06102 (37.80 g) were firstly sonicated in 0.5 l of MeOH using an ultrasonic bath with 240 W, 35 kHz for 10 min to disrupt the cells. The biomass was then exhaustively extracted using MeOH (methanol, 7 x 0.5 l) at room temperature and CH_2Cl_2 (dichloromethane, 2 x 1 l). The evaporation of the solvents from crude extracts occurred in a rotavapor under vacuum and at 30 °C. This process yielded organic residues of 6.97 g and 10.80 g for *S. salina* LEGE 06099 and *N. nodulosa* LEGE 06102, respectively.

The organic extraction of *Nodosilinea* sp. LEGE 06001 and the first extraction of *S. salina* LEGE 06099 were not performed by the author of this work but by other researchers from the laboratory. Each crude extract and subsequent fractions were given increasing numeric codes (Table 1). These organic residues of three cyanobacterial strains were then chromatographed over silica columns.

Table 1 – Crude extracts codes from the chemical fractionated cyanobacterial strains.

Cyanobacterial strains	**Extract codes**
***Nodosilinea* sp. LEGE 06001**	E17161
***Synechocystis salina* LEGE 06099**	E15074 and E18179
***Nodosilinea nodulosa* LEGE 06102**	E17165

2.3.2. Bioassay-guided fractionation

2.3.2.1. Study of E17161 originated from the strain *Nodosilinea* sp. LEGE 06001

In a previous work the crude extract of *Nodosilinea* sp. LEGE 06001 was chromatographed by normal phase VLC yielding 11 fractions, from A to Iy. Fraction E (35.27 mg) eluted with 2:3 *n*-hexane/EtOAc – hexane and ethyl acetate, was reported to have the most interesting activity in the zebrafish bioassay.

Figure 5 synopsis all the fractionation procedures performed for strain *S. salina* LEGE 06099, as follows.

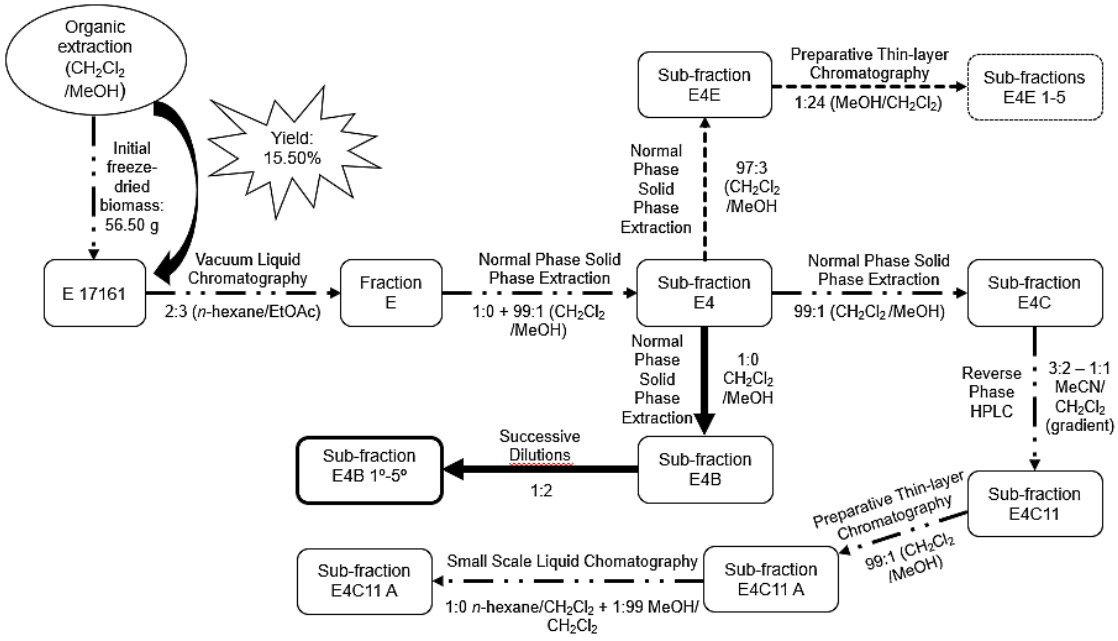

Figure 5 - Schematic diagram of chemical fractionation and sub-fractionation procedures and consequently fractions and sub-fractions of interest for strain Nodosilinea sp. LEGE 06001 (E17161). Dashed arrows indicate the chemical pathway that led to the isolation of the pure compound. Dotted arrows indicate the chemical pathway that follow sub-fractionation based on NMR information. Thicker arrows indicate a sub-fraction with different bioactivity from the others.

A normal phase SiO_2 SPE (2 g, 12 ml) with step-wise crescent polar solvent gradient from 1:0 until 0:1 CH_2Cl_2/MeOH was realized for fraction E. Six fractions were obtained from E1 to E7. These were joined according with information obtained from TLC, and all sub-fractions were submitted to ^{1}H NMR (400 MHz) and zebrafish bioassay. Due the bioactivity level presented, sub-fraction E4 (15.98 mg, eluted with 1:0 and 99:1 CH_2Cl_2/MeOH) was subjected to another round of normal phase chromatography. Hence, E4 was chromatographed through SiO_2 SPE (2 g, 12 ml) with 7:3 *n*-hexane/CH_2Cl_2 to 0:1 CH_2Cl_2/MeOH series of crescent polar solvent gradient originating 6 sub-fractions from E4A to EAF. Again, a TLC analysis was done to ensure the efficacy of the separation and to group the mixtures with similar composition. A preparative TLC was performed for sub-fraction E4E (3.18 mg, eluted with 97:3 MeOH/CH_2Cl_2), being developed twice in a mixture of 1:24 MeOH/CH_2Cl_2, affording 5 new sub-fractions from E4E1 to E4E5 (Figure 6). For these fractions obtained from preparative TLC, each one of the bands were scraped off the glass backing to a vial and then filtrated. Moreover, after ^{1}H NMR (400 MHz) and zebrafish analysis no more sub-fractionations were applied for E17161 E4E.

Sub-fraction E4C (4.72 mg, eluted with 99:1 CH_2Cl_2/MeOH) was submitted to further sub-fractionation after desirable compliance with zebrafish bioassay results with a RP (reverse phase)-HPLC.

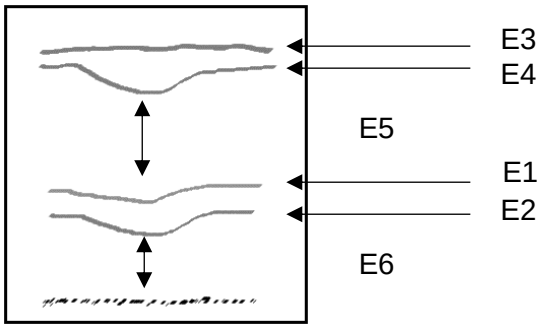

Figure 6 – Preparative TLC of sub-fraction E17161 E4E. Elucidatory scheme of band layout that originated sub-fractions E4E1 to E4E5.

In this method was used a Luna 10 µm C18 100 Å column (250 x 10 mm) and occur two rounds of purification. The initial separation was carried out under a polar isocratic mixture of 9:11 MeCN (acetonitrile)/H_2O with a flow of 3 ml.min^{-1} for 22 min. The sample was eluted with MeOH and the injection volume was 90 µl. Afterwards, the sample was re-injected with the same volume used previously to HPLC system. The separation occur with a continuously polar gradient of 3:2 to 1:1 MeCN/CH_2Cl_2, with a flow of 2 ml.min^{-1} for 25 min. The sample was eluted in a mixture of 1:1 MeCN/CH_2Cl_2. In the end, 11 sub-fractions were obtained and after analysis of ^{1}H NMR (400 MHz) spectrum and zebrafish bioassay, the sub-fraction E4C11 (1.46 mg) was subjected to low-resolution LC-MS. The chromatographic analytical column used was Luna 5 µm C18 100 Å (250 x 4.6 mm; Phenomenex). The elution was done with acidified solvents with 0.1 % formic acid in a flow of 0.8 ml.min^{-1} for 30 min with the following gradient: 15 minutes 1:1 to 0:1 H_2O/MeCN and 15 minutes 0:1 H_2O/MeCN. The injection volume was 20 µl. The MS data were collected in negative mode with full scan (200-2000 *m/z*). The sample was further sub-fractionated by preparative TLC chromatography with mixture of 1:99 MeOH/CH_2Cl_2 affording two new sub-fractions E4C11A and E4C11B (Figure 7).

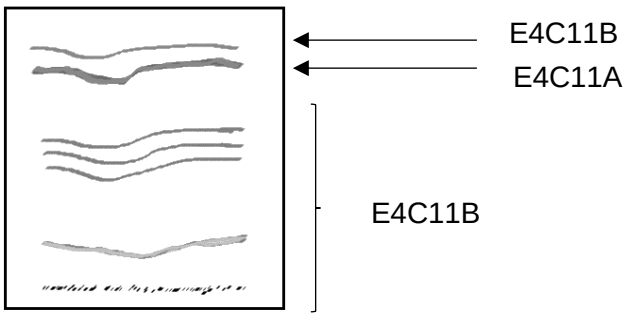

Figure 7 - Elucidatory scheme of preparative TLC band layout of sub-fractions E4C11A and E4C11B.

These two sub-fractions had the same methodology applied as mentioned above. Once again, after analysis of ^{1}H NMR (400 MHz) spectra, sub-fraction E4C11A was the one who had a set of signals more similar to the one that was being followed. Additionally, sub-fraction E4C11B was tested in zebrafish bioassay however E4C11A was not immediately tested because of limitation of mass of the compound. First all chemical structure characterization analyses were completed, and only then was the potential bioactivity of the compound access.

Compound **(1)** was isolated from sub-fraction E4C11A, with only one more step of filtration necessary. Finally, bioactivity of sub-fraction E4C11A was confirmed through zebrafish bioassay

Compound (1):

Brownish green powder;

Low-resolution LC-MS (negative mode) *m/z*: 815.46 $[M - H]^-$.

^{1}H NMR (600 MHz, $CDCl_3$): δ 9.77 (1H, s, H-10), 9.56 (1H, s, H-5), 8.71 (1H, s, H-20), 8.03 (1H, dd, *J* = 17.8, 11.5 Hz, H-3^1), 6.35 (2H, d, *J* = 18.7 Hz, H-3^2), 6.19 (2H, d, *J* = 11.4 Hz, H-3^2), 6.11 (1H, s, 0H-13^2), 5.14 (2H, t, *J* = 6.5 Hz, H-F2), 4.50 (2H, m, H-F1), 4.46 (1H, m, H-18), 4.44 (2H, m, H-F1), 4.07 (1H, dd, *J* = 7.4 Hz, H-17), 3.90 (3H, s, H-12^1), 3.77 (2H, m, H-8^1), 3.76 (3H, s, H-13^4), 3.64 (2H, m, H-8^1), 3.44 (3H, s, H-2^1), 3.28 (3H, s, 7^1), 2.56 (2H, dd, *J* = 7.7 Hz, H-17^1), 2.46 (2H, m, H-17^2), 2.35 (2H, t, *J* = 7.5 Hz, H-F8), 2.17 (2H, m, H-17^2), 1.89 (2H, m, H-F4), 1.83 (2H, dd, *J* = 9.1 Hz, H-17^1), 1.72 (3H, t, *J* = 7.7 Hz, H-8^2), 1.65 (2H, m, H-F9), 1.61 (3H, s, H-F3^1), 1.59 (3H, m, H-18^1), 1.51 (1H, m, H-F11), 1.33 (1H, m, H-F7), 1.29 (2H, m, H-F5), 1.11 (2H, m, H-F10), 1.01(2H, m, H-F6), 0.85 (3H, d, *J* = 6.6 Hz, H-F11^1), 0.85 (3H, m, H-F12), 0.80 (3H, m, H-F7^1) ppm.

^{13}C NMR (600 MHz, $CDCl_3$): *δ* 173.4 (C, C-17^3), 171 (C, C-19), 170.8 (C, C-13^3), 166.3 (C, C-16), 155.7 (C, C-6), 149.9 (C, C-9), 145.6 (C, C-8), 141.3 (C, C-1), 140.2 (C, C-14), 138.8 (C, C-11), 136.6 (C, C-7), 135.9 (C, C-4), 133.4 (C, C-3), 133.2 (C, C-13), 131.5 (C, C-2), 131.5 (C, C-12), 128.3 (CH, C-3^1), 122.1 (CH_2, C-3^2), 117.7 (C, C-F3), 117.1 (CH, C-F2), 103.4 (CH, C-10), 102 (C, C-15/13^2) 100.4 (C, C-13^2/15), 99.1 (CH, C-5), 93.3 (CH, C-20), 60.8 (CH_2, C-F1), 53.4 (CH_3, C-13^4), 53.1 (CH, C-17), 49.7 (CH, C-18), 39.3 (CH_2, C-F4), 38.9 (CH_2, C-F10), 36.6 (CH_2, C-F6), 32.6 (CH_2, C-F8), 32.1 (CH, C-F7), 31.7 (CH_2, C-17^2), 30.7 (CH_2, C-17^1), 27.4 (CH, C-F11), 24.3 (CH_2, C-F9), from 22 to 24 (CH_2, C-F5), 22.1 (CH_3, C-F11^1), 22.1 (CH_3, C-F12), 21.7 (CH_3, C-18^1), 19.2 (CH_3, C-F7^1), 19 (CH_2, C-8^1), 17 (CH_3, C-8^2), 15.8 (CH_3, C-F3^1), 11.9 (CH_3, C-12^1), 11.5 (CH_3, C-2^1), 10.8 (CH_3, C-7^1) ppm.

2.3.2.2. Study of E15074 and E18179 originated from *Synechocystis salina* LEGE 06099

In a previous work the organic extract E15074 from *S. salina* LEGE 06099 was fractionated by normal phase VLC yielding 10 fractions, from A to I. These fractions were submitted to the zebrafish assay and fraction B presented activity.

Figure 8 shows a schematic diagram with all the fractionation procedures accomplished to strain S. salina LEGE 06099.

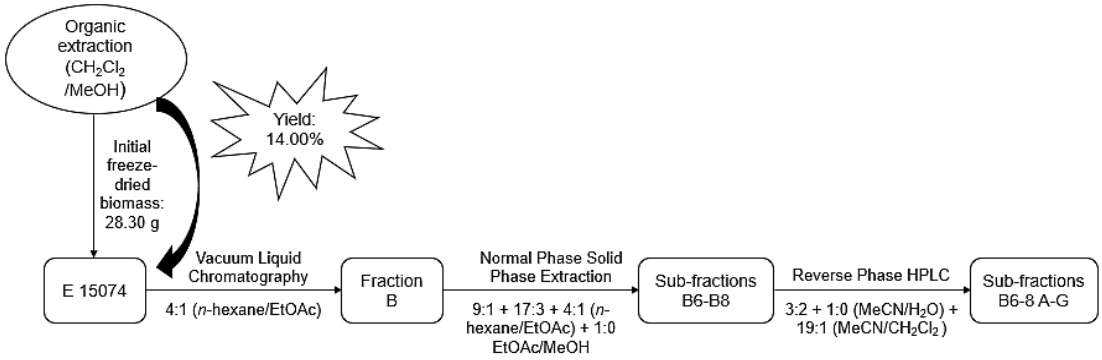

Figure 8 - Schematic diagram of chemical fractionation and sub-fractionation procedures and consequently fractions and sub-fractions of interest for strain Synechocystis salina LEGE 06099 (E15074).

Fraction B (23.83 mg eluted with 4:1 *n*-hexane/EtOAc), as the result of activity level presented, was sub-fractionated through a normal phase SiO_2 SPE (2g, 12 ml) using step-wise increasing polar solvent mixtures from 1:0 *n*-hexane/EtOAc to 0:1 EtOAc/MeOH originating 11 sub-fractions from B1 to B11. These sub-fractions were grouped according with information obtained from TLC and were submitted to zebrafish bioassay and ^{1}H NMR analysis. According to the bioactivity assays, fractions B6 to B8 were the most active and since they showed a similar proton profile they were joined. Sub-fraction B6-8 (4.95 mg, eluted with 9:1, 17:3, 4:1 and 0:1 *n*-hexane/EtOAc) was subjected to a RP-HPLC using a Synergy 4 µm Fusion-RP 80 Å column (250 x 10 mm). The separation occurred with an isocratic mixture of 3:2 $MeCN/H_2O$. The joined sub-fractions had a sample volume injected of 100 µl and flow of 3 $ml.min^{-1}$ for 25 min. Additionally, two more rounds were carried out to clean the column with isocratic mixtures of 1:0 $MeCN/H_2O$, and 19:1 $MeCN/CH_2Cl_2$. As a result, from initial purification step were obtained 5 sub-fractions, B6-8 A to E, and from cleaning of column two more sub-fractions were afforded, B6-8 F and G.

The crude extract E18179 obtained from *S. salina* LEGE 06099 (6.97 g) was fractionated by normal phase VLC over SiO_2 (320 g) and was used an increasingly polar

solvent mixtures, since *n*-hexane/EtOAc (9:1 to 0:1) until EtOAc/MeOH (3:1 and 0:1) according with the Table 2, yielding 10 fractions, from A to Ix.

Table 2 - Crude fractions obtained by vacuum liquid chromatography of extract of strain Synechocystis salina LEGE 06099, E18179.

	ELUENTS (V/V)			
FRACTION	Amount (mg)	*n*-hexane:EtOAc	EtOAc:MeOH	Column volume (ml)
A	98.85	9:1	-	750
B	74.15	4:1	-	750
C	99.65	7:3	-	750
D	314.92	3:2	-	750
E	229.85	2:3	-	750
F	444.73	1:4	-	750
G	86.43	0:1	-	750
H	1128.67	-	3:1	500
I	1951.73	-	0:1	500
Ix	401.39	-	0:1	750

Succinct information about the fractionation steps of the dried biomass of E18179 from this strain is illustrated in Figure 9. The initial fractions were submitted to zebrafish and ^{1}H NMR. Fractions D and E were found to be the most active and with very similar proton profile, so they were joined for the further sub-fractionation.

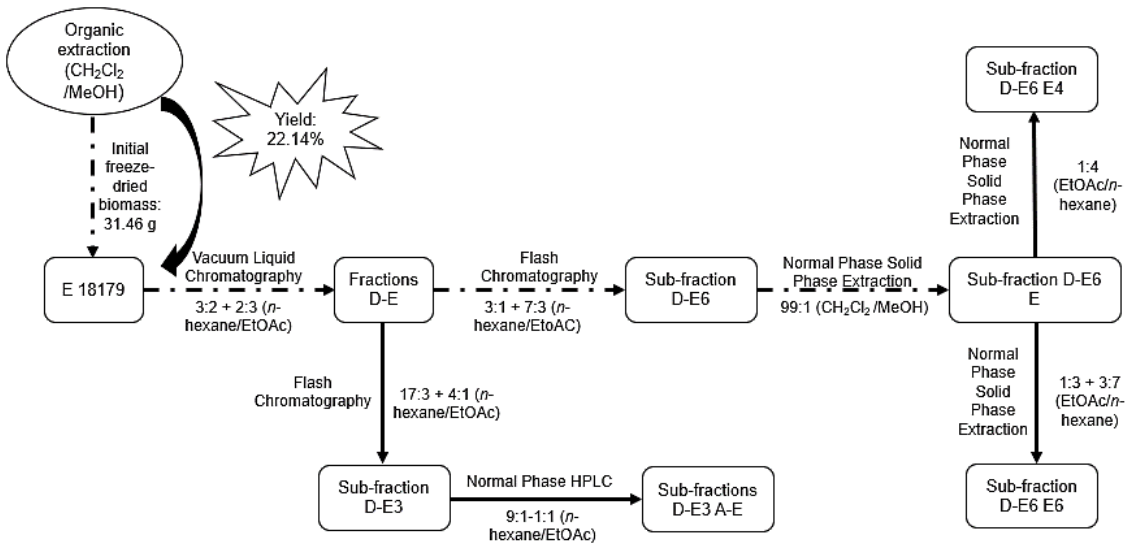

Figure 9 - Schematic diagram of chemical fractionation and sub-fractionation procedures and consequently fractions and sub-fractions of interest for strain Synechocystis salina LEGE 06099 (E18179).

A flash chromatography was performed for fractions D-E (456.06 mg, eluted with 3:2 and 2:3 *n*-hexane/EtOAc) with a step-wise crescent polar solvent gradient from 1:0 *n*-hexane/EtOAc to 0:1 EtOAc/MeOH yielding 12 sub-fractions from D-E1 to D-E12. TLC was performed to assemble the final sub-fractions and two of these according to zebrafish bioassay were further chromatographed, D-E3 and D-E6.

A normal phase SiO_2 SPE (5 g, 20 ml) was performed for D-E6 (139.3 mg, eluted with 3:1-7:3 *n*-hexane:EtOAc) with a crescent polar gradient from 1:1 until 0:1 *n*-hexane/CH_2Cl_2 and then 0:1 CH_2Cl_2/MeOH, with a total of 8 sub-fractions originated (D-E6 A to H). A normal phase HPLC of the D-E3 sub-fraction (2.3 mg eluted with 17:3 - 4:1 *n*-hexane:EtOAc) was done using a Luna 5 µm Silica 100 Å column (250 x 4.6 mm). The separation occur under polar gradient from 9:1 to 1:1 *n*-hexane:EtOAc with a flow of 1 $ml.min^{-1}$ for 35 min. The sample was eluted with *n*-hexane and injection volume was 30 µl. This analytical-scale HPLC purification yield 5 sub-fractions (D-E3 A to E). Each sub-fraction was tested in zebrafish bioassay and ^1H NMR spectra was obtained. According with the information provided by these analyses, only sub-fraction D-E6 E was further sub-fractionated. D-E6 E (66.6 mg, eluted with 1:99 MeOH/CH_2Cl_2) was chromatographed using a normal phase SiO_2 SPE (5 g, 20 ml) with a series of crescent polar solvent gradient from 1:0 *n*-hexane:EtOAc until 0:1 EtOAc:MeOH with a total of 8 sub-fractions originated (D-E6E 1 to 8). These were subjected to ^1H NMR and zebrafish bioassay analysis. Accordingly, two sub-fractions displayed the desirable bioactivity and the ^1H NMR spectra contained the proper set of signals that were being followed.

2.3.2.3. Study of E17165 originated from *Nodosilinea nodulosa* LEGE 06102

The crude extract obtained (10.80 g) for this strain was fractionated over SiO_2 (320 g) and was used a step-wise increasingly polar solvent mixtures, since *n*-hexane/EtOAc (9:1 to 0:1) until EtOAc/MeOH (3:1 and 0:1) according with Table 3, yielding 12 fractions, from A to Iz. No further work was developed for this strain because there was no available time to proceed the following sub-fractionations.

Table 3 - Crude fractions obtained by vacuum liquid chromatography of extract of strain Nodosilinea nodulosa LEGE 06102, E17165.

		ELUENTS (V/V)		
FRACTION	Amount (mg)	*n*-hexane:EtOAc	EtOAc:MeOH	Column Volume (ml)
A	103.92	9:1	-	1500
B	68.04	4:1	-	750
C	113.79	7:3	-	750
D	328.59	3:2	-	750
E	301.48	2:3	-	750
F	94.66	1:4	-	750
G	84.94	0:1	-	750
Hx	424.26	-	3:1	750
Hy	473	-	3:1	750
Ix	1765.76	-	0:1	500
Iy	2485.3	-	0:1	750
Iz	630.62	-	0:1	750

3. Results and Discussion

3.1. Growth of strains *Romeria* sp. LEGE 06013, *Romeria* aff. *gracilis* LEGE 07310 and *Cyanobium* sp. LEGE 06097

Cyanobacterial strains were grown during several months in a large-scale culture, at laboratory level. The strain *Romeria* sp. LEGE 06013 was successively cultured in seven 20 l Nalgene flask, while the strain *R. gracilis* LEGE 07310 was cultured in 100 l plastic bag system (Figure 11). The strain *R. gracilis* throughout its culture time was frequently monitored using optical density (OD) of different absorbance wavelengths and the results are shown in the Figure 10.

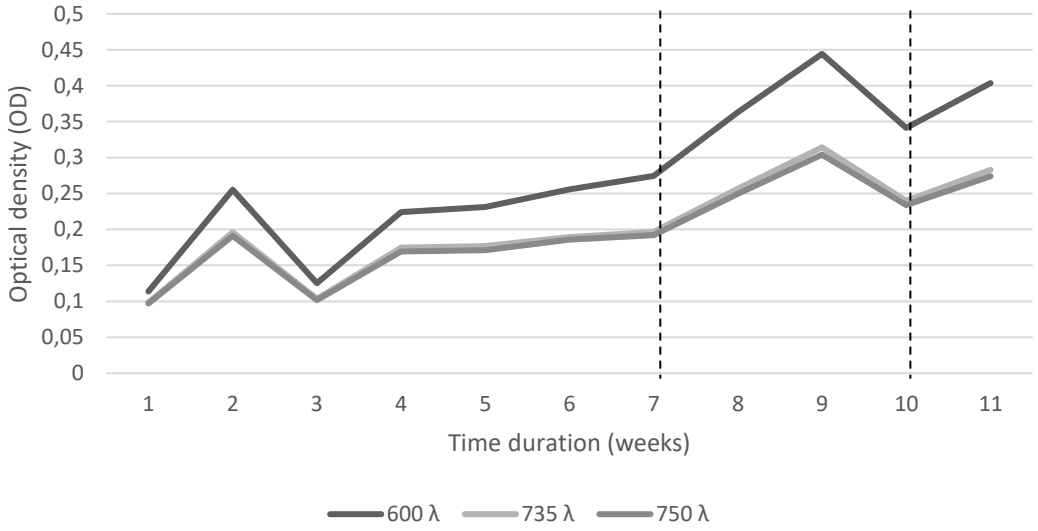

Figure 10 - Continuous reading of the optical density of strain Romeria aff. gracilis LEGE 07310, in the plastic bag system for three months, in three different absorbance wavelengths, 600, 735 and 750 nm. In dashed is indicating the sampling period of culture medium and subsequent renewal.

Cyanobacteria contain various pigments, and the most common are chlorophylls and phycocyanin. These pigments can be affected by physiological state of the organisms (*e.g.* availability of light, nutrient limitations), which means that the cellular content of pigments is different depending upon environmental conditions (Lawton *et al*., 1999; Myers *et al*., 2013). One of the most commons methods to estimate cyanobacterial growth is the microscopic biomass determination, however it is very time-consuming. Another less time-consuming method is the quantification of chlorophyll-a or phycocyanin. Quantification of pigment content is a widely used and accepted measure of biomass. Nonetheless is open to

interference depending on the physiological state of the microorganism (*e.g.* content increase if light availability is low). So, to prevent possible bias in measurements due to pigment cell content, the measurements used need to not interfere with the pigment's absorption spectra, and in this way assess growth qualitatively as the turbidity of culture (Lawton *et al*., 1999; Myers *et al*., 2013). Therefore, the wavelengths chosen were 735 and 750 nm, above 700 nm to allow light scatter but not absorb by the organism's pigments and thus measure the abundance of particles (cells) in suspension, however 600 nm was also used to compare with chromophore content in culture. Nonetheless, is necessary to keep in mind that this method is reliable and robust for routine monitorization of cultures even without sample preparation, as occur in this case, but not for specific research purposes.

By examining Figure 10 is possible to recognize that from all the three absorbance wavelengths used, there are two with quantifications very similar, which are the ones that are indeed measuring the cyanobacteria cells in culture (735 and 750 λ), and on other hand the quantification from 600 λ was much higher, indicated the possible overestimation of cyanobacteria growth when using wavelengths that are absorbed by pigments. Also, two abrupt drops in the OD values can be detected in week 2 to 3 and week 9 to 10. The last one correspond to the harvest of half the plastic bag system followed by the replacement of the same amount of culture, while the first may be indication of the adaptation of the culture to this system. Additionally, a slower drop is evidenced in dashed in week 7 that correspond to the first harvest of the culture. There is a noticeable difference between both collection periods, which could imply a different response of the culture dependent on the cellular content or an error in the measurement. Except for the week 3, in the intermediate period there was a continuous growth of the culture. Overall, this confirm a healthy growth of cultures in plastic bags systems, with possible identification of stage of growth for culture harvest.

In the end, for the purposes of these work the final yield of the collected biomass, was 97.20 g and 117.70 g, for strains *R. gracilis* LEGE 07310 and *Romeria* sp. LEGE 06013, respectively. Biomass differences may be dependent on strain or culture growth method and considering the much more time-consuming culture in 20 l Nalgene flask, plastic bags systems should be prioritized for large scale culture in laboratories. The culture of the strain *Cyanobium* sp. LEGE 06097 was only possible to reach the 6 l glass flask culture due the lack of space and material during this work period to transfer to a plastic bag system.

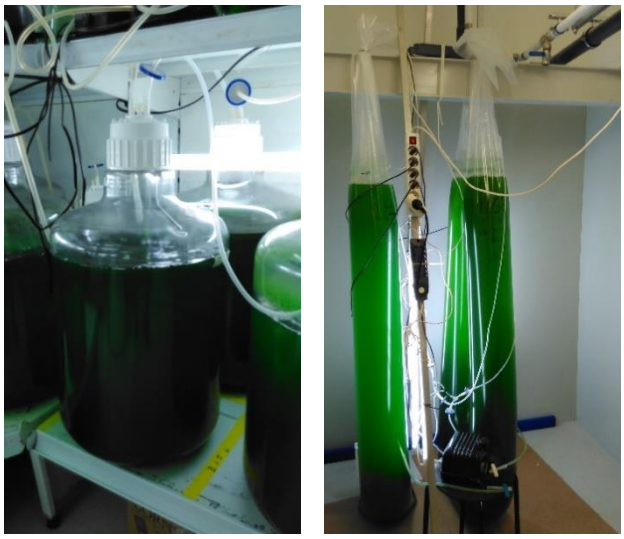

Figure 11 – Strains growth culture. Left: Romeria sp. LEGE 06013 in 20 l Nalgene flask growth culture; Right: Romeria aff. gracilis LEGE 07310 in plastic bag system growth culture.

3.2. Bioassay-guided fractionation

3.2.1. Study of E17161 derived from strain *Nodosilinea* sp. LEGE 06001

The *Nodosilinea* sp. LEGE 06001 undergoes a series of chromatographic and other procedures to obtain the different fractions that were tested in zebrafish bioassay and followed by proton NMR.

An initial bioactivity screening was previously performed in another work and indicated that the fraction E17161 E had the desirable activity. After sub-fractionation through SiO_2 SPE, the results from the zebrafish bioassay showed that only sub-fractions E17161 E4 and E17161 E4C, had a reduction on fluorescence intensity compared to solvent control group (DMSO) (Figure 12).

Statistical analysis confirmed that sub-fractions E4 and E4C had significant lipid-reducing activity in comparison with DMSO group at 48 h, as illustrated in Figure 13. A reduction of about 40% of the stained neutral lipids in the zebrafish larvae were observed for both fractions, more exactly 37.25 ± 13.76% and 38.59 ± 11.03%, respectively.

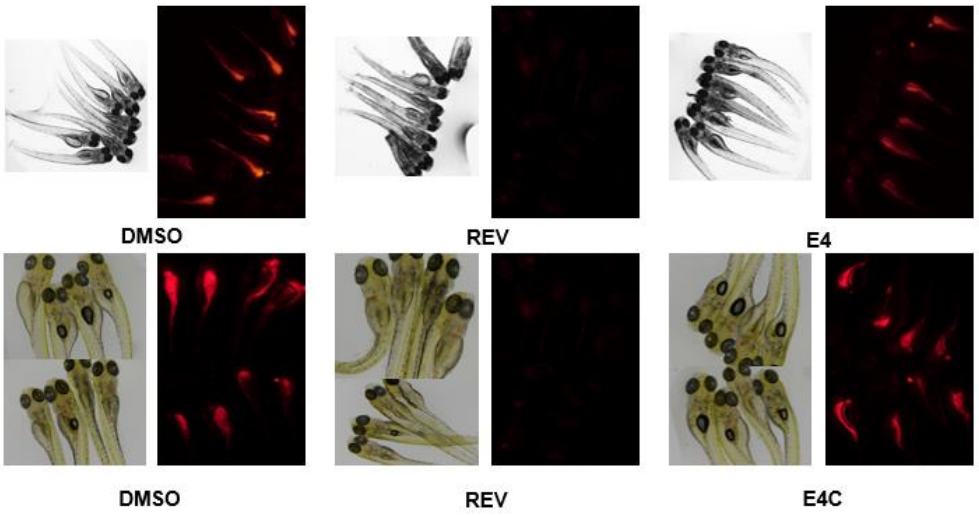

Figure 12 - Representative images of the zebrafish Nile Red fat metabolism assay of sub-fractions E17161 E4 and E4C. In left are represent the phase contrast image of zebrafish larvae and the right images show the fluorescence with red contrast in fractions with bioactivity. DMSO, solvent control 0.1%; REV, positive control 50 µM.

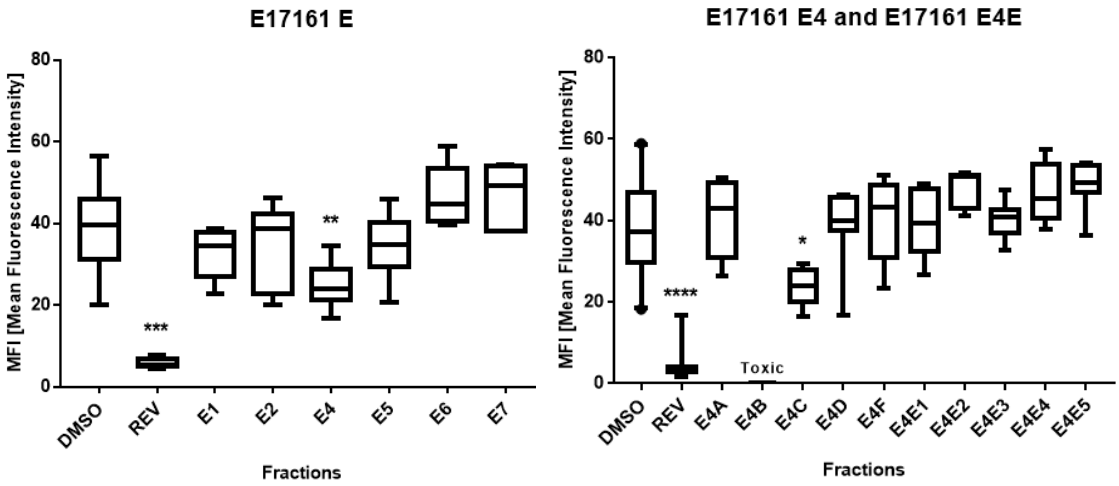

*Figure 13 – Lipid-reducing activity in the zebrafish Nile Red fat metabolism assay for sub-fractions E17161 E1 to E7 (left), E4A to E4F (right) and E4E1 to E4E5 (right). Solvent control had 0.1% DMSO and the positive control received 50 µM REV. Values are expressed as mean fluorescence intensity (MFI) relative to the DMSO group, and each treatment group had 6 to 8 replicates. The data are represented as box-whisker plots. Statistical differences were analysed by Kruskal-Wallis with Dunn´s posthoc test and are indicated to the solvent control with the symbol * p < 0.05; ** p < 0.01; *** p < 0.001; **** p < 0.0001.*

Interestingly sub-fraction E17161 E4B caused death for all exposed zebrafish larvae after 24 h, while all the other sub-fractions, apart from E4C, did not have any significant effects different from DMSO group (Figure 14).

This toxicity activity at final concentration 10 µg.ml^{-1}, applied for all solutions tested in this bioassay-guided fractionation study, could be masking a positive obesity activity at lower concentrations.

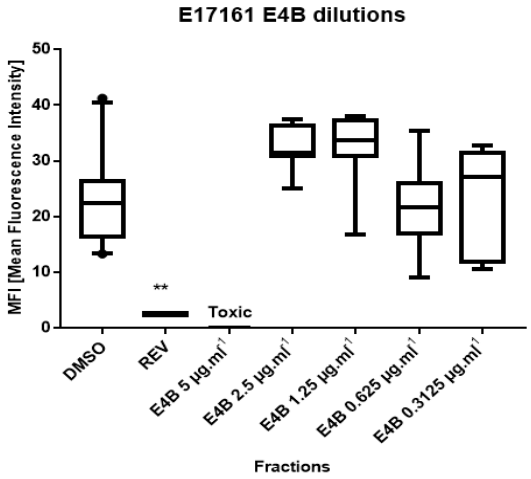

*Figure 14 – Lipid-reducing activity in the zebrafish Nile Red fat metabolism assay for sub-fractions E17161 E4B 1º dilution to E4B 5º dilution. Solvent control had 0.1% DMSO and the positive control received 50 µM REV. Values are expressed as mean fluorescence intensity (MFI) relative to the DMSO group, and each treatment group had 6 to 8 replicates. The data are represented as box-whisker plots. Statistical differences were analysed by Kruskal-Wallis with Dunn´s posthoc test and are indicated to the solvent control with the symbol * p < 0.05; ** p < 0.01; *** p < 0.001; **** p < 0.0001.*

For example, this situation may occur when the compound would possess a very strong activity - the concentration tested could induce an excessive reduction of the larvae lipids content, crucial for live maintenance. To test this hypothesis, a successive dilution of sub-fraction E4B was prepared and tested, in which the diluted sub-fractions did not display any statistically significant difference from DMSO group (Figure 14). Therefore, it can be concluded that the mixture of compounds in this sub-fraction did not have lipid-reducing properties. However, other bioactivities may be present, the most likely cytotoxicity, considering the toxicity activity also displayed at 5 $\mu g.ml^{-1}$. For this aim, an MTT bioassay for cytotoxic activity on cancer cells was performed by a colleague.

Throughout these steps of purification, sub-fractions proton composition was followed by ^{1}H NMR (Appendix II). Parsing these spectra was possible to confirm that overall proton profile became more defined, including very clear (1) downfield peaks between 0.5 to 2.5, normally correspondent to polymeric aliphatic chains, (2) peaks between 3 to 4, that could indicate the presence of either, amines or alcohols groups and finally (3) upfield peaks between 6 to 7 and between 8 to 10 that could imply the presence of varies heteroaromatic rings besides carboxylic acid groups, aldehydes groups, amides groups, among others. Nevertheless, the proton profile of sub-fractions with activity (E17161 E4 and E4C) showed that predominant peaks were preserved, and no loss occurred of possible bioactive compounds.

Additionally, a ^{1}H NMR-guided sub-fractionation was applied to E17161 E4E because seemed chemically interesting. So, as result of preparative TLC, was obtained 5 sub-fractions that did not display any significantly different activity from control group, as shown

in Figure 13. Therefore, not further work was developed for these sub-fractions E4E1 to E4E5.

Further sub-fractionation was performed for the active E17161 E4C sub-fraction by RP-HPLC with two different rounds of purification. The Figure 15 A demonstrates that sub-fractions E4C 1, 2, 4, 5, 6, 7 and 8 correspond to the several peaks highlighted in rectangles, while sub-fractions 3, 6 and 9 correspond to the remaining content during the run of sample. ^{1}H NMR data analysis revealed that the compounds existing in sub-fractions E4C1 to E4C8 were lost, and that apparent proton signals profile in the spectra did not resemble the ones of previous sub-fractions E4 and E4C (Appendix II, Figures II.1.1 and II.1.2). A possibility existed that the compounds were trapped in the column. Consequently, a non-polar mixture of solvents, a stronger mixture, was used to recover the two peaks illustrated in Figure 15 B. The first peak (10) had a retention time of 11.16 min and was colourless, while the second peak (11) had a retention time of 12.37 min and a greenish colour indicating the presence of the pigment. However, both sub-fractions, E4C9 and E4C10, did not have any significant lipid-reducing activity (Figure 16). The proton spectra of sub-fraction E4C11 contained a profile of peaks with similar predominant peaks as E4C, which was the reason to continue work on that sub-fraction (Appendix II, II.1.3).

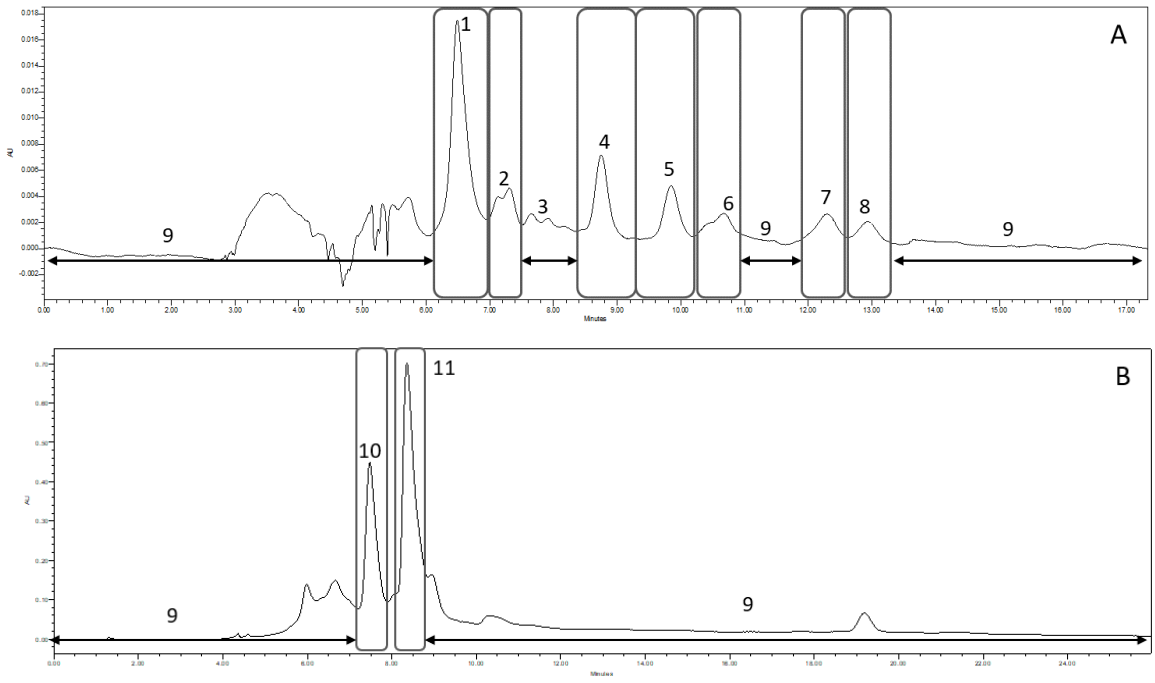

Figure 15 - Reverse phase HPLC chromatograms of E17161 E4C using a Luna 10 µm C18 100 Å column (250 x 10 mm). (A) Initial separation was carried out under a polar isocratic mixture of 9:11 MeCN/H_2O with a flow of 3 ml.min^{-1} for 22 min. The sample was eluted with MeOH and the injection volume was 90 µl. (B) Second separation occur with a step-wise polar gradient of 3:2 to 1:1 MeCN/CH_2Cl_2, with a flow of 2 ml.min^{-1} for 25 min. The sample was eluted in a mixture of 1:1 MeCN/CH_2Cl_2 and the injection volume was 90 µl. Peak 10 had a retention time of 11.16 min and peak 11 of 12.37 min (UV detection at 254 nm).

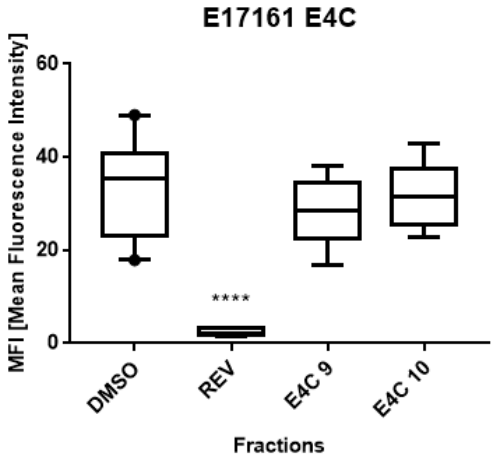

*Figure 16 – Lipid-reducing activity in the zebrafish Nile Red fat metabolism assay for sub-fractions E17161 E4C 9 and 10. Solvent control had 0.1% DMSO and the positive control received 50 µM REV. Values are expressed as mean fluorescence intensity (MFI) relative to the DMSO group, and each treatment group had 6 to 8 replicates. The data are represented as box-whisker plots. Statistical differences were analysed by Kruskal-Wallis with Dunn´s posthoc test and are indicated to the solvent control with the symbol * p < 0.05; ** p < 0.01; *** p < 0.001; **** p < 0.0001.*

Analysis of the proton NMR of sub-fraction E4C11 revealed some similarities between this compound and hydroxy-pheophytin-a, although with some differences (Jerz *et al*., 2007; Matsuo *et al*., 1996). In order to further purify E4C11, a preparative TLC was preformed originating sub-fractions E4C11A and E4C11B. At this point, the mass of the sub-fractions began to be scarce, therefore only sub-fraction E4C11B was tested in zebrafish bioassay and did not show activity towards reducing lipids, which suggested sub-fraction E4C11A to be the one of interest (Figure 17). Only one more step of purification was required which lead to the pure compound **(1)**, sub-fraction E4C11A.

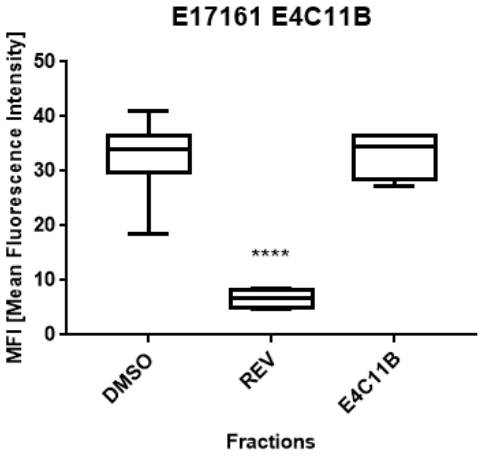

*Figure 17 – Lipid-reducing activity in the zebrafish Nile Red fat metabolism assay for sub-fraction E17161 E4C11B. Solvent control had 0.1% DMSO and the positive control received 50 µM REV. Values are expressed as mean fluorescence intensity (MFI) relative to the DMSO group, and each treatment group had 6 to 8 replicates. The data are represented as box-whisker plots. Statistical differences were analysed by One-way ANOVA with Dunnett posthoc test and are indicated to the solvent control with the symbol * p < 0.05; ** p < 0.01; *** p < 0.001; **** p < 0.0001.*

3.2.1.1. Structural elucidation of compound (1)

Compound **(1)** was obtained as a brownish green amorphous solid. The ^{1}H NMR spectrum of compound **(1)** showed similarities with the proton profiles of hydroxy pheophytin-a. The comparison was realized using a proton profile of a lab colleague and literature data available (Jerz *et al*., 2007; Li *et al*., 2012). Additionally, these similarities suggested the central Mg ion was absent comparing with proton NMR spectral data obtained for pheophorbide-a and pheophytin-a, in opposition of chlorophyll-a (Abraham and Rowan, 1991; Jerz *et al*., 2007; Kang *et al*., 2018; Li *et al*., 2012). Low resolution ESI-MS spectrum presented a pseudomolecular ion at *m/z* 815.46 $[M - H]^-$ (Figure 18 A), that suggested the molecular formula $C_{50}H_{64}N_4O_6$. An ion at *m/z* 607.07 $[M - C_{15}H_{29}]^-$ correspond to the data literature to the porphyrin part of hydroxy pheophytin-a, that exhibited an ion at *m/z* 606.00 [M - H-phytyl]$^-$ (Jerz *et al*., 2007). The difference between the *m/z* 606.00 fragment of hydroxy pheophytin and the monoisotopic mass of 885.70 $[M - H]^-$ is *m/z* 279.70 corresponding to the phytyl moiety. However, in compound **(1)** it corresponds to Δ *m/z* 208.39, which indicates the presence of a farnesyl moiety instead of a phytyl group (Figure 18 B).

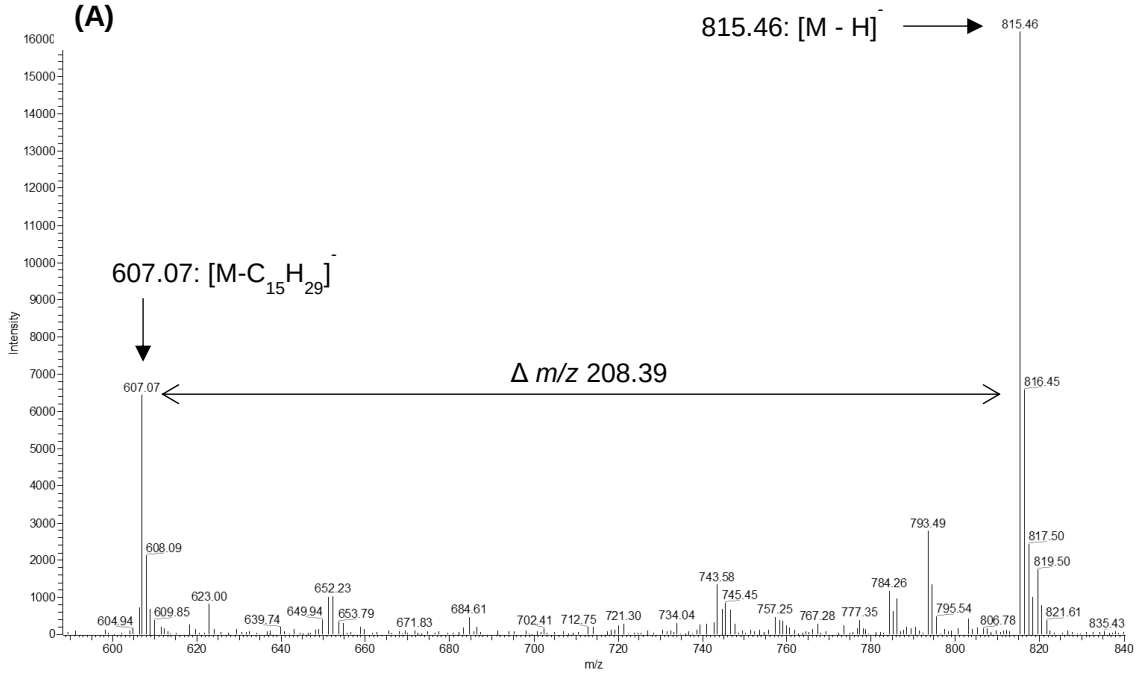

*Figure 18 – Mass data enable confirmation of the structure of compound **(1)**. (A) Low resolution ESI-MS spectrum, in the negative-ion mode, of compound **(1)** at 13.70 min. The signal at m/z 815.46 corresponds to the pseudomolecular ion [M - H]$^-$, and the observed peak at m/z 607.07 [M - $C_{15}H_{29}$]$^-$ corresponds to the porphyrin system. (B) Structure of compound **(1)** with indication of the location of fragmentation described above and corresponding to the ion at m/z 607.07 [M - $C_{15}H_{29}$]$^-$.*

(B)

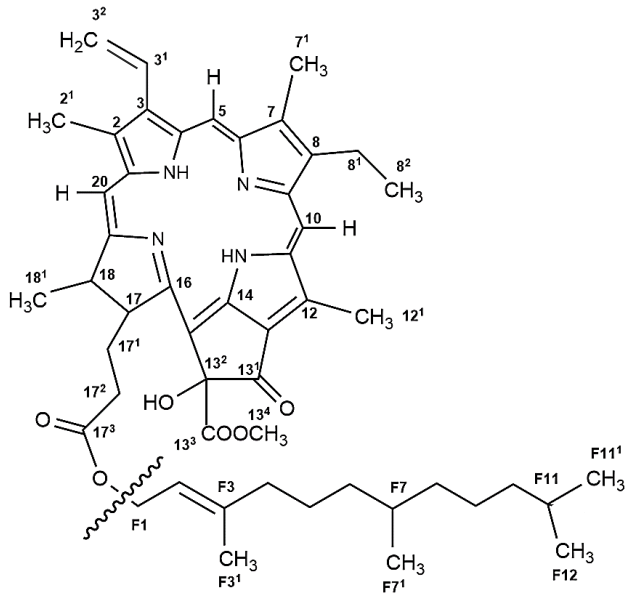

Figure 18 – (Continued)

To confirm the structure of the compound, 1D and 2D NMR analyses, including ^{1}H and ^{13}C NMR, COSY, TOCSY, HSQC, HMBC, and ROESY experiments were carried out.

The ^{1}H NMR spectrum showed all resonances of the compound **(1)** backbone: four aromatic methyl groups (δ 1.59, 3.28, 3.44, 3.9 ppm), one aromatic ethyl group (δ 1.72, 3.64, 3.77 ppm), three olefinic singlets (δ 8.71, 9.56, 9.77 ppm), a methoxyl group (δ 3.76 ppm) and a vinyl substitution (δ 6.19, 6.35, 8.03 ppm) with a characteristic exomethylene coupling pattern (*J* 18.7 and 11.4 Hz) (Table 4). The attached farnesyl moiety was recognized by a large number of overlapping proton signals of aliphatic methylene and methyl functions. Indicative proton resonances for the farnesyl moiety were the carbinol resonances (δ 4.44, 4.5 ppm at F1), the olefinic proton (δ 5.14 ppm at F2), the first methyl group (δ 1.61 ppm at $F3^{1}$) and the final methyl groups of the tail (δ 0.85 ppm at $F11^{1}$ and F12) (Figure 19).

No carbon was assigned by ^{13}C NMR spectrum directly since only in the downfield, between chemical shifts of 0 to 40 ppm, signals were detected with enough intensity. This is predominantly the aliphatic region of the farnesyl moiety with partially overlapping set of signals hindering their assignment. An attempt for determining the nature of all carbons (CH, CH_2, CH_3, quaternary C) was done by a standard DEPT-135 experiment, however the same problem occurred. Despite this, the integration of all data obtained for all experiments (HMBC, COSY and TOCSY) allowed to determine the nature of almost all carbons (including the ones of the aliphatic region), except for the carbon at position 13^{1}.

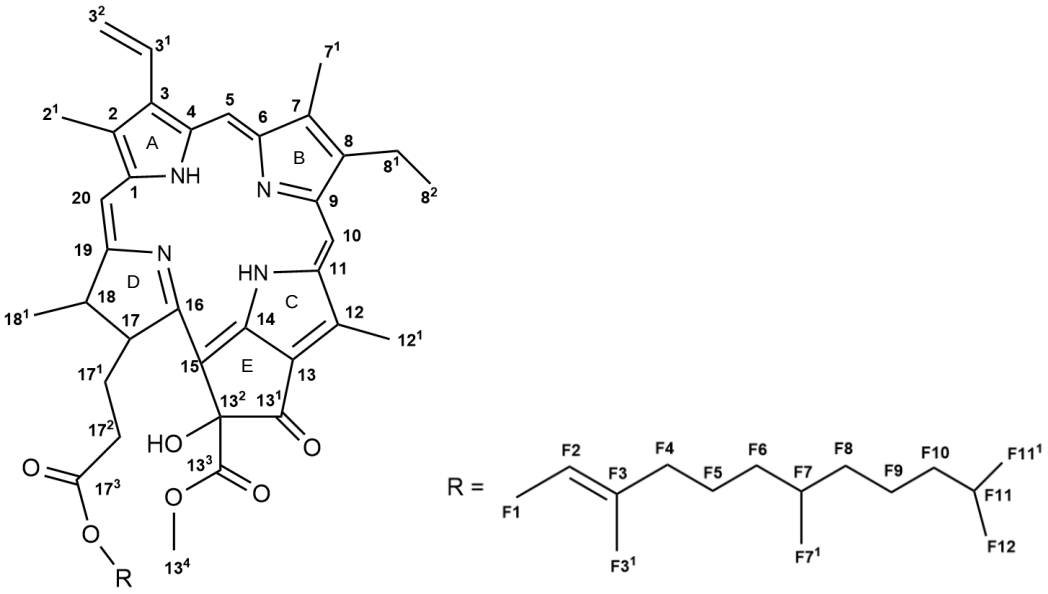

*Figure 19 - Structure proposed for compound **(1)**.*

Using HSQC experiments, thirty four carbons signals were detected in the spectrum, by one bond ^{1}H-C correlation with the already known proton signals allowing the assignment of the carbon chemical shifts. These signals were detected for the porphyrin system along with the fifth ring system. The aliphatic region of compound **(1)**, had partly overlapping set of signals in this region (Appendix III, Figure III.3).

Direct ^{13}C NMR detection of imine carbons of the porphyrin system, as mentioned above, was hampered by the low signal intensities. Yet, the shifts of these could be confirmed from the HMBC experiment that showed long range CH correlations to imine carbons (Figure 20).

The HMBC experiment allowed all two and three bond ($^{2,3}J$) C-^{1}H correlations to be deduced, confirming the proposed structure of compound **(1)** that is presented in Figure 19, Table 4 and 5. For the porphyrin moiety the detected $^{2,3}J$ CH long range correlations of the olefinic proton H-5 to C-4 (ring A) , H-10 to C-8 (ring B), C-11 and C-12 (ring C), and H-20 with C-18 (ring D), C-1 and C-2 (ring A) allowed the connections between the four pyrrole rings (Figure 20).

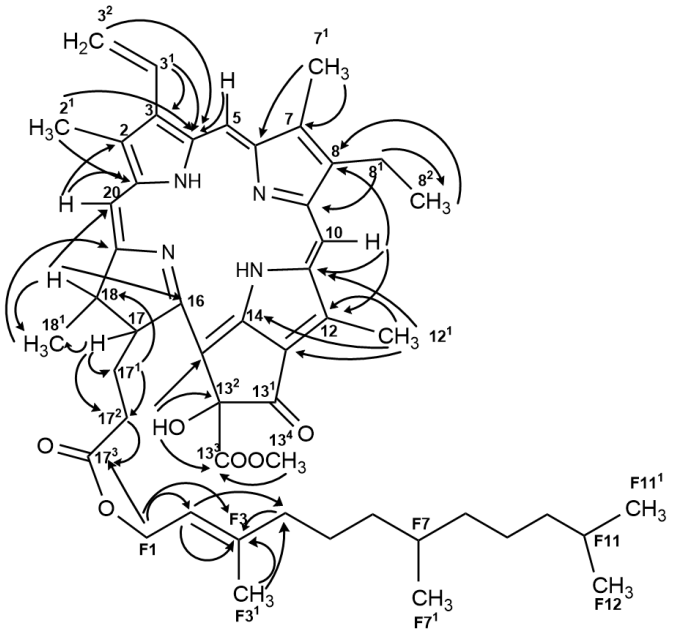

*Figure 20 - Relevant long range C-^{1}H correlation signals observed in the HMBC experiment of compound **(1)**.*

The constitution of ring A was deduced from long range signals as showed by Figure 20 and described in Table 4. Interestingly, two ^{4}J C-^{1}H correlations were deduced: from the methylene protons of vinyl group at 3^{2} position (δ 6.19/6.35 ppm) to C-4, and the other from the protons of methyl group at 2^{1} position (δ 3.44 ppm) to also C-4. The confirmation of the vinyl substitution was also confirmed by ^{1}H-^{1}H COSY correlation as illustrated in Figure 21. Another substitution confirmed by $^{2,3}J$ C-^{1}H long range correlation was the ethyl group at ring B (Figure 20 and Table 4). Similarly, substitution of ring C was deduced by another ^{4}J C-^{1}H correlation from protons of methyl group at 12^{1} position (δ 3.9 ppm) to C-14. Additionally, the constitution of ring D was also determined by these long range signals ($^{2,3}J$ C-^{1}H correlation).

The constitution of ring E include a carboxyl group and four quaternary carbons by analogy with hydroxy pheophytin-a. As previously mentioned, was not possible to confirm the existence of the carboxyl group at C-13^{1}, however the attribution of the hydroxy group and methyl-ester to ring system E was achieved. The position of the methyl-ester in this ring was deduced by the long ^{3}J C-^{1}H correlation of the singlet protons of methyl group O$C\underline{H_3}$-13^{4} (δ 3.76 ppm) to carboxyl group C-13^{3}. Hydroxylation of this ring was deduced by the significant low field shifts of carbons 13^{2} and 15 (δ 100.4 and 102 ppm, respectively) indicating that both carbons must be influenced by the presence of oxygen. Moreover, a proton at δ 6.11 ppm without an HSQC correlation suggested it to be the proton of the hydroxy group. Additionally, the hydroxylation was confirmed by three important $^{2,3}J$ C-^{1}H long range correlations between O$\underline{H}$-13^{2} position to C-13^{2}, C-13^{3} and C-15.

*Table 4 - ^{1}H (600 MHz), ^{13}C (600 MHz), DEPT, ^{1}H-^{1}H COSY, ROESY and $^{2,3}J$ C-^{1}H long range correlations (HMBC) for the porphyrin system of compound **(1)** (δ, ppm; J, Hz) in $CDCl_3$ and DMSO-d6 (*).*

Position	δ^{1}H (*J in Hz*)	COSY	ROESY (*)	δ ^{13}C	DEPT	HMBC
1				**141.3**	C	
2				**131.5**	C	
2^{1}	3.44 s		CH_2-3^{2}, H-20	**11.5**	CH_3	C-1, C-4
3				**133.4**	C	
3^{1}	8.03 dd (11.5, 17.8)	CH_2-3^{2}	H-5	**128.3**	CH	C-3, C-4
3^{2}	6.35 d (18.7) 6.19 d (11.4)	H-3^{1}	CH_3-2^{1}, CH_2-3^{2}, H-5	**122.1**	CH_2	C-4
4				**135.9**	C	
5	9.56 s		H-3^{1}, CH_2-3^{2}	**99.1**	CH	C-4
6				**155.7**	C	
7				**136.6**	C	
7^{1}	3.28 s		CH_2-8^{2}	**10.8**	CH_3	C-6, C-7
8				**145.6**	C	
8^{1}	3.77 m 3.64 m			**19**	CH_2	C-8^{2}, C-9
8^{2}	1.72 t (7.7)		CH_3-7^{1}	**17**	CH_3	C-8, C8^{1}
9				**149.9**	C	
10	9.77 s		CH_3-12^{1}	**103.4**	CH	C-8, C-11, C-12
11				**138.8**	C	
12				**131.5**	C	
12^{1}	3.90 s		H-10	**11.9**	CH_3	C-11, C-12,C-13, C-14
13				**133.2**	C	
13^{1}				**[a]**	C	
13^{2}-OH	6.11 s			**110.4/102 [a]**	C	C-13^{2}, C-13^{3}, C-15
13^{3}				**170.8**	C	
13^{4}-OCH$_3$	3.76 s			**53.4**	CH_3	C-13^{3}
14				**140.2**	C	
15				**102/100.4 [a]**	C	
16				**166.3**	C	
17	4.07 dd (7.4)	CH_2-17^{1}	CH_2-17^{2}	**53.1**	CH	C-17^{1}, C-17^{2}, C-18^{1}
17^{1}	2.56 dd (7.7) 1.83 dd (9.1)	H-17, CH_2-17^{1}, CH_2-17^{2}		**30.7**	CH_2	C-17, C-17^{2}, C-18
17^{2}	2.46 m 2.17 m	CH_2-17^{1}, CH_2-17^{2}	H-17, CH_3-18^{1}	**31.7**	CH_2	C-17, C-17^{1}, C-17^{3}
17^{3}				**173.4**	C	
18	4.46 m (7.8)			**49.7**	CH	C-17^{1}, C-18^{1}, C-16, C-20
18^{1}	1.59 m		CH_2-17^{2}, H-20	**21.7**	CH_3	C-17, C-18, C-19
19				**171**	C	
20	8.71 s		CH_3-2^{1}, CH_3-18^{1}	**93.3**	CH	C-1, C-2, C-18

[a] – Indicate that was not possible to attribute the chemical shift by 1D and 2D NMR experiments, however its assignment was consistent with mass data

The attachment of the farnesyl moiety to the porphyrin system was indicated by the ^{3}J C-^{1}H correlation of the methylene group H_2-F1 (δ 4.44/4.5 ppm) to the carboxyl group C-17^{3}. Likewise, $^{2,3}J$ C-^{1}H correlations were established for the positions H_2-F1 to C-F2 and

C-F3, H-F2 (δ 5.14 ppm) to C-F3 and C-F4, and H_3-F3[1] (δ 1.61 ppm) to C-F3 and C-F4 of the aliphatic region. Thereafter, to confirm and complete the assignments of positions F1 to F12 in aliphatic region a TOCSY and ^{1}H-^{1}H COSY experiments were performed (Figure 21). In the TOCSY experiment ^{1}H-^{1}H TOCSY correlations confirmed the assignments of the methylene group at F1 position (δ 4.44/4.5 ppm), the olefinic proton at F2 position (δ 5.14 ppm) and the methyl group at F3[1] position (δ 1.61 ppm). Additionally, allowed the deduction of correlations of the methylene group at F6 position (δ 1.01 ppm) to the methyl group at F7[1] position (δ 0.8 ppm), the olefinic proton at F7 position (δ 1.33 ppm) to the methylene group at F8 position (δ 2.35 ppm), and of this last group to another methylene group at F9 position (δ 1.65 ppm). Furthermore, was possible to deduce the assignments of the final olefinic proton and methyl groups of the tail, and the attachment of this group to the rest of the chain by a long ^{1}H-^{1}H TOCSY correlations with the methylene groups at F9 and F10 positions (δ 1.65 ppm and 1.11 ppm, respectively). In addition ^{1}H-^{1}H COSY correlations indicated the positions of the methylene groups at F4 and F5 positions (δ 1.89 ppm and 1.29 ppm, respectively) and combining with ^{1}H-^{1}H TOCSY correlations confirmed the double bond between C-F2 and C-F3.

The chemical shift of the carbon at F5 position of the aliphatic region was not possible to be completely deduced, due very low signal intensity, and so this carbon is referred being at δ 22-24 ppm chemical shift (Figures 20 and 21, Table 5).

*Table 5 - ^{1}H (600 MHz), ^{13}C (600 MHz), DEPT, ^{1}H-^{1}H COSY, ^{1}H-^{1}H TOCSY and $^{2,3}J$ C-^{1}H long range correlations (HMBC) for the farnesyl moiety of compound **(1)** (δ, ppm; J, Hz) in $CDCl_3$.*

Pos.	δ^{1}H (*J*)	COSY	TOCSY	δ ^{13}C	DEPT	HMBC
F1	4.5 m 4.44 m (6.8)	H-F2	H-F2, CH_3-F3[1]	**60.8**	CH_2	C-17[3], C-F2, C-F3
F2	5.14 t (6.5)	CH_2-F1	CH_2-F1	**117.1**	CH	C-F1, C-F3, C-F4
F3						
F3[1]	1.61 s		CH_2-F1	**15.8**	CH_3	C-F3, C-F4
F4	1.89 m (7.7)	CH_2-F5		**39.9**	CH_2	C-F2, C-F3, C-F3[1]
F5	1.29 m (7.4)	CH_2-F4, CH_2-F6		**22-24**	CH_2	
F6	1.01 m	CH_2-F5, H-F7	CH_3-F7[1]	**36.6**	CH_2	
F7	1.33 m	CH_3-F7[1], CH_2-F6	CH_2-F8	**32.1**	CH	
F7[1]	0.8 m	H-F7	CH_2-F6	**19.2**	CH_3	
F8	2.35 t (7.5)	CH_2-F9	H-F7, CH_2-F9	**32.6**	CH_2	
F9	1.65 m (7.3)	CH_2-F8	CH_2-F8, CH_3-F11[1], CH_3-F12	**24.3**	CH_2	
F10	1.11 m	H-11, CH_3-F11[1], CH_3-F12	CH_3-F11[1], CH_3-F12	**38.9**	CH_2	
F11	1.51 m	CH_2-F10, CH_3-F11[1], CH_3-F12	CH_3-F11[1], CH_3-F12	**27.4**	CH	
F11[1]	0.85 m (6.6)	CH_2-F10, H-F11	CH_2-F9, CH_2-F10, H-F11	**22.1**	CH_3	
F12	0.85 m (6.6)	CH_2-F10, H-F11	CH_2-F9, CH_2-F10, H-F11	**22.1**	CH_3	

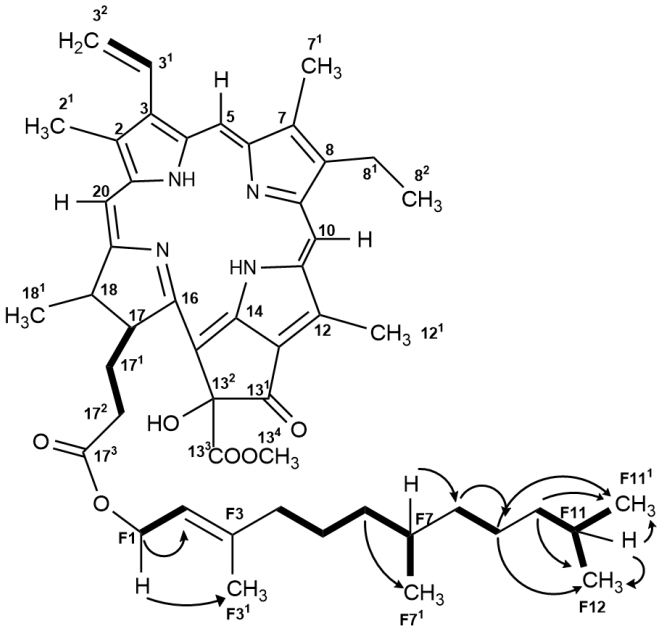

*Figure 21 - Relevant one bond ^{1}H-^{1}H correlation signals detected in the COSY (highlighted in bold) and long range correlations signals detected in the TOCSY (highlighted in arrows) experiments of compound **(1)**.*

Summing up, overall ^{1}H NMR and carbon assignments data for the porphyrin of compound **(1)**, were in accordance with the literature data (Jerz *et al*., 2007; Lee *et al*., 2008; Li *et al*., 2012; Matsuo et al., 1996; Mizoguchi et al., 2005). The predominant difference in both ^{1}H NMR and carbon shifts, as compared with that of literature for hydroxy pheophytin-a was the increase in 0.58-0.68 ppm of the chemical shift of the proton and carbon of hydroxy group at position 13^2, probably caused by some substituent or conformational change nearby.

The relative configuration of compound **(1)** was achieved through ROESY experiments (Figure 22).

In order to establish the configuration of quaternary carbon at C-13^2 position the signals of the Overhauser enhancements in the ROESY spectra of compound **(1)** were analyzed. There was no detection of any signals from the hydroxyl and methyl-ester groups of C-13^2. Consequently, the 13^2S stereochemistry configuration was achieved by comparison with literature data. The proton signal of hydroxy group at δ 6.11 ppm (13^2 position) suggested this configuration in good agreement with reference data (δ 6.04 to 6.18 ppm in acetone-d6: Hyvärinen *et al*., 1995; Hyvärinen *et al*., 1998). Additionally, the value pinpointed in literature for the proton of the hydroxyl group in alpha position is δ 6.01 ppm in acetone-d6 (Hyvärinen *et al*., 1995).

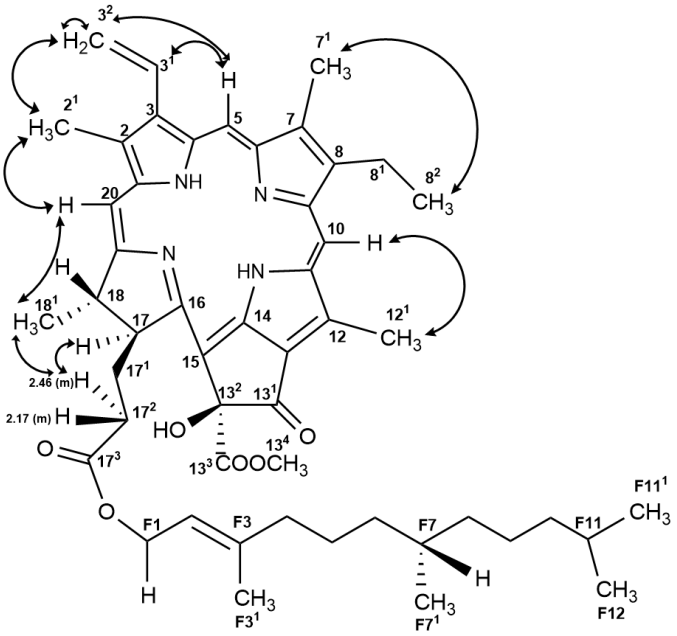

*Figure 22 - Relevant ROESY correlation signals observed in structure of compound **(1)** showing proton-proton through space interactions in the porphyrin ring system, suggesting the (13^2 S)-configuration.*

However, to establish the configuration of carbon at C-17 position, signals were observed between the methylene of H_2-17^2 at δ 2.46 ppm and H-17 at δ 4.07 ppm, and also between H_2-17^2 and the methyl group of H_3-18^1 at δ 1.59 ppm. These correlations suggest that the protons are on the same side of the molecule plane. A comparison with data from the literature indicates that the protons H-17, H_2-17^2 and H_3-18^1 have alfa (α) orientation (Figure 22, Table 4).

3.2.1.2. Bioactivity assessment of compound (1)

As far we aware, compound **(1)** is a new reported secondary metabolite from cyanobacteria, and more precisely from *Nodosilinea* sp. strain. Confirmation of bioactivity was assessed through a zebrafish Nile Red fat metabolism assay using several concentrations in order to obtain a dose-response curve and consequently an IC_{50} value.

Compound **(1)** was able to reduce the fluorescence intensity, mainly at concentration 20 $\mu g.ml^{-1}$ (Figure 23). Comparing this result with the previous obtained by sub-fractions E17161 E4 and E4C there is some reduction of the level of bioactivity at 10 $\mu g.ml^{-1}$, since the last mentioned sub-fractions had significant different activity from control group DMSO. Nevertheless, this isolated compound **(1)** at concentration 10 $\mu g.ml^{-1}$ reduced the amount of neutral lipids in yolk sac by 27.69 ± 14.35%, while the highest concentration tested in the bioassay reduced 51.67 ± 15.59% with significant difference compared with the control

(Figure 24). Therefore, the existence of lipid-reducing properties of the compound isolated was confirmed and could be used in therapies to attenuate obesity settings.

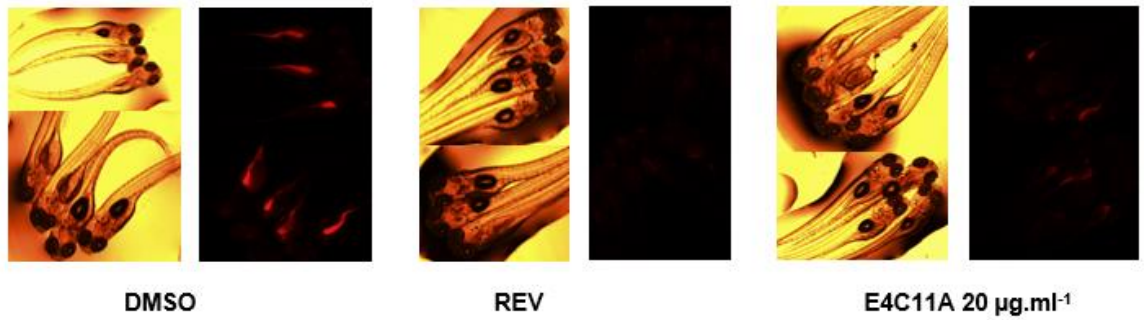

Figure 23 - Representative images of the zebrafish Nile Red fat metabolism assay of compound (1). In left are represent the phase contrast image of zebrafish larvae and the right images show the fluorescence with red contrast in treatment with significant bioactivity. DMSO, solvent control 0.1%; REV, positive control 50 µM.

Furthermore, dose-response curve revealed an IC_{50} value of 15.23 µg.ml^{-1} corresponding to 18.64 µM (Figure 24). High interindividual variance was present in the assay, and results should be repeated to confirm the obtained potency of the compound.

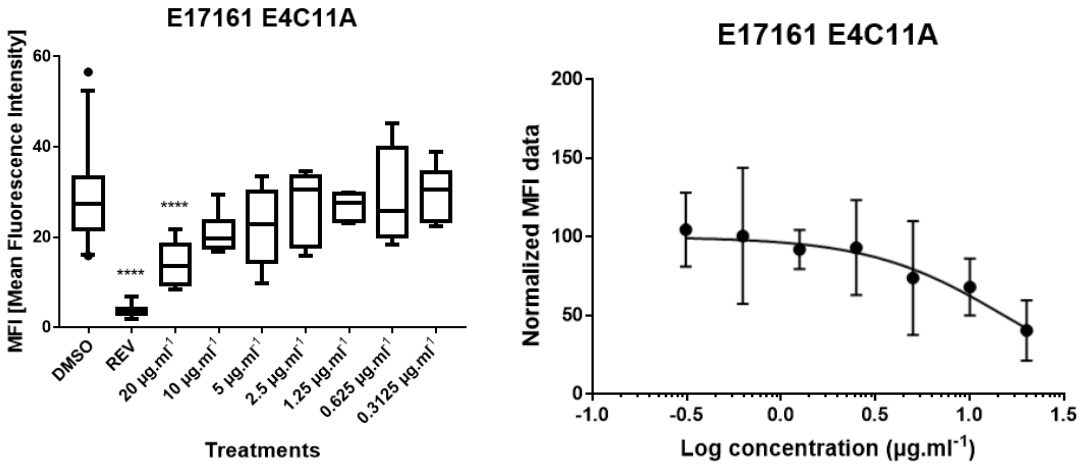

*Figure 24 - Lipid-reducing activity in the zebrafish Nile Red fat metabolism assay for sub-fraction E17161 E4C11A. Solvent control had 0.1% DMSO and positive control received 50 µM REV. On the right is the statistical analysis wherein values are expressed as mean fluorescence intensity (MFI) relative to the DMSO group, and each treatment group had 6 to 8 replicates. The data are represented as box-whisker plots. Statistical differences were analysed by One-way ANOVA with Dunnett posthoc test and are indicated to the solvent control with the symbol * $p < 0.05$; ** $p < 0.01$; *** $p < 0.001$; **** $p < 0.0001$. On the left is the dose-response curve wherein values are expressed as normalized MFI and log-transformed concentrations using nonlinear regression.*

Chlorophyll is one of the most abundant biological molecules on earth and is essential for photosynthesis so is found ubiquitous and mainly in photoautotrophic organisms, as cyanobacteria. There is a vast variety of chlorophylls structures, and as result the nomenclature was somewhat untidy (Aronoff, 1966; Scheer, 1991).

Chlorophylls are porphyrins which comprises all closed and completely conjugated rings, also referred as tetrapyrroles. The natural structure of chlorophyll-a, the most widely distributed chlorophyll in nature, include features as a chelated magnesium atom in the centre of tetrapyrrole macrocycle, a characteristic isocyclic fifth ring (ring E) conjoined with ring C, a vinyl group at carbon-3, a ketone at carbon-13[1], a carbomethoxy group at carbon-13[2] and a propionic acid moiety at carbon-17 esterified with phytol (Aronoff, 1966; Scheer, 1991; Tanaka and Tanaka, 2007; Vavilin and Vermaas, 2002). As mentioned above, natural modifications of the main structure of the pigment chlorophyll-a may occur, originating for instance, pheophytin-a, if not contain magnesium, and pheophorbide-a, if additionally not incorporate phytol. Nowadays, the universally applied numbering system for these structures, as for all organic compounds, is IUPAC nomenclature, depicted in the Figure 25.

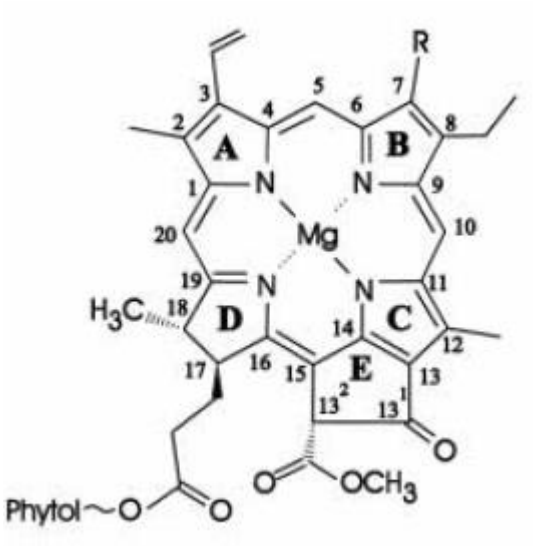

Figure 25 - Currently accepted IUPAC system for numbering carbon atoms of chlorophylls (Vavilin and Vermaas, 2002). Chlorophyll-a has a methyl group in position C-7, and chlorophyll-b has a formyl group in C-7.

The study of the biosynthetic pathway of tetrapyrroles was changeling for many years, hindered by the lack of knowledge or misconception of certain sequence of steps. Biosynthesis of chlorophyll is complex and biochemical heterogeneous characterized by a multibranched biosynthetic pathway resulting in various biosynthetic intermediates and end products. The first elucidations and considerable breakthroughs of this biochemical pathway were reviewed by Ellsworth in 1968 and in the book “The Chlorophylls”, and our knowledge has been greatly enhanced since these pioneering studies.

Tetrapyrrole pathway (Figure 26) produces chlorophyllide (chlorin moiety) including magnesium incorporation while methylerythritol phosphate (MEP) metabolic pathway (Figure 27) accomplish phytol chain incorporation (Kim *et al*., 2013; Masuda and Fujita, 2008; Moulin and Smith, 2005; Tanaka and Tanaka, 2007). Within tetrapyrrole pathway

there are common steps for chlorophylls, hemes and other tetrapyrroles in which there are share of a set of specific enzymes.

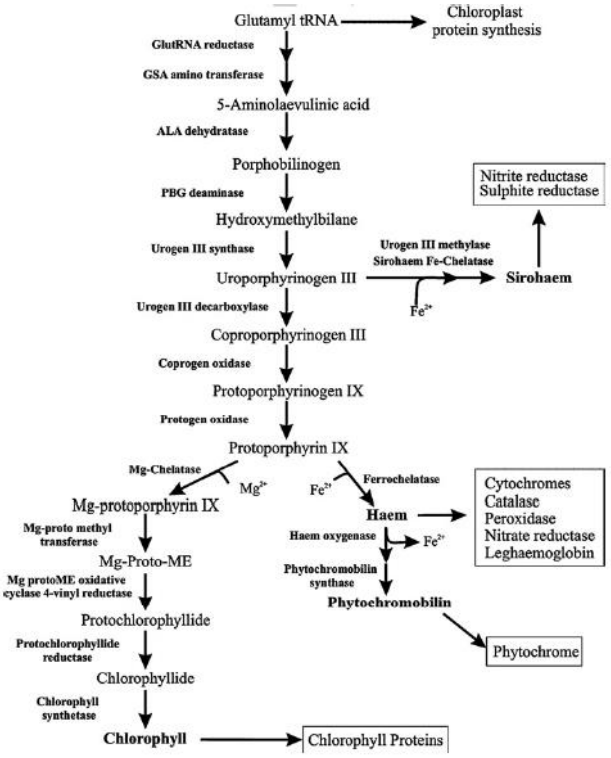

Figure 26 - Abbreviated scheme of the tetrapyrrole biosynthetic pathway in plants, including the end-products heme, chlorophyll, siroheme and phytochromobilin (Moulin and Smith, 2005).

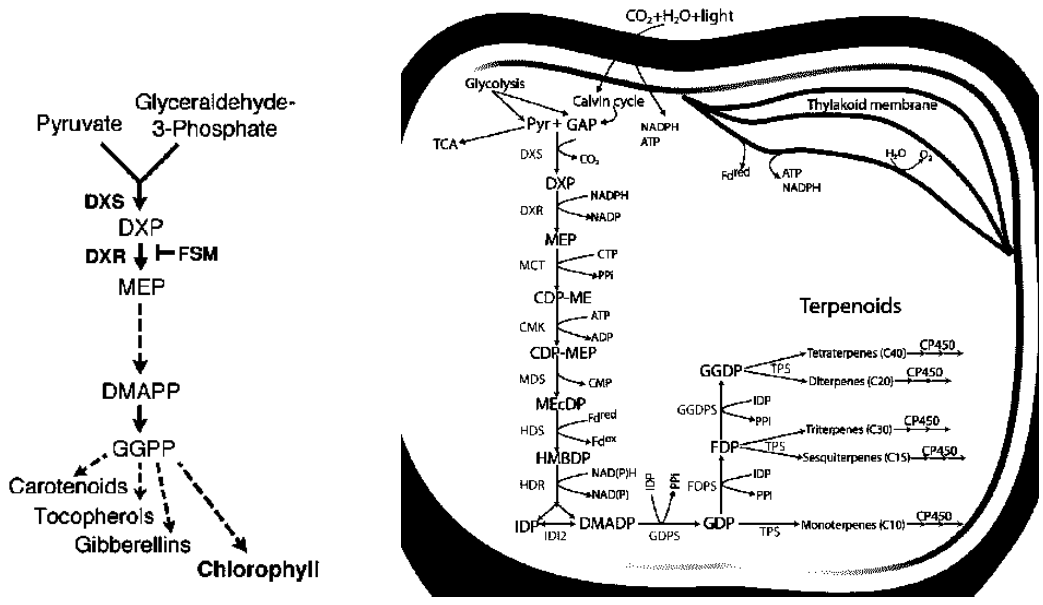

Figure 27 - Scheme of the MEP metabolic pathway. On the left is the abbreviated MEP pathway with the relevant steps of phytol chain incorporation into chlorophyll in plants (dotted lines indicate several biochemical pathways). On the right is the proposed terpenoid biosynthesis via MEP pathway in cyanobacteria (Kim et al., 2013; Pattanaik and Lindberg, 2015).

Numerous alterations occur naturally for chlorophyll-a. Basic structural modifications may include the formation of metal-free pheophorbides and pheophytins, as well as metallo-chlorophyll derivatives. Several research studies and reviews indicate that the natural pigments, chlorophyll and their derivatives such as pheophytin-a and pheophorbide-a, mentioned above, have the potential to exhibit therapeutic properties with human health benefit. These biological properties include (1) antioxidant properties which are associated with (2) anti-inflammatory activity, (3) anti-mutagenic activity related with (4) cancer preventive effects, (5) antiviral activity, more precisely against hepatitis C virus and HIV (human immunodeficiency virus), (6) antimicrobial activity and (7) neuroprotection properties also associated with their anti-oxidant and anti-inflammatory activities (Barbosa *et al*., 2014; Ferruzzi *et al*., 2002; Gomes *et al*., 2015; Kang *et al*., 2018; Pangestuti and Kim, 2011; Subramoniam *et al*., 2012; Wang *et al*., 2009; Zhao *et al.*, 2014).

The intact nature of porphyrin system has been suggested to be important to their capacity to display some bioactivities, such anti-oxidant and anti-cancer activities. Anti-oxidant capacity can be explained by the π-cation radical in the porphyrin structure and the existence of a chelated metal ion (Ferruzzi *et al*., 2002; Kang *et al*., 2018). In contrast, to reduce mutagen bioavailability and consequently mutagenicity and carcinogenicity the porphyrin system, with or without metal atom, is an essential component (Ferruzzi *et al*., 2002). Furthermore, the porphyrin system was also suggested to be important to anti-inflammatory and anti-viral activities, since pheophorbide-a display this bioactivity, excluding the aliphatic chain as an important structure (Subramoniam *et al*., 2012). Therefore, because of the similarity between chlorophyll-a and its derivatives, as pheophytin-a and pheophorbide-a, and compound **(1)** it would be interesting to assess the possibility of this isolated compound to display these bioactivities in future studies, besides the reducing-lipid activity demonstrated in this study. However, in these future works some cautions would be necessary in the bioactive capacities of this compound because of some relevant structural differences, as the location of the hydroxy functional group of the molecule in 13^2 position.

Bioactivities capable of attenuate diabetes complications were also linked to intact nature of porphyrin system of pheophytin-a and pheophorbide-a isolated from *L. japonica*. These compounds demonstrated capacity towards inhibition of formation of AGE (advanced glycation end-products) (IC_{50} 228.71 µM and 49.43 µM, respectively) and of aldose reductase activity (IC_{50} superior to 100 µM and 12.31 µM, respectively), in which pheophorbide-a had inhibitory activities relatively stronger compared with pheophytin-a (Sharifuddin *et al*., 2015). So, in the future work, is also necessary to confirm other bioactivities capable of attenuate obesity related co-morbidities, even if due to the greater resemblance to pheophytin-a, compound **(1)** may not displayed a stronger activity.

Additionally, three metabolites, sargahydroquinoic acid, sargachromenol and sargaquinoic acid, isolated from brown algae *Sargassum serratifolium*, were capable of inhibit TG (triglycerides) accumulation in 3T3-L1 adipocytes, and consequently may been able to inhibit adipogenesis. The IC_{50} values estimated were 3.2 ± 0.21, 2.4 ± 0.20, and 2.0 ± 0.14 μM, respectively (Kwon *et al*., 2018). Thus, these metabolites displayed a stronger activity in reducing the amount of fat storage compared with compound **(1)**, however, they were tested through an *in vitro* bioassay which does not count the diversity of the physiological processes that influence this activity in a whole organism and the interspecific variations between different organisms. Furthermore, recently was studied the capacity of several polyphenol derivatives to lipid-reducing activity without any cytotoxic effects in pre-adipocytes or toxic effects in zebrafish larvae. For 18 compounds were determined the IC_{50} values, that ranged between 0.07 and 1.67 μM in zebrafish organism model (Urbatzka *et al*., 2018). The biggest similarities between these compounds is the existence of many aromatic rings connected, in which one of them possess a ketone group and other possess a methoxy or hydroxy group. Comparing to IC_{50} value of compound **(1)** these natural phenolic compounds have a stronger bioactivity beneficial towards reducing obesity. Nevertheless, many studies of chlorophyll derivatives support a potential role for these natural compounds in many human health and disease prevention, besides obesity and related co-morbidities.

Besides, further studies of other possible bioactivities of this compound is essential to elucidate possible mechanism(s) of action. Currently, research studies identified several possible targets, in which the most common is through transcription factor PPARγ pathway, that could encourage preadipocyte recruitment, avoid local hypoxic state, or inhibit adipocyte differentiation, reducing in this way related co-morbidities associated with lipid deposition in peripheral tissues, insulin resistance, diabetes, fatty liver disease, cardiovascular diseases, among others (Gustafson *et al*., 2013; Henninger *et al*., 2014; Khan *et al*., 2009; Lefterova and Lazar, 2009; Mariman and Wang, 2010; Park *et al*., 2014; Pasarica *et al*., 2009). Obviously, many more targets are involved in these physiological processes, such as growth factor TGFβ (transforming growth factor beta) pathway, GLP-1 (glucagon-like peptide-1) pathway, TRPV1 (transient receptor potential cation channel subfamily V member 1) receptor pathway, among others.

The lower lipid accumulation would lead to weight loss and acute remodelling of adipose tissue which could lower macrophages content and consequently inflammation in adipose tissue (Kosteli *et al*., 2010). A moderate weight loss (85%) achieved through diet is associated with decreased hepatic insulin resistance and hepatic steatosis, but no change occur for glucose uptake (Petersen *et al*., 2005). These effects are a result of a chronic

weight loss and not acute, so compound **(1)** of this study may not be able to achieve these effects.

As demonstrated previously, obesity is a complex multifactorial disease, so different endpoints may be useful in the study of obesity treatments, sometimes even considering a strategy using different endpoints at the same time.

3.2.2. Study of E15074 and E18179 derived from strain *Synechocystis salina* LEGE 06099

Strain *Nodosilinea* sp. LEGE 06001 was extracted twice using different biomass from distinct growth experiments. Since the first fractionation resulted in low weights of the E15074 fractions, a new organic extraction procedure was performed originating E18179.

An initial screening was performed which indicated that the initial fraction E15074 B originated from 1:4 EtOAc/*n*-hexane had bioactivity in comparison with solvent control group with great reduction of fluorescence intensity and reduction of 50.17 ± 6.45 % of the stained neutral lipids in the zebrafish larvae (Figure 28). According with the Figure 29 three fractions had statistically significant different activity from the control, but only fraction B reduced significantly the amount of lipids, while fraction F significantly enhanced in the same proportion. From this information could be predicted that this bioactive compound would be more potent for the study than the previous isolated (E17161 E4C11A), since it seems to possess a slightly higher activity.

Subsequently SiO_2 SPE chromatographic separation lead to sub-fractions E15074 B6, B7 and B8 that reduced fluorescence intensity (Figure 28). Sub-fraction B6 and B8 had statistically significant bioactivity compared with the DMSO group, reducing stained neutral lipids for 42.46 ± 7.91% and 41.06 ± 12.13%, respectively (Figure 29). However, sub-fractions B6, B7 and B8 were joint together for the next sub-fractionation with a total of 4.95 mg, because the ^{1}H NMR indicated a similar chemical nature (Appendix II, Figure II.2.2).

Afterwards, a RP-HPLC was performed for the joined sub-fractions, and the sub-fractions B6-8 A and B correspond to the first and second peak highlighted with rectangles, while sub-fractions C, D and E correspond to remaining content during the run of sample (Figure 30). In the end of separation, all sub-fractions were colourless instead of greenish brown colour of the original fraction. A column cleaning was performed that resulted in sub-fractions F and G with mixtures of 1:0 and 1:19 CH_2Cl_2/MeCN, respectively. However, this non-polar mixture was not enough for the recovery of the compound responsible for the colour.

Following, zebrafish bioassay was performed for the sub-fractions B6-8 A to G, but none of those reduced the neutral lipids in the zebrafish larvae, but instead enhanced the amount of these lipids (Figure 31).

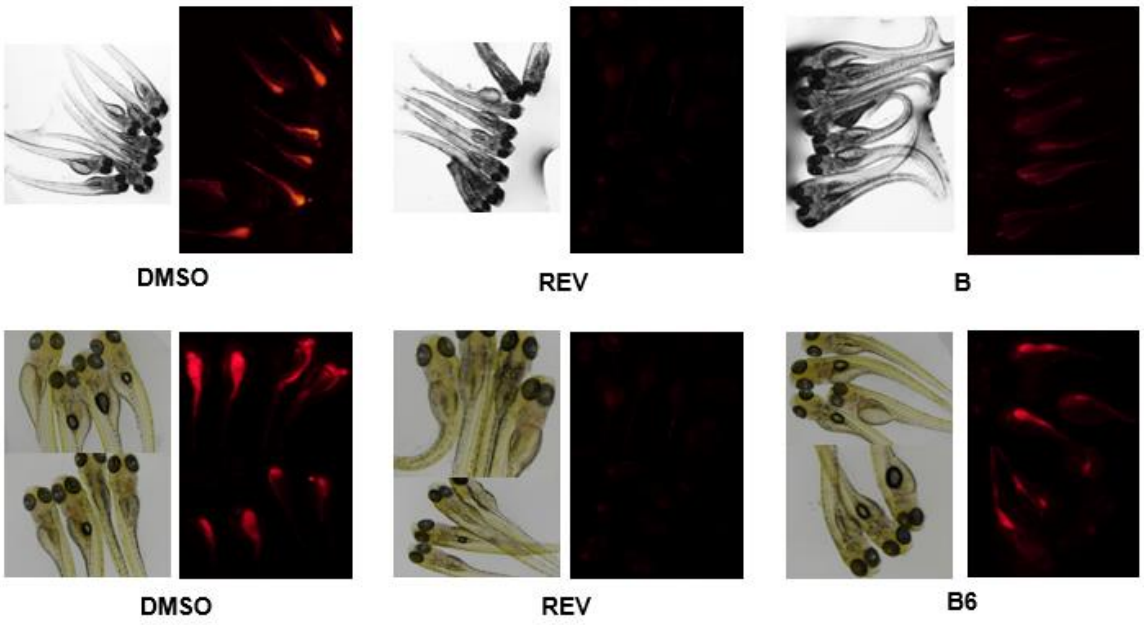

Figure 28 - Representative images of the zebrafish Nile Red fat metabolism assay of fraction E15074 B and sub-fractions B6 to B8. In left are represent the phase contrast image of zebrafish larvae and the right images show the fluorescence with red contrast in fractions with bioactivity. DMSO, solvent control 0.1%; REV, positive control 50 µM.

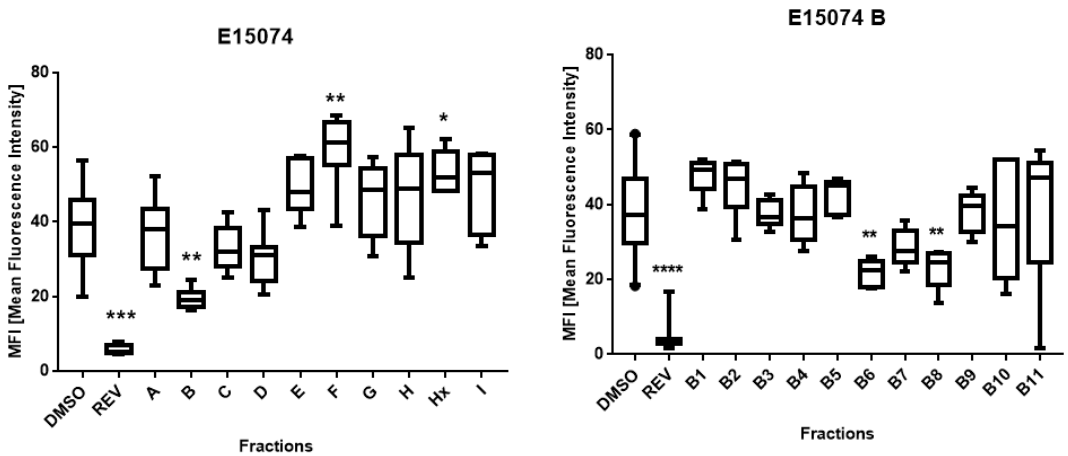

*Figure 29 – Lipid-reducing activity in the zebrafish Nile Red fat metabolism assay for fractions E15074 A to I (left) and sub-fractions B1 to B11 (right). Solvent control had 0.1% DMSO and the positive control received 50 µM REV. Values are expressed as mean fluorescence intensity (MFI) relative to the DMSO group, and each treatment group had 6 to 8 replicates. The data are represented as box-whisker plots. Statistical differences were analysed by Kruskal-Wallis with Dunn´s posthoc test and are indicated to the solvent control with the symbol * $p < 0.05$; ** $p < 0.01$; *** $p < 0.001$; **** $p < 0.0001$.*

These results suggest a potential loss of the compounds responsible for the lipid-reducing activity, which could have been a pigment, since the original sub-fractions B6 to B8 were coloured greenish brown and the resultant sub-fractions (B6-8 A-G) were colourless. This activity loss is also mirrored by the missing peaks between chemical shifts of 9 to 10.5 ppm and 5 to 7 ppm in proton profile NMR spectra in Appendix II (Figure II.2.3).

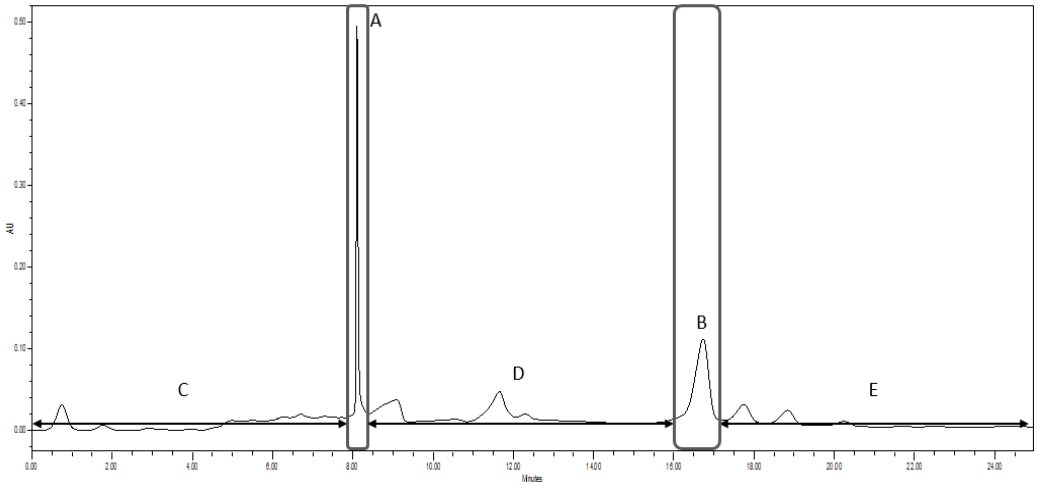

Figure 30 - Reverse phase HPLC chromatogram of joined sub-fractions E15074 B6-8 using a Synergy 4 µm Fusion-RP 80 Å (250 x 10 mm) semi-preparative column. Separation occur under an isocratic mixture of 3:2 MeCN/H_2O with and a flow of 3 ml.min^{-1} for 25 min. The sample was eluted with MeOH and the injection volume was 100 µl. Peak A had a retention time of 8.2 min and peak B of 16.7 min (Detection at 314.6 nm).

The loss of the bioactivity may have occurred due to the degradation of the compound(s) by several reasons or even by the loss of synergetic effects.

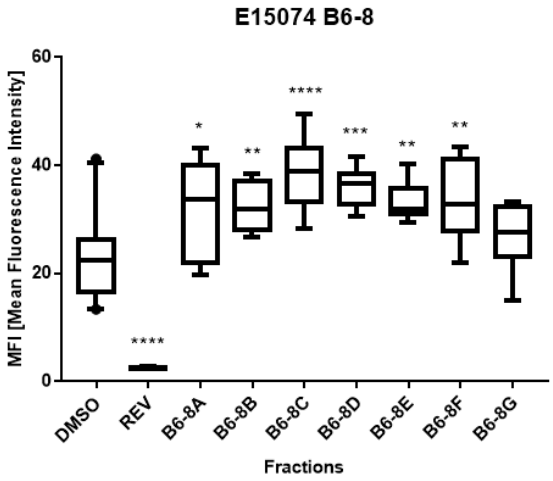

*Figure 31 - Lipid-reducing activity in the zebrafish Nile Red fat metabolism assay for sub-fractions E15074 B6-8A to B6-8G. Solvent control had 0.1% DMSO and the positive control received 50 µM REV. Values are expressed as mean fluorescence intensity (MFI) relative to the DMSO group, and each treatment group had 6 to 8 replicates. The data are represented as box-whisker plots. Statistical differences were analysed by One-way ANOVA with Dunnett posthoc test and are indicated to the solvent control with the symbol * $p < 0.05$; ** $p < 0.01$; *** $p < 0.001$; **** $p < 0.0001$.*

In addition, the second biomass of the strain LEGE 06099 was first organically extracted, and then the resultant crude extract (E18179) was fractionated by VLC. The results of first fractions D and E, originated from a mixture of 2:3 and 3:2 EtOAc/*n*-hexane respectively, showed very similarity with the results of the first fraction E15074 B. In zebrafish bioassay both sub-fractions caused a decreased of the fluorescence intensity, illustrated by Figure 32, which translated in a reduction of the stained neutral lipids in the zebrafish larvae by 48.3 ± 22.67% and 51.16 ± 15.8% for sub-fraction D and E, respectively. These reductions were statically significantly different from the solvent control group, similar to E15074 B, indicating a strong evidence in favour of lipid-reducing activity (Figure 33). Since the chemical nature of both fractions was not very discrepant they were joined for sub-fractionation (Appendix II, Figure II.2.4). Beyond that, considering the proton profile of fraction D and E we could assume that the molecule would had very similarities with chlorophylls (Abraham and Rowan, 1991; Kang *et al*., 2018). Although the process of fractionation was identical on both E15074 and E18179, the compounds with bioactivity may not be the same, which could be later verified by the comparison of both proton profile of the fractions. Slightly different culture conditions in different periods of times, could be the reason of this difference, since the cyanobacteria produce secondary metabolites according with the conditions of the environment in which they are. Even if the compound would be the same, nothing guarantees that it would appear in the same fraction, because many variables influence the fractionation procedure, as initial mass of biomass, volume of the solvents, column size, among others.

Additionally, a lab colleague performed an *in vitro* bioassay with E18179 fractions resultant from VLC fractionation, mentioned above, in order to confirm the existing bioactivity. In this bioassay was assessed lipid content in three dimensions (spheroids) 3T3-L1 cell lines through fluorescence with the use of Nile Red staining. The results confirmed that both fractions E18179 D and E at concentration of 30 $\mu g.ml^{-1}$ significantly reduced the fluorescence signal which mean the reduction of content of lipids and could suggested the inhibition of adipocyte differentiation.

Sub-fractions E18179 D-E3 and 6, resultant from flash chromatography, demonstrated to have a very promising lipid-reducing activity, visible in “naked eye” by the great reduction of fluorescence intensity illustrated in Figure 32, with reduction of 62.57 ± 11.9% and 57.86 ± 4.2% of the stained neutral lipids in the zebrafish larvae by D-E3 and D-E6, respectively. The chemical composition of both sub-fractions became more defined and stayed quite similar to the fractions that gave them rise (Appendix II, Figures II.2.5 and II.2.7). So, applying flash chromatography to fraction D-E was a good choice which allowed a good separation.

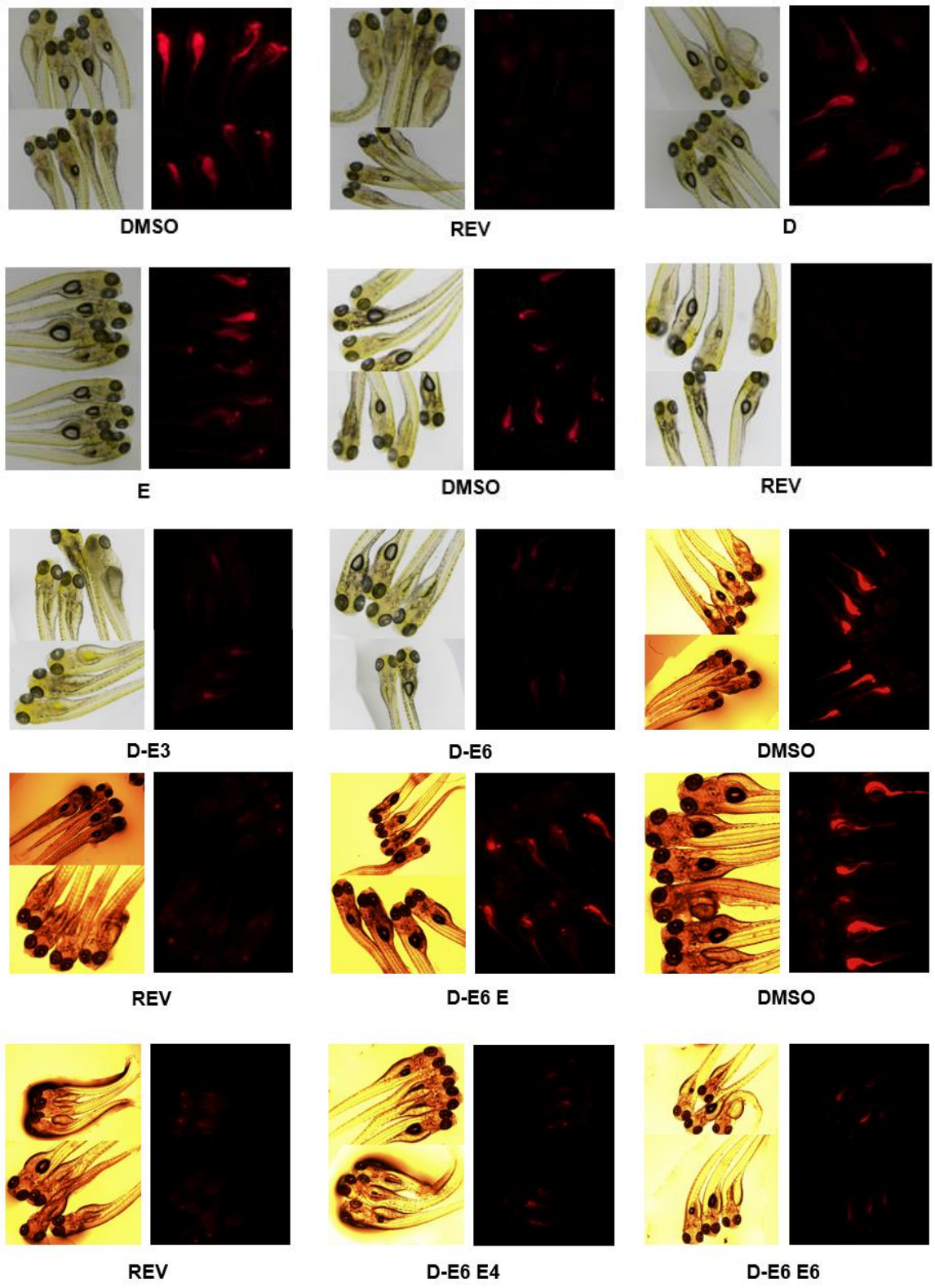

Figure 32 - Representative images of the zebrafish Nile Red fat metabolism assay of fractions E18179 D and E and sub-fractions D-E3, D-E6, D-E6E, D-E6E4 and D-E6E6. In left are represent the phase contrast image of zebrafish larvae and the right images show the fluorescence with red contrast in fractions with bioactivity. DMSO, solvent control 0.1%; REV, positive control 50 µM.

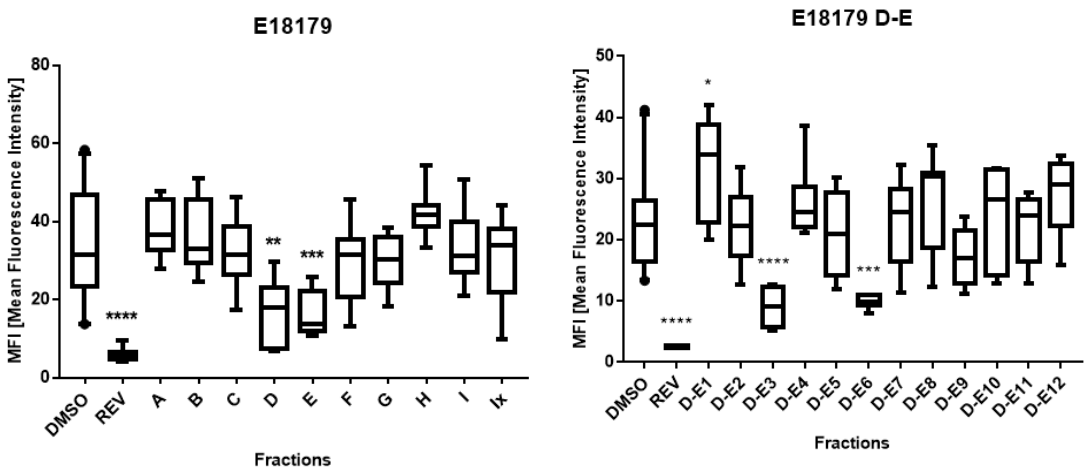

*Figure 33 – Lipid-reducing activity in the zebrafish Nile Red fat metabolism assay for fractions E18179 A to Ix (left) and sub-fractions D-E1 to D-E12 (right). Solvent control had 0.1% DMSO and the positive control received 50 µM REV. Values are expressed as mean fluorescence intensity (MFI) relative to the DMSO group, and each treatment group had 6 to 8 replicates. The data are represented as box-whisker plots. Statistical differences were analysed by One-way ANOVA with Dunnett posthoc test and are indicated to the solvent control with the symbol * p < 0.05; ** p < 0.01; *** p < 0.001; **** p < 0.0001.*

Then, sub-fraction D-E3 was subjected to a normal phase HPLC, in which peaks A, B, C and D highlighted with rectangles correspond to their homologous sub-fractions, and sub-fraction D-E3E correspond to the remaining content during the run of sample (Figure 34).

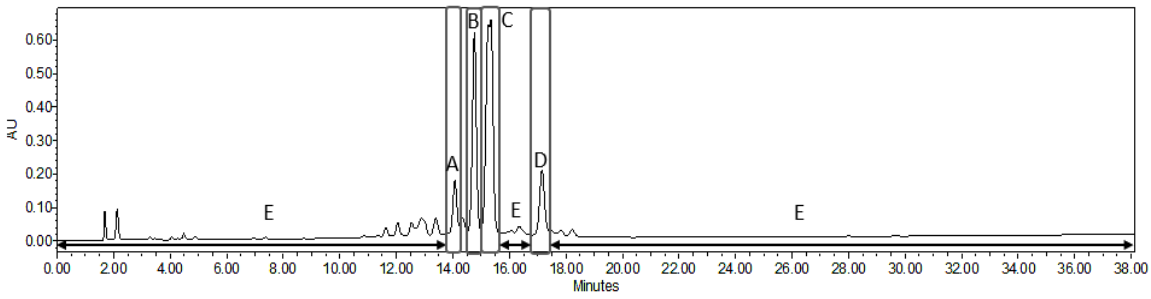

Figure 34 - Normal phase HPLC chromatogram of fraction E18179 D-E3 using Luna 5 µm Silica 100 Å (250 x 4.6 mm) analytical column. Separation result from a gradient of 9:1 to 1:1 n-hexane/EtOAc with a flow of 1 ml.min^{-1} for 35 min. The sample was eluted with n-hexane and the injection volume was 30 µl. Peak A had a retention time of 14.1 min, peak B of 14.8 min, peak C of 15.4 min and peak D of 17.1 min (UV detection at 254 nm).

In similarity with the previous case (E15074 B6-8A to G), sub-fractions originated from HPLC lost their strong lipid-reducing bioactivity (Figure 35). Sub-fraction D-E3C, with a chemical composition very similar to D-E3 (Appendix II, Figures II.2.5 and II.2.6) had a reduction of 29.41 ± 21.94% of stained neutral lipids of zebrafish larvae, while sub-fraction D-E3D exhibited toxicity towards zebrafish larvae at 48 h (Figure 35 A). However, a considerable delay in the development of zebrafish larvae was presented in this assay, and

consequently another bioassay was performed to confirm these results. In the second bioassay (Figure 35 B), none of the sub-fractions caused a reduction of the fluorescence intensity or toxicity, suggesting a potential loss of the compound(s). However, the colour, was recovered during the separation indicating the presence of the pigment and the chemical and structural integrity of the compounds.

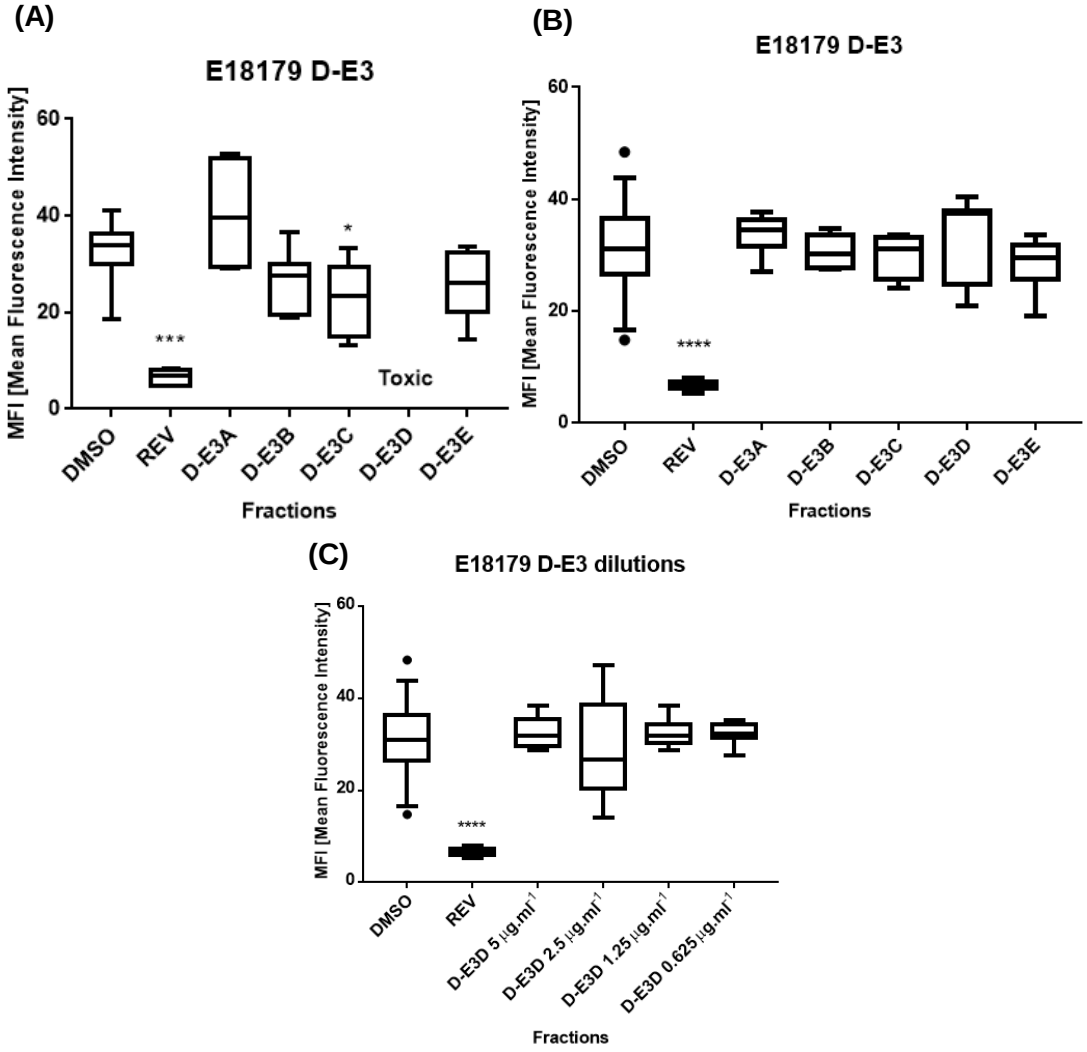

*Figure 35 – Lipid-reducing activity in the zebrafish Nile Red fat metabolism assay for sub-fractions E18179 D-E3A to D-E3E (A and B) and D-E3D 1º dilution to 4º dilution (C). Solvent control had 0.1% DMSO and the positive control received 50 µM REV. Values are expressed as mean fluorescence intensity (MFI) relative to the DMSO group, and each treatment group had 6 to 8 replicates. The data are represented as box-whisker plots. Statistical differences were analysed by Kruskal-Wallis with Dunn´s posthoc test and are indicated to the solvent control with the symbol * p < 0.05; ** p < 0.01; *** p < 0.001; **** p < 0.0001.*

Then, the loss of activity could be due synergetic effects or loss of bioactive compound during the chromatographic separation. A successive dilution (1:2) of the initial test solution of D-E3D was realized to check possible hidden bioactivity, which did not occur (Figure 35 C).

After SiO_2 SPE sub-fractionation of D-E6, according with the results of zebrafish Nile Red metabolism assay, the sub-fraction D-E6E exhibited reduction of the fluorescence intensity by 39.24 ± 20.73% (Figure 32). The following SiO_2 SPE sub-fractionation showed that D-E6E4 and D-E646 had a lipid-reducing activity of 74.61 ± 6.07% and 67.8 ± 9.1%, respectively (Figures 32 and 36). Although, a reduction of the bioactivity of the compound occur in sub-fraction D-E6E, the subsequent sub-fractions displayed an increment of the bioactivity, one of the greatest values obtained in all the study. In addition, ^{1}H NMR spectra throughout the fractionation process, becomes more and more defined. The last sub-fractions (D-E6E4 and D-E6E6) only need a few more chromatographic purification steps to isolate the compounds that both share similarities to chlorophylls (Appendix II, Figures II.2.9 and II.2.10).

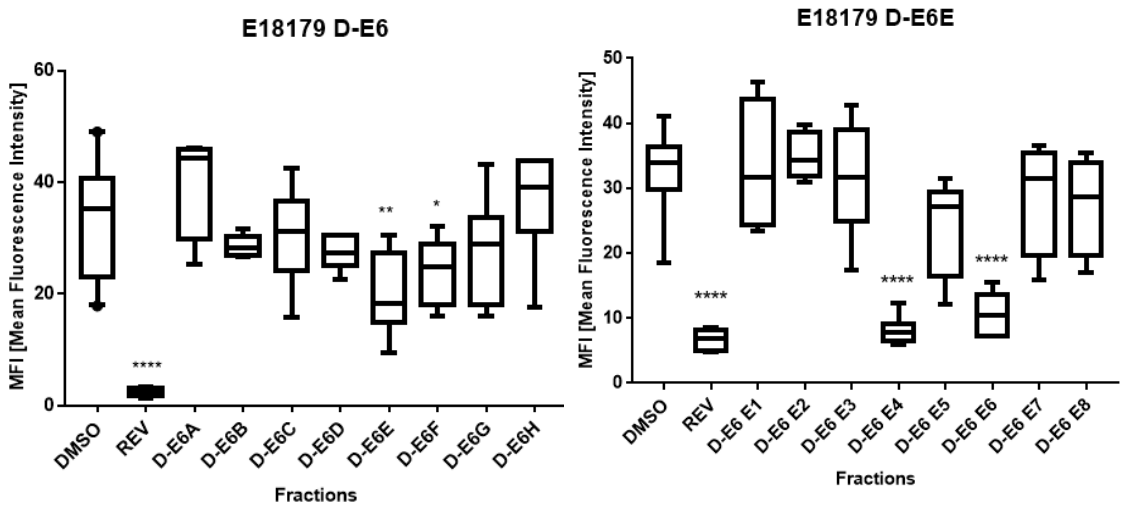

*Figure 36 – Lipid-reducing activity in the zebrafish Nile Red fat metabolism assay for sub-fractions E18179 D-E6A to D-E6H (left) and D-E6E1 to D-E6E8 (right). Solvent control had 0.1% DMSO and the positive control received 50 µM REV. Values are expressed as mean fluorescence intensity (MFI) relative to the DMSO group, and each treatment group had 6 to 8 replicates. The data are represented as box-whisker plots. Statistical differences were analysed by Kruskal-Wallis with Dunn´s posthoc test (left) or by One-way ANOVA with Dunnett posthoc test (right) and are indicated to the solvent control with the symbol * p < 0.05; ** p < 0.01; *** p < 0.001; **** p < 0.0001.*

After isolation and structure elucidation of the compound(s) in sub-fractions E18179 D-E6E4 and D-E6E6 responsible for the lipid-reducing activity, it would also be interesting to assess its potential in other bioactivities, such as anti-oxidant, anti-cancer, anti-inflammatory, anti-viral activities and attenuation of obesity related complications (Ferruzzi *et al*., 2002; Kang *et al*., 2018; Subramoniam *et al*., 2012). These compounds, as mentioned before, have resemblances with chlorophyll derivatives in similarity with compound **(1)**, so some considerations of possible structural differences also will have to be applied.

Possible capacity to inhibit adipocyte differentiation was suggested by results of the *in vitro* bioassay performed by a lab colleague of the initial fractions with bioactivity. In the same direction, the natural compounds yoshinone-a and kalkipyrone have the ability to inhibit adipocyte differentiation with IC_{50} values of 420 nM (0.153 $\mu g.ml^{-1}$) and 67.5 nM in 3T3-L1 cells (Inuzuka *et al*., 2014). Despite the great inhibition, the study revealed that kalkipyrone induced cytotoxic effects at the concentrations tested while yoshinone-a did not at concentration of 50 µM (18.22 $\mu g.ml^{-1}$). Additionally, fucoxanthinol, a degradation product of natural carotenoid fucoxanthin, at lowest concentration tested of 2.5 µM (1.54 $\mu g.ml^{-1}$) significantly inhibited lipids accumulation and differentiation of adipocytes (Maeda *et al*., 2006). In the period duration of this study was not possible to achieve the isolation and elucidation of the compound(s) in these sub-fractions, consequently an IC_{50} value was not determined, so there is only the knowledge that at 30 $\mu g.ml^{-1}$ fractions D and E were able to display this bioactivity without cytotoxicity.

So, besides isolation and elucidation of the compound(s) in sub-fractions D-E6E4 and D-E6E6 will be also required to assess the IC_{50} values for inhibition of lipid accumulation and possible adipocyte differentiation, preferably in whole organism models in order to better evaluate their potential either for future dietary intake of extracts or purified pharmacological agents.

Additionally, in this study was not possible to completely elucidate possible mechanism(s) of action that would reduce the amount of neutral lipids in the yolk sac of zebrafish larvae. The *in vitro* results suggested inhibition of adipocyte differentiation, however there is no information on possible targets affected, such as transcription factor PPARγ, growth factor TGFβ, GLP-1, TRPV1 receptor pathways, mentioned before, or even through other targets still not explained. At this point we can only speculate, and further studies of these compounds will be necessary.

3.2.3. Study of E17165 derived from strain *Nodosilinea nodulosa* LEGE 06102

All fractions were tested for their lipid-reducing activity using the zebrafish Nile Red fat metabolism assay. This initial screening provides evidence for lipid-reducing activity, since fractions F and G, originated from a mixture of 4:1 and 1:0 EtOAc/*n*-hexane, respectively, displayed a reduction of the fluorescence intensity (Figure 37) by 35.75 ± 14.45% and 26.15 ± 12.57%, respectively. As expected, statistical analysis of this bioassay data confirmed that fractions F and G possess significant activity in comparison with solvent control group, favouring the anti-obesity activity of fraction F with adoption of a p-value of 0.01 (Figure 38).

One fraction statistically significantly increased the stained neutral lipids content in the zebrafish larvae, an activity which may be of interest for some studies.

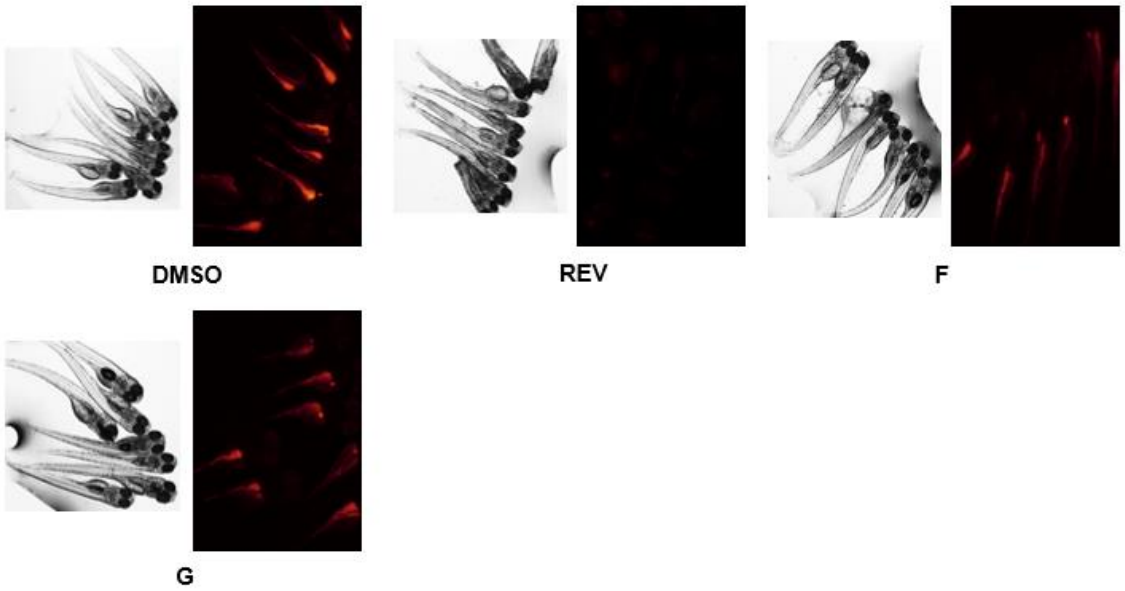

Figure 37 - Representative images of the zebrafish Nile Red fat metabolism assay of fractions E17165 F and G. In left are represent the phase contrast image of zebrafish larvae and the right images show the fluorescence with red contrast in fractions with bioactivity. DMSO, solvent control 0.1%; REV, positive control 50 µM.

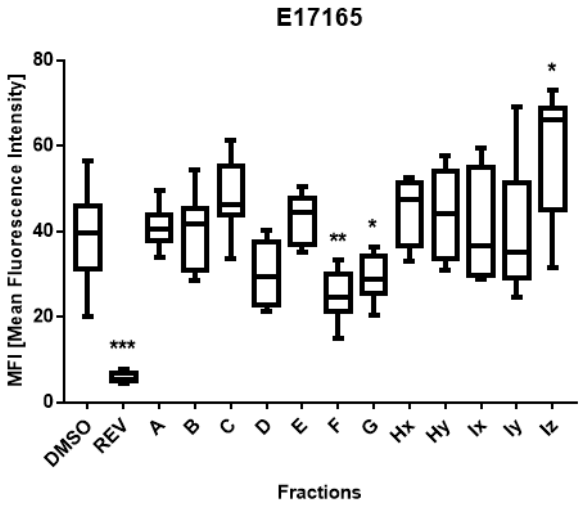

*Figure 37 - Lipid-reducing activity in the zebrafish Nile Red fat metabolism assay for fractions E17165 A to Iz. Solvent control had 0.1% DMSO and the positive control received 50 µM REV. Values are expressed as mean fluorescence intensity (MFI) relative to the DMSO group, and each treatment group had 6 to 8 replicates. The data are represented as box-whisker plots. Statistical differences were analysed by Kruskal-Wallis with Dunn´s posthoc test and are indicated to the solvent control with the symbol * $p < 0.05$; ** $p < 0.01$; *** $p < 0.001$; **** $p < 0.0001$.*

More analyses will have to be carried out, namely ^{1}H NMR to decide the steps that will follow for E17165 fractions from strain *N. nodulosa* LEGE 06102.

3.3. Future Perspectives

Regarding future work, further isolation and structure elucidation of the bioactive compounds of sub-fractions E181719 D-E6E4 and D-E6E6 will be required. Once fully characterized, the work may focus in possible other bioactivities and mechanism(s) of action of these sub-fractions and compound **(1)**, since as the result of this study is already known that are able to reduce the amount of neutral lipids, such as triacylglycerol, in the yolk sac of zebrafish model organism.

Additionally, besides the use of purified pharmacological compounds, may be useful to consider the use of dry biomass extracts of this studied strains as possible dietary supplements. As highlighted before cyanobacteria hold many beneficial effects as well treat obesity and related co-morbidities.

The administration of cyanobacteria extracts *Arthrospira* sp. and *L. japonica* helped mitigate metabolic complications associated to adipose tissue dysfunction in obesity states (Jang and Choung, 2013; Jarouliya *et al*., 2012; Ku *et al*., 2013). So, considering the results showed in this study and the data from literature, is reasonable to consider the administration of cyanobacterial extracts from *S. salina*, *N. nodulosa* and *Nodosilinea* sp. strains as dietary supplements for not only obesity and related co-morbidities treatment but also to attenuate other diseases.

The first fractions of this strains resulting from midpolarity organic extracts did not pose toxicity towards the animal model organism, zebrafish. Nonetheless, throughout the fractionation procedure were identified sub-fractions E17161 E4B from *Nodosilinea* sp. and possibly E18179 D-E3D from *S. salina* with toxicity to zebrafish embryos at 48 h. Moreover, in the context of this study was considered the acute effects of the fractions which could be completely different from the chronic administration purpose as an alternative treatment of metabolic diseases. In the end, further studies need to be carried out in order to elucidate if the administration of these strains represents a health hazard.

4. Conclusion

The main goal of this study was to identify novel cyanobacterial secondary metabolites in order to purpose new hits for the treatment of obesity and/or associated metabolic complications.

In this way, 5 fractions and sub-fractions were identified (E17165 F and G from strain *N. nodulosa* LEGE 06102; E18179 D-E6E4 and D-E6E6 from strain *S. salina* LEGE 06099; E17161 E4C11A from strain *Nodosilinea* sp.) with significant lipid-reducing activity. In addition, compound **(1)** was isolated and structural characterized from sub-fraction E4C11A. To the best of our knowledge, compound **(1)** is a new secondary metabolite from *Nodosilinea* sp. strain not previously described in the literature or related to activity towards reducing obesity or associated co-morbidities.

These results confirmed that cyanobacteria are prolific in secondary metabolites with bioactivity of interest. In addition, the potential bioactivity of chlorophyll derivatives was demonstrated and supported a potential role of these natural compounds in human health and disease prevention.

5. References

Abraham RJ and Rowan A (1991) Nuclear magnetic resonance spectroscopy of chlorophyll.

Afonso TB, Costa MS, Rezende de Castro R, Freitas S, Silva A, Schneider MPC, Martins Rr and Leão PN (2016) Bartolosides E–K from a Marine Coccoid Cyanobacterium. *Journal of Natural Products* **79**:2504-2513.

Alfeus A (2016) *Cyanobacteria as a source of compounds with cosmetics potential*, p 69, University of Porto (Master dissertation). Retrieved from UP open repository

Aronoff S (1966) The Chlorophylls – An Introductory Survey, in *The Chlorophylls* (Vernon LP and Seely GR eds) pp 3-20, Academic Press.

Balaji M, Ganjayi MS, Hanuma Kumar GEN, Parim BN, Mopuri R and Dasari S (2016) A review on possible therapeutic targets to contain obesity: The role of phytochemicals. *Obesity Research & Clinical Practice* **10**:363-380.

Barbosa M, Valentão P and Andrade PB (2014) Bioactive compounds from macroalgae in the new millennium: implications for neurodegenerative diseases. *Marine Drugs* **12**:4934-4972.

Barboza GF, Gorlach-Lira K, Sassi CF and Sassi R (2017) Microcystins production and antibacterial activity of cyanobacterial strains of Synechocystis, Synechococcus and Romeria from water and coral reef organisms (Brazil). *Revista de Biologia Tropical* **65**:890-899.

Baskaran P, Markert L, Zimmerman L, Bennis J and Thyagarajan B (2018) Sub-Chronic Oral Safety Analysis of MetabocinTM. *Biophysical Journal* **114**:484a.

Blunt JW, Copp BR, Keyzers RA, Munro MH and Prinsep MR (2015) Marine natural products. *Natural Product Reports* **32**:116-211.

Bogorad L (1966) The Biosynthesis of Chlorophylls, in *The Chlorophylls* (Vernon LP and Seely GR eds) pp 481-510, Academic Press.

Brito Â, Gaifem J, Ramos V, Glukhov E, Dorrestein PC, Gerwick WH, Vasconcelos VM, Mendes MV and Tamagnini P (2015) Bioprospecting Portuguese Atlantic coast cyanobacteria for bioactive secondary metabolites reveals untapped chemodiversity. *Algal Research* **9**:218-226.

Brito Â, Ramos V, Seabra R, Santos A, Santos CL, Lopo M, Ferreira S, Martins A, Mota R, Frazão B, Martins R, Vasconcelos V and Tamagnini P (2012) Culture-dependent characterization of cyanobacterial diversity in the intertidal zones of the Portuguese coast: A polyphasic study. *Systematic and Applied Microbiology* **35**:110-119.

Castro M, Preto M, Vasconcelos V and Urbatzka R (2016) Obesity: The metabolic disease, advances on drug discovery and natural product research. *Current Topics in Medicinal Chemistry* **16**:2577-2604.

Chen K, Ríos JJ, Roca M and Pérez-Gálvez A (2015) Development of an accurate and high-throughput methodology for structural comprehension of chlorophylls derivatives.(II) Dephytylated derivatives. *Journal of Chromatography A* **1412**:90-99.

Cheong SH, Kim MY, Sok D-E, Hwang S-Y, Kim JH, Kim HR, Lee JH, Kim Y-B and Kim MR (2010) Spirulina prevents atherosclerosis by reducing hypercholesterolemia in rabbits fed a high-cholesterol diet. *Journal of Nutritional Science and Vitaminology* **56**:34-40.

Cinti S, Mitchell G, Barbatelli G, Murano I, Ceresi E, Faloia E, Wang S, Fortier M, Greenberg AS and Obin MS (2005) Adipocyte death defines macrophage localization and function in adipose tissue of obese mice and humans. *Journal of Lipid Research* **46**:2347-2355.

Cooke D and Bloom S (2006) The obesity pipeline: current strategies in the development of anti-obesity drugs. *Nature Reviews Drug Discovery* **5**:919.

Costa M, Garcia M, Costa-Rodrigues J, Costa MS, Ribeiro MJ, Fernandes MH, Barros P, Barreiro A, Vasconcelos V and Martins R (2014) Exploring bioactive properties of

marine cyanobacteria isolated from the Portuguese coast: high potential as a source of anticancer compounds. *Marine Drugs* **12**:98-114.

Costa MS, Rego A, Ramos V, Afonso TB, Freitas S, Preto M, Lopes V, Vasconcelos V, Magalhães C and Leão PN (2016) The conifer biomarkers dehydroabietic and abietic acids are widespread in Cyanobacteria. *Scientific Reports* **6**:23436.

Daneschvar HL, Aronson MD and Smetana GW (2016) FDA-approved anti-obesity drugs in the United States. *The American Journal of Medicine* **129**:879. e871-879. e876.

De Rivera CG, Miranda-Zamora R, Diaz-Zagoya J and Juárez-Oropeza M (1993) Preventive effect of Spirulina maxima on the fatty liver induced by a fructose-rich diet in the rat, a preliminary report. *Life Sciences* **53**:57-61.

Dixit RB and Suseela M (2013) Cyanobacteria: Potential candidates for drug discovery. *Antonie Van Leeuwenhoek* **103**:947-961.

Duarte K, Justino CIL, Pereira R, Freitas AC, Gomes AM, Duarte AC and Rocha-Santos TAP (2014) Green analytical methodologies for the discovery of bioactive compounds from marine sources. *Trends in Environmental Analytical Chemistry* **3**:43-52.

Ellsworth RK (1968) Chlorophyll a biogenesis. Retrieved from Dissertations and Theses database. (UMI No. 3732)

Ferruzzi M, Böhm V, Courtney P and Schwartz S (2002) Antioxidant and antimutagenic activity of dietary chlorophyll derivatives determined by radical scavenging and bacterial reverse mutagenesis assays. *Journal of Food Science* **67**:2589-2595.

Frühbeck G, Toplak H, Woodward E, Yumuk V, Maislos M and Oppert J-M (2013) Obesity: the gateway to ill health-an EASO position statement on a rising public health, clinical and scientific challenge in Europe. *Obesity Facts* **6**:117-120.

Gaio V, Antunes L, Namorado S, Barreto M, Gil A, Kyslaya I, Rodrigues AP, Santos A, Bøhler L, Castilho E, Vargas P, do Carmo I, Nunes B and Dias CM (2018) Prevalence of overweight and obesity in Portugal: Results from the First Portuguese Health Examination Survey (INSEF 2015). *Obesity Research & Clinical Practice* **12**:40-50.

Gerwick WH, Coates RC, Engene N, Gerwick L, Grindberg RV, Jones AC and Sorrels CM (2008) Giant marine cyanobacteria produce exciting potential pharmaceuticals. *Microbe-American Society for Microbiology* **3**:277.

Giacomotto J and Ségalat L (2010) High-throughput screening and small animal models, where are we? *British Journal of Pharmacology* **160**:204-216.

Gogineni V and Hamann MT (2018) Marine natural product peptides with therapeutic potential: Chemistry, biosynthesis, and pharmacology. *Biochimica et Biophysica Acta (BBA) - General Subjects* **1862**:81-196.

Gomes RA, Teles YCF, Pereira FdO, Rodrigues LAdS, Lima EdO, Agra MdF and Souza MdFVd (2015) Phytoconstituents from Sidastrum micranthum (A. St.-Hil.) Fryxell (Malvaceae) and antimicrobial activity of pheophytin a. *Brazilian Journal of Pharmaceutical Sciences* **51**:861-867.

Graber MA and Gerwick WH (1998) Kalkipyrone, a Toxic γ-Pyrone from an Assemblage of the Marine Cyanobacteria Lyngbya majuscula and Tolypothrix sp. *Journal of Natural Products* **61**:677-680.

Gustafson B, Hammarstedt A, Hedjazifar S and Smith U (2013) Restricted adipogenesis in hypertrophic obesity: the role of WISP2, WNT, and BMP4. *Diabetes* **62**:2997-3004.

Henninger AJ, Eliasson B, Jenndahl LE and Hammarstedt A (2014) Adipocyte hypertrophy, inflammation and fibrosis characterize subcutaneous adipose tissue of healthy, non-obese subjects predisposed to type 2 diabetes. *PloS one* **9**:e105262.

Hölttä-Vuori M, Salo VT, Nyberg L, Brackmann C, Enejder A, Panula P and Ikonen E (2010) Zebrafish: gaining popularity in lipid research. *Biochemical Journal* **429**:235-242.

Hoseini S, Khosravi-Darani K and Mozafari M (2013) Nutritional and medical applications of spirulina microalgae. *Mini Reviews in Medicinal Chemistry* **13**:1231-1237.

Hosogai N, Fukuhara A, Oshima K, Miyata Y, Tanaka S, Segawa K, Furukawa S, Tochino Y, Komuro R and Matsuda M (2007) Adipose tissue hypoxia in obesity and its impact on adipocytokine dysregulation. *Diabetes* **56**:901-911.

Hu X, Tao N, Wang X, Xiao J and Wang M (2016) Marine-derived bioactive compounds with anti-obesity effect: A review. *Journal of Functional Foods* **21**:372-387.

Hyvärinen K, Helaja J and Hynninen PH (1998) An unexpected allomer of chlorophyll: 132 (S)-hydroxy-10-methoxychlorophyll b. *Tetrahedron Letters* **39**:9813-9814.

Hyvärinen K, Helaja J, Kuronen P, Kilpeläinen I and Hynninen PH (1995) 1H and 13C NMR spectra of the methanolic allomerization products of 132 (R)-chlorophyll a. *Magnetic Resonance in Chemistry* **33**:646-656.

Inuzuka T, Yamamoto K, Iwasaki A, Ohno O, Suenaga K, Kawazoe Y and Uemura D (2014) An inhibitor of the adipogenic differentiation of 3T3-L1 cells, yoshinone A, and its analogs, isolated from the marine cyanobacterium Leptolyngbya sp. *Tetrahedron Letters* **55**:6711-6714.

Iwata K, Inayama T and Kato T (1990) Effects of Spirulina platensis on plasma lipoprotein lipase activity in fructose-induced hyperlipidemic rats. *Journal of Nutritional Science and Vitaminology* **36**:165-171.

Jain S, Prajapat G, Abrar M, Ledwani L, Singh A and Agrawal A (2017) Cyanobacteria as efficient producers of mycosporine-like amino acids. *Journal of Basic Microbiology* **57**:715-727.

Jang WS and Choung SY (2013) Antiobesity effects of the ethanol extract of Laminaria japonica Areshoung in high-fat-diet-induced obese rat. *Evidence-Based Complementary and Alternative Medicine* **2013**.

Jarouliya U, Anish ZJ, Kumar P, Bisen P and Prasad G (2012) Alleviation of metabolic abnormalities induced by excessive fructose administration in Wistar rats by Spirulina maxima. *The Indian Journal of Medical Research* **135**:422.

Jerz G, Arrey TN, Wray V, Du Q and Winterhalter P (2007) Structural characterization of 132-hydroxy-(132-S)-phaeophytin-a from leaves and stems of Amaranthus tricolor isolated by high-speed countercurrent chromatography. *Innovative Food Science & Emerging Technologies* **8**:413-418.

Jones KS, Alimov AP, Rilo HL, Jandacek RJ, Woollett LA and Penberthy WT (2008) A high throughput live transparent animal bioassay to identify non-toxic small molecules or genes that regulate vertebrate fat metabolism for obesity drug development. *Nutrition & Metabolism* **5**:1-11.

Kanda H, Tateya S, Tamori Y, Kotani K, Hiasa K-i, Kitazawa R, Kitazawa S, Miyachi H, Maeda S and Egashira K (2006) MCP-1 contributes to macrophage infiltration into adipose tissue, insulin resistance, and hepatic steatosis in obesity. *The Journal of Clinical Investigation* **116**:1494-1505.

Kang JG and Park C-Y (2012) Anti-Obesity Drugs: A Review about Their Effects and Safety. *Diabetes & Metabolism Journal* **36**:13-25.

Kang Y-R, Park J, Jung SK and Chang YH (2018) Synthesis, characterization, and functional properties of chlorophylls, pheophytins, and Zn-pheophytins. *Food Chemistry* **245**:943-950.

Khan T, Muise ES, Iyengar P, Wang ZV, Chandalia M, Abate N, Zhang BB, Bonaldo P, Chua S and Scherer PE (2009) Metabolic dysregulation and adipose tissue fibrosis: role of collagen VI. *Molecular and Cellular Biology* **29**:1575-1591.

Kim S, Schlicke H, Van Ree K, Karvonen K, Subramaniam A, Richter A, Grimm B and Braam J (2013) Arabidopsis chlorophyll biosynthesis: an essential balance between the methylerythritol phosphate and tetrapyrrole pathways. *The Plant Cell* tpc-113.

Kirti K, Amita S, Priti S, Mukesh Kumar A and Jyoti S (2014) Colorful world of microbes: carotenoids and their applications. *Advances in Biology* **2014**.

Kosteli A, Sugaru E, Haemmerle G, Martin JF, Lei J, Zechner R and Ferrante AW (2010) Weight loss and lipolysis promote a dynamic immune response in murine adipose tissue. *The Journal of Clinical Investigation* **120**:3466-3479.

Kotai J (1972) Instructions for preparation of modified nutrient solution Z8 for algae. *Norwegian Institute for Water Research*, Oslo **11**:5.

Koyama T, Kawazoe Y, Uemura D, Iwasaki A, Ohno O and Suenaga K (2016) Anti-obesity activities of the yoshinone A and the related marine γ-pyrone compounds. *The Journal of Antibiotics* **69**:348- 351.

Ku CS, Yang Y, Park Y and Lee J (2013) Health benefits of blue-green algae: prevention of cardiovascular disease and nonalcoholic fatty liver disease. *Journal of Medicinal Food* **16**:103-111.

Kwon M, Lim S-J, Lee B, Shin T and Kim H-R (2018) Ethanolic extract of Sargassum serratifolium inhibits adipogenesis in 3T3-L1 preadipocytes by cell cycle arrest. *Journal of Applied Phycology* **30**:559-568.

Lawton L, Marsalek B, Padisák J and Chorus I (1999) Determination of cyanobacteria in the laboratory. *Toxic cyanobacteria in water: A guide to their public health consequences, monitoring and management*: 1-28.

Leão PN, Engene N, Antunes A, Gerwick WH and Vasconcelos V (2012) The chemical ecology of cyanobacteria. *Natural Product Reports* **29**:372-391.

Leão PN, Nakamura H, Costa M, Pereira AR, Martins R, Vasconcelos V, Gerwick WH and Balskus EP (2015) Biosynthesis-Assisted Structural Elucidation of the Bartolosides, Chlorinated Aromatic Glycolipids from Cyanobacteria. *Angewandte Chemie International Edition* **54**:11063-11067.

Leão PN, Ramos V, Goncalves PB, Viana F, Lage OM, Gerwick WH and Vasconcelos VM (2013) Chemoecological Screening Reveals High Bioactivity in Diverse Culturable Portuguese Marine Cyanobacteria. *Marine Drugs* **11**:1316-1335.

Lee M-J, Wu Y and Fried SK (2010) Adipose tissue remodeling in pathophysiology of obesity. *Current Opinion in Clinical Nutrition and Metabolic Care* **13**:371.

Lee TH, Lu CK, Kuo YH, Lo JM and Lee CK (2008) Unexpected novel pheophytin peroxides from the leaves of Biden pilosa. *Helvetica Chimica Acta* **91**:79-84.

Lefterova MI and Lazar MA (2009) New developments in adipogenesis. *Trends in Endocrinology & Metabolism* **20**:107-114.

Li H, Li L, Zheng Q, Kuroda C and Wang Q (2012) Phaeophytin analogues from Ligularia knorringiana. *Molecules* **17**:5219-5224.

Liang S, Liu X, Chen F and Chen Z (2004) Current microalgal health food R & D activities in China, in *Asian Pacific Phycology in the 21st Century: Prospects and Challenges* pp 45-48, Springer, Dordrecht.

Lumeng CN, Bodzin JL and Saltiel AR (2007) Obesity induces a phenotypic switch in adipose tissue macrophage polarization. *The Journal of Clinical Investigation* **117**:175-184.

Machado J, Azevedo J, Vasconcelos V and Campos A (2016) Mode of Action and Toxicity of Major Cyanobacterial Toxins and Corresponding Chemical Variants. In: Gopalakrishnakone P., Stiles B., Alape-Girón A., Dubreuil J., Mandal M. (eds) *Microbial Toxins* 1-24. Toxinology. Springer, Dordrecht.

Maeda H, Hosokawa M, Sashima T, Takahashi N, Kawada T and Miyashita K (2006) Fucoxanthin and its metabolite, fucoxanthinol, suppress adipocyte differentiation in 3T3-L1 cells. *International Journal of Molecular Medicine* **18**:147-152.

Mariman EC and Wang P (2010) Adipocyte extracellular matrix composition, dynamics and role in obesity. *Cellular and Molecular Life Sciences* **67**:1277-1292.

Martins R, Fernandez N, Beiras R and Vasconcelos V (2007) Toxicity assessment of crude and partially purified extracts of marine Synechocystis and Synechococcus cyanobacterial strains in marine invertebrates. *Toxicon* **50**:791-799

Mascher D, Paredes-Carbajal MC, Torres-Durán PV, Zamora-González J, Díaz-Zagoya JC and Juárez-Oropeza MA (2006) Ethanolic extract of Spirulina maxima alters the vasomotor reactivity of aortic rings from obese rats. *Archives of Medical Research* **37**:50-57.

Masuda T and Fujita Y (2008) Regulation and evolution of chlorophyll metabolism. *Photochemical & Photobiological Sciences* **7**:1131-1149.

Matsuo A, Ono K, Hamasaki K and Nozaki H (1996) Phaeophytins from a cell suspension culture of the liverwort Plagiochila ovalifolia. *Phytochemistry* **42**:427-430.

Mi Y, Zhang J, He S and Yan X (2017) New peptides isolated from marine cyanobacteria, an overview over the past decade. *Marine Drugs* **15**:132.

Mizoguchi T, Oh-oka H and Tamiaki H (2005) Determination of Stereochemistry of Bacteriochlorophyll gF and 81-Hydroxy-chlorophyll aF from Heliobacterium modesticaldum. *Photochemistry and Photobiology* **81**:666-673.

Modiri S, Sharafi H, Alidoust L, Hajfarajollah H, Haghighi O, Azarivand A, Zamanzadeh Z, Zahiri HS, Vali H and Noghabi KA (2015) Lipid production and mixotrophic growth features of cyanobacterial strains isolated from various aquatic sites. *Microbiology* **161**:662-673.

Moulin M and Smith A (2005) Regulation of tetrapyrrole biosynthesis in higher plants, Portland Press Limited.

Myers JA, Curtis BS and Curtis WR (2013) Improving accuracy of cell and chromophore concentration measurements using optical density. *BMC Biophysics* **6**:4.

Nguyen M, Yang E, Neelkantan N, Mikhaylova A, Arnold R, Poudel MK, Stewart AM and Kalueff AV (2013) Developing 'integrative' zebrafish models of behavioral and metabolic disorders. *Behavioural Brain Research* **256**:172-187.

Noinart J, Buttachon S, Dethoup T, Gales L, Pereira JA, Urbatzka R, Freitas S, Lee M, Silva A and Pinto MM (2017) A New Ergosterol Analog, a New Bis-Anthraquinone and Anti-Obesity Activity of Anthraquinones from the Marine Sponge-Associated Fungus Talaromyces stipitatus KUFA 0207. *Marine Drugs* **15**:139.

Nunnery JK, Mevers E and Gerwick WH (2010) Biologically active secondary metabolites from marine cyanobacteria. *Current Opinion in Biotechnology* **21**:787-793.

Oka T, Nishimura Y, Zang L, Hirano M, Shimada Y, Wang Z, Umemoto N, Kuroyanagi J, Nishimura N and Tanaka T (2010) Diet-induced obesity in zebrafish shares common pathophysiological pathways with mammalian obesity. *BMC Physiology* **10**:21.

Pangestuti R and Kim S-K (2011) Biological activities and health benefit effects of natural pigments derived from marine algae. *Journal of Functional Foods* **3**:255-266.

Park M, Lee JH, Choi JK, Hong YD, Bae IH, Lim KM, Park YH and Ha H (2014) 18β-glycyrrhetinic acid attenuates anandamide-induced adiposity and high-fat diet induced obesity. *Molecular Nutrition & Food Research* **58**:1436-1446.

Pasarica M, Gowronska-Kozak B, Burk D, Remedios I, Hymel D, Gimble J, Ravussin E, Bray GA and Smith SR (2009) Adipose tissue collagen VI in obesity. *The Journal of Clinical Endocrinology & Metabolism* **94**:5155-5162.

Pattanaik B and Lindberg P (2015) Terpenoids and their biosynthesis in cyanobacteria. *Life* **5**:269-293.

Paul DGN and J V (1999) Production of secondary metabolites by filamentous tropical marine cyanobacteria: ecological functions of the compounds. *Journal of Phycology* **35**:1412-1421.

Pellecchia M, Bertini I, Cowburn D, Dalvit C, Giralt E, Jahnke W, James TL, Homans SW, Kessler H, Luchinat C, Meyer B, Oschkinat H, Peng J, Schwalbe H and Siegal G (2008) Perspectives on NMR in drug discovery: a technique comes of age. *Nature Reviews Drug Discovery* **7**:738.

Petersen KF, Dufour S, Befroy D, Lehrke M, Hendler RE and Shulman GI (2005) Reversal of nonalcoholic hepatic steatosis, hepatic insulin resistance, and hyperglycemia by moderate weight reduction in patients with type 2 diabetes. *Diabetes* **54**:603-608.

Plaza M, Santoyo S, Jaime L, Reina GG-B, Herrero M, Señoráns FJ and Ibáñez E (2010) Screening for bioactive compounds from algae. *Journal of Pharmaceutical and Biomedical Analysis* **51**:450-455.

Raja R, Hemaiswarya S, Ganesan V and Carvalho IS (2016) Recent developments in therapeutic applications of Cyanobacteria. *Critical Reviews in Microbiology* **42**:394-405.

Ramos V, Morais J, Castelo-Branco R, Pinheiro Â, Martins J, Regueiras A, Pereira AL, Lopes V, Frazão B, Gomes D, Moreira C, Costa MS, Brûle S, Faustino S, Martins

R, Saker M, Osswald J, Leão PN and Vasconcelos VM (2018a) Cyanobacterial diversity held in mBRCs as a biotechnological asset: the case study of the newly established LEGE Culture Collection. *Journal of Applied Phycology*:415.

Ramos V, Morais J, Castelo-Branco R, Pinheiro Â, Martins J, Regueiras A, Pereira AL, Lopes VR, Frazão B, Gomes D, Moreira C, Costa MS, Brûle S, Faustino S, Martins R, Saker M, Osswald J, Leão PN and Vasconcelos VM (2018b) Cyanobacterial diversity held in microbial biological resource centers as a biotechnological asset: the case study of the newly established LEGE culture collection. *Journal of Applied Phycology* **30**:1437-1451.

Raposo MFdJ, de Morais RMSC and Bernardo de Morais AMM (2013) Bioactivity and applications of sulphated polysaccharides from marine microalgae. *Marine Drugs* **11**:233-252.

Rodgers RJ, Tschöp MH and Wilding JPH (2012) Anti-obesity drugs: past, present and future. *Disease Models & Mechanisms* **5**:621-626.

Sakthivel K and Kathiresan K (2012) Antimicrobial activities of marine cyanobacteria isolated from mangrove environment of south east coast of India. *Journal of Natural Products* **5**:147-156.

Scheer H (1991) Chlorophylls, in *Structure and occurrence of chlorophylls* (Scheer H ed) pp 3-30, CRC Press, Florida.

Schipper HS, Prakken B, Kalkhoven E and Boes M (2012) Adipose tissue-resident immune cells: key players in immunometabolism. *Trends in Endocrinology & Metabolism* **23**:407-415.

Shah SAA, Akhter N, Auckloo BN, Khan I, Lu Y, Wang K, Wu B and Guo Y-W (2017) Structural Diversity, Biological Properties and Applications of Natural Products from Cyanobacteria. A Review. *Marine Drugs* **15**:354.

Sharifuddin Y, Chin Y-X, Lim P-E and Phang S-M (2015) Potential bioactive compounds from seaweed for diabetes management. *Marine Drugs* **13**:5447-5491.

Sharma NK, Tiwari SP, Tripathi K and Rai AK (2011) Sustainability and cyanobacteria (blue-green algae): facts and challenges. *Journal of Applied Phycology* **23**:1059-1081.

Singh R, Parihar P, Singh M, Bajguz A, Kumar J, Singh S, Singh VP and Prasad SM (2017) Uncovering Potential Applications of Cyanobacteria and Algal Metabolites in Biology, Agriculture and Medicine: Current Status and Future Prospects. *Frontiers in Microbiology* **8**:515.

Singh S, Kate BN and Banerjee UC (2005) Bioactive Compounds from Cyanobacteria and Microalgae: An Overview. *Critical Reviews in Biotechnology* **25**:73-95.

Subramoniam A, Asha VV, Nair SA, Sasidharan SP, Sureshkumar PK, Rajendran KN, Karunagaran D and Ramalingam K (2012) Chlorophyll revisited: Anti-inflammatory activities of chlorophyll a and inhibition of expression of TNF-α gene by the same. *Inflammation* **35**:959-966.

Suleria HAR, Gobe G, Masci P and Osborne SA (2016) Marine bioactive compounds and health promoting perspectives; innovation pathways for drug discovery. *Trends in Food Science & Technology* **50**:44-55.

Sun K, Kusminski CM and Scherer PE (2011) Adipose tissue remodeling and obesity. *The Journal of Clinical Investigation* **121**:2094-2101.

Tabassum N, Tai H, Jung D-W and Williams DR (2015) Fishing for Nature's Hits: Establishment of the Zebrafish as a Model for Screening Antidiabetic Natural Products. *Evidence-based Complementary & Alternative Medicine (eCAM)*:1-16.

Tan LT (2013) Pharmaceutical agents from filamentous marine cyanobacteria. *Drug Discovery Today* **18**:863-871.

Tanaka R and Tanaka A (2007) Tetrapyrrole biosynthesis in higher plants. *Annual Review of Plant Biology* **58**:321-346.

Tingaud-Sequeira A, Ouadah N and Babin PJ (2011) Zebrafish obesogenic test: a tool for screening molecules that target adiposity. *Journal of Lipid Research* **52**:1765-1772.

Torres-Durán P, Miranda-Zamora R, Paredes-Carbajal M, Mascher D, Blé-Castillo J, Dıaz-Zagoya J and Juárez-Oropeza M (1999) Studies on the preventive effect of Spirulina

maxima on fatty liver development induced by carbon tetrachloride, in the rat. *Journal of Ethnopharmacology* **64**:141-147.

Tremmel M, Gerdtham U-G, Nilsson PM and Saha S (2017) Economic burden of obesity: a systematic literature review. *International Journal of Environmental Research and Public Health* **14**:435.

Urbatzka R, Freitas S, Palmeira A, Almeida T, Moreira J, Azevedo C, Afonso C, Correia-da-Silva M, Sousa E, Pinto M and Vasconcelos V (2018) Lipid reducing activity and toxicity profiles of a library of polyphenol derivatives. *European Journal of Medicinal Chemistry* **151**:272-284.

Vandevijvere S, Chow CC, Hall KD, Umali E and Swinburn BA (2015) Increased food energy supply as a major driver of the obesity epidemic: a global analysis. *Bulletin of the World Health Organization* **93**:446-456.

Vavilin DV and Vermaas WF (2002) Regulation of the tetrapyrrole biosynthetic pathway leading to heme and chlorophyll in plants and cyanobacteria. *Physiologia Plantarum* **115**:9-24.

Vijayakumar S, Manogar P and Prabhu S (2016) Potential therapeutic targets and the role of technology in developing novel cannabinoid drugs from cyanobacteria. *Biomedicine & Pharmacotherapy* **83**:362-371.

Wang S-Y, Tseng C-P, Tsai K-C, Lin C-F, Wen C-Y, Tsay H-S, Sakamoto N, Tseng C-H and Cheng J-C (2009) Bioactivity-guided screening identifies pheophytin a as a potent anti-hepatitis C virus compound from Lonicera hypoglauca Miq. *Biochemical and Biophysical Research Communications* **385**:230-235.

Weisberg SP, Hunter D, Huber R, Lemieux J, Slaymaker S, Vaddi K, Charo I, Leibel RL and Ferrante Jr AW (2006) CCR2 modulates inflammatory and metabolic effects of high-fat feeding. *The Journal of clinical investigation* **116**:115-124.

World Health Organization. (2014). *Global status report on noncommunicable diseases 2014.* Geneva, Switzerland: World Health Organization.

Ye J, Gao Z, Yin J and He Q (2007) Hypoxia is a potential risk factor for chronic inflammation and adiponectin reduction in adipose tissue of ob/ob and dietary obese mice. *American Journal of Physiology-Endocrinology and Metabolism* **293**:E1118-E1128.

Yumuk V, Tsigos C, Fried M, Schindler K, Busetto L, Micic D, Toplak H and for the Obesity Management Task Force of the European Association for the Study of O (2015) European Guidelines for Obesity Management in Adults. *Obesity Facts* **8**:402-424.

Yun JW (2010) Possible anti-obesity therapeutics from nature – A review. *Phytochemistry* **71**:1625-1641.

Zhao Y, Wang X, Wang H, Liu T and Xin Z (2014) Two new noroleanane-type triterpene saponins from the methanol extract of Salicornia herbacea. *Food Chemistry* **151**:101-109.

6. Appendixes

Appendix I – Macro and micronutrients composition of Z8 medium

Table I.1 - Composition and concentration of stock solutions of Z8 medium.

Solution A	
Reagent	Concentration ($g.l^{-1}$ UPW*)
Sodium Nitrate ($NaNO_3$)	46.7
Calcium Nitrate Tetrahydrate ($Ca(NO_3)_2.4H_2O$)	5.9
Magnesium Sulphate Heptahydrate ($MgSO_4.7H_2O$)	2.5
Solution B	
Reagent	Concentration ($g.l^{-1}$ UPW*)
Potassium Phosphate dibasic (K_2HPO_4)	3.1
Sodium Carbonate (Na_2CO_3)	2.1
Solution Fe-EDTA	
Reagent	Concentration ($g.l^{-1}$ HCL)
Iron(III)chloride ($FeCl_3$)	
$FeCl_3.6H_2O$	20.8
Sodium EDTA (EDTA-Na)	
Reagent	Concentration ($g.l^{-1}$ NaOH)
EDTA	39
Reagent	Concentration ($ml.l^{-1}$ UPW*)
Iron(III)chloride ($FeCl_3$)	10
Sodium EDTA (EDTA-Na)	9.5
Micronutrients	
Reagent	Concentration ($g.l^{-1}$)
1 - Sodium tungstate dihydrate ($Na_2WO_4.2H_2O$)	0.33
2 - Ammonium paramolybdate dihydrate ($(NH_4)6Mo_7O_{24}.2H_2O$)	0.88

3 - Potassium bromide (KBr)	1.2
4 - Potassium iodide (KI)	0.83
5 - Zinc Sulfate Heptahydrate ($ZnSO_4.7H_2O$)	2.87
6 - Cadmium nitrate tetrahydrate ($Cd(NO_3)_2.4H_2O$)	1.55
7 - Cobalt(II) Nitrate Hexahydrate ($Co(NO_3)_2.6H_2O$)	1.46
8 - Copper(II) sulfate pentahydrate ($CuSO_4.5H_2O$)	1.25
9 - Nickel (II) ammonium bi-sulfate hexahydrate ($NiSO_4(NH_4)2SO_4.6H_2O$)	1.98
10 - Chromium(III) Nitrate Nonahydrate ($Cr(NO_3)3.9H_2O$)	0.41
11 - Vanadium pentoxide (V_2O_5)	0.089
12 - Aluminium potassium bi-sulfate dodecahydrate $Al_2(SO_4)3K_2SO_4.24H_2O$	4.74
13 - Boric acid (H_3BO_3)	3.1
14 - Manganese(II) Sulfate Tetrahydrate ($MnSO_4.4H_2O$)	2.23
Reagent	Concentration ($ml.l^{-1}$)
Solution 1-12	10
Solution 13 and 14	100
*** UPW - ultra-pure water**	

Appendix II – ^{1}H NMR data for fractions resulting from the successive fractionations studies of E17161, E15074/E18179 and E171615 belonging to strains *Nodosilinea* sp. LEGE 06001, *Synechocystis salina* LEGE 06099 and *Nodosilinea nodulosa* LEGE 06102, respectively.

Fractions E17161 from strain *Nodosilinea* sp. LEGE 06001

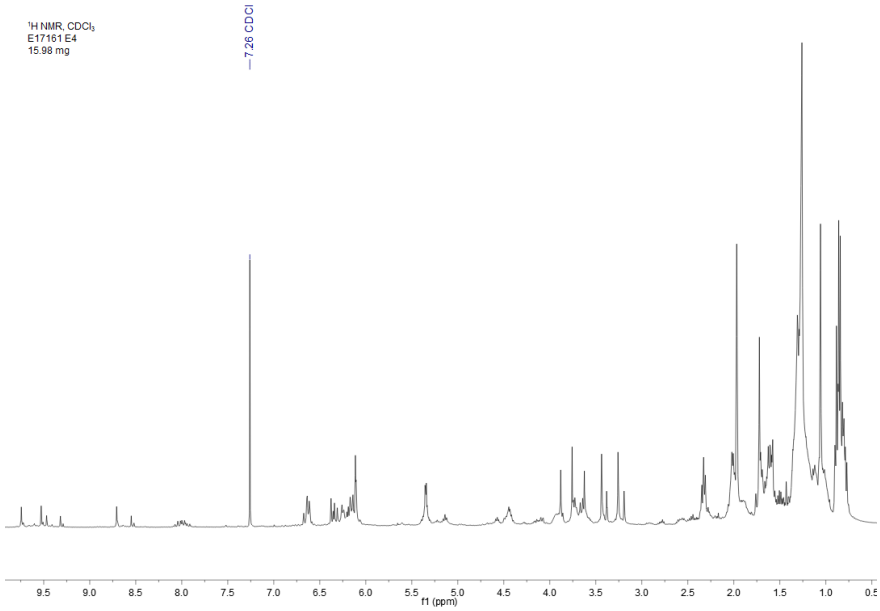

Figure II.1.1 - ^{1}H NMR spectrum for E17161 E4 in $CDCl_3$ (recorded at 400 MHz).

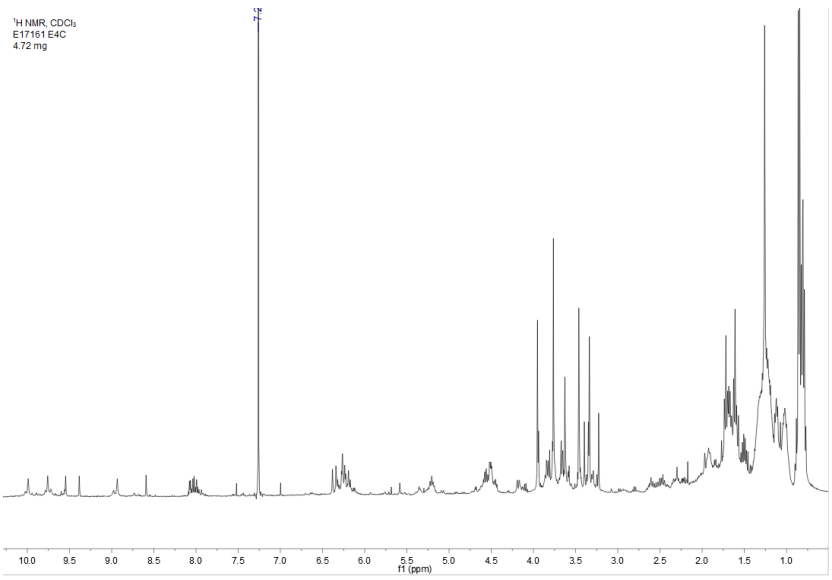

Figure II.1.2 - ^{1}H NMR spectrum for E17161 E4C in $CDCl_3$ (recorded at 400 MHz).

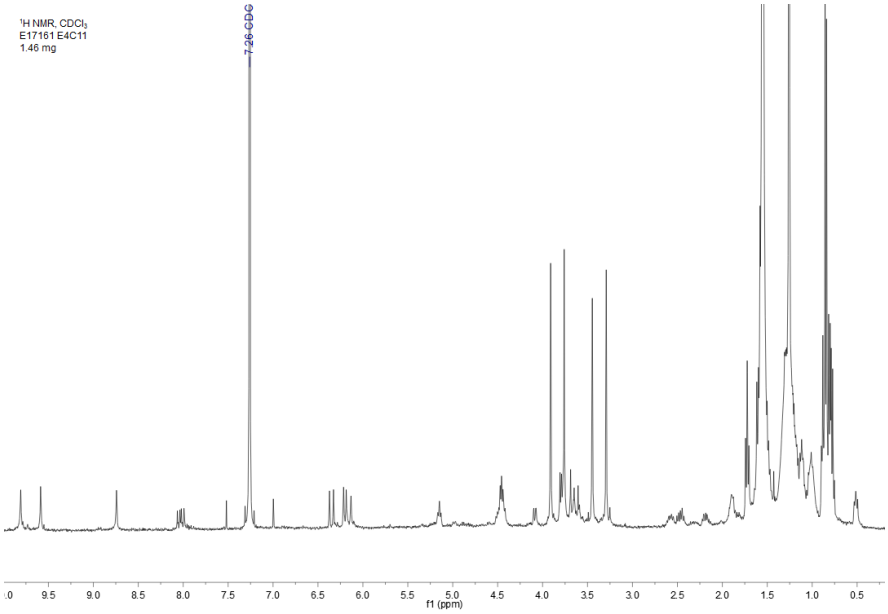

Figure II.1.3 - ^{1}H NMR spectrum for E17161 E4C11 in $CDCl_3$ (recorded at 400 MHz).

Fractions E15074 and E18179 from strain *S. salina* LEGE 06099

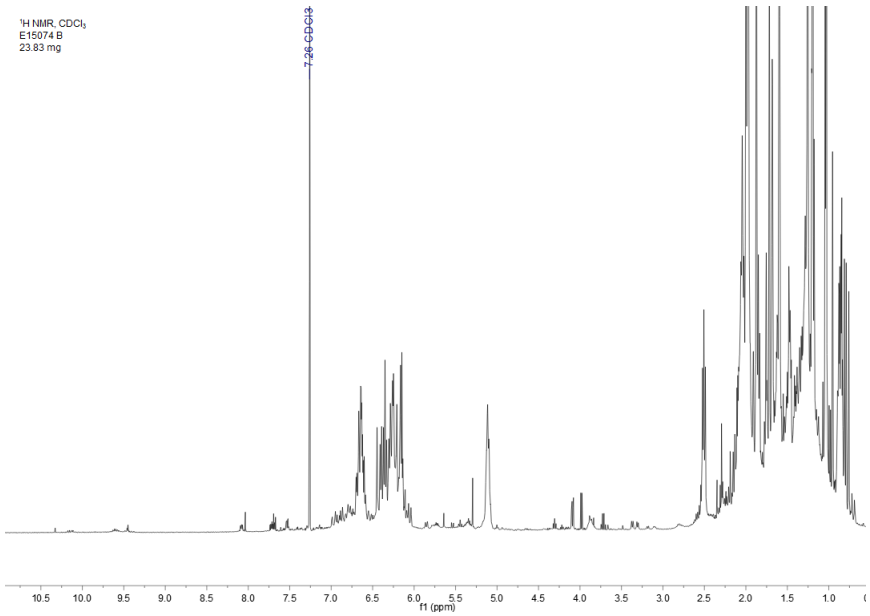

Figure II.2.1 - ^{1}H NMR spectrum for E15074 B in $CDCl_3$ (recorded at 400 MHz).

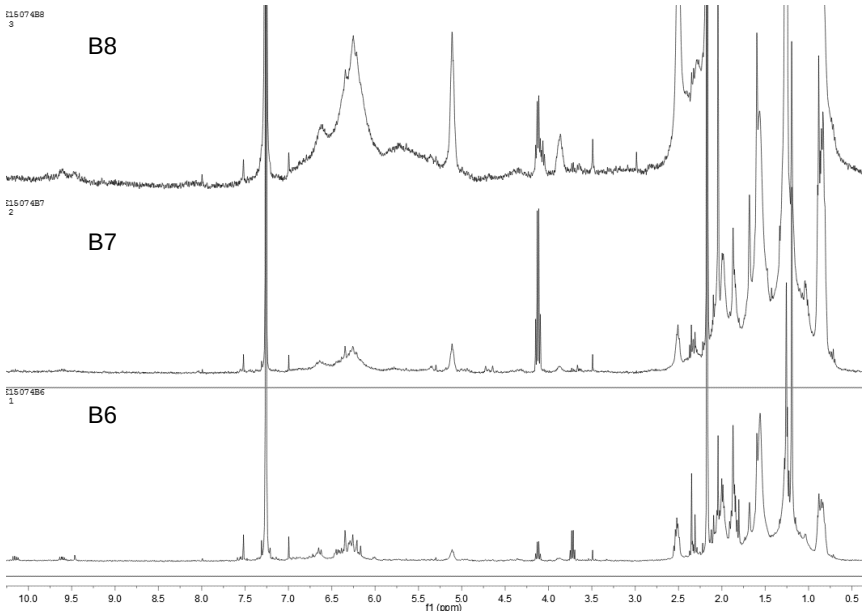

Figure II.2.2 - ^{1}H NMR spectra with comparison of proton profile between sub-fractions E15074 B6, B7 and B8 in $CDCl_3$ (recorded at 400 MHz).

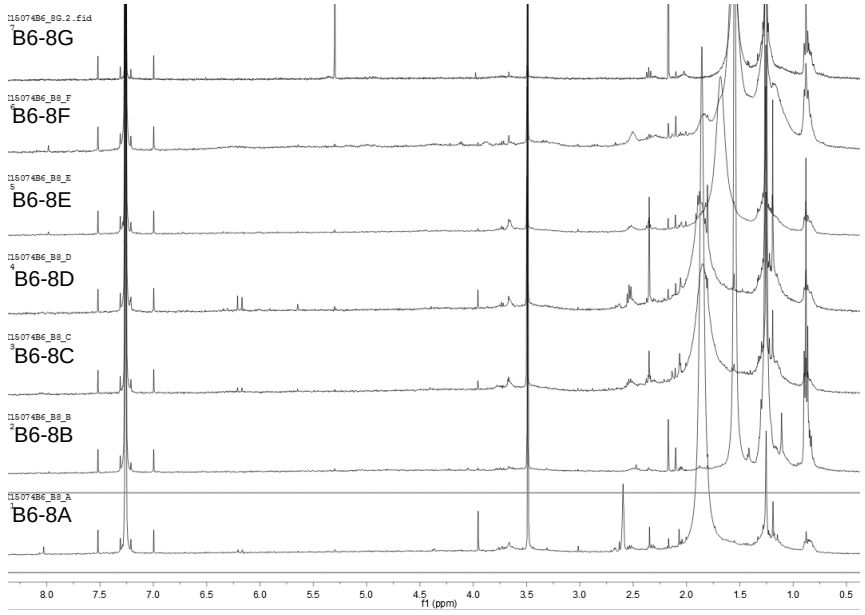

Figure II.2.3 - ^{1}H NMR spectra with comparison of proton profile between sub-fractions E15074 B6-8A to B6-8G in $CDCl_3$ (recorded at 400 MHz).

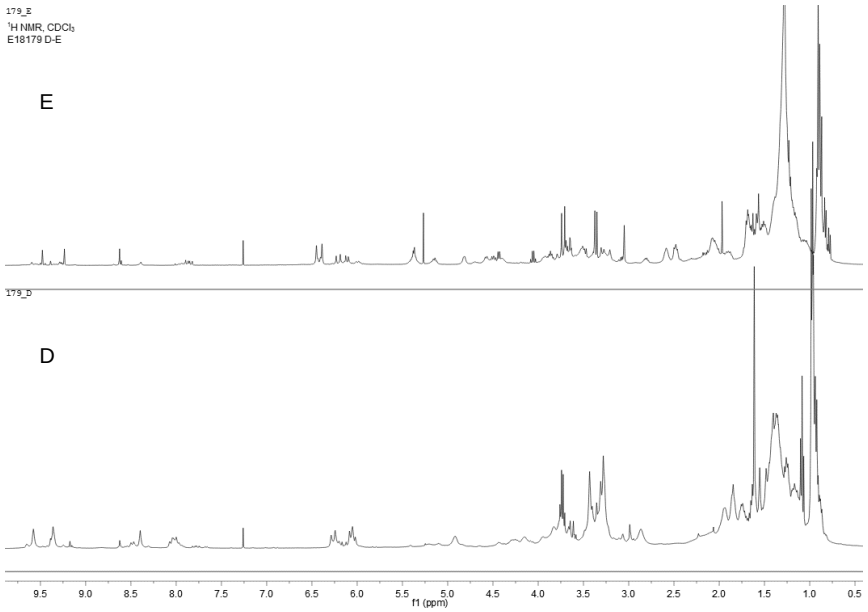

Figure II.2.4 - ^{1}H NMR spectra with comparison of proton profile between sub-fractions E18179 D and E in $CDCl_3$ (recorded at 400 MHz).

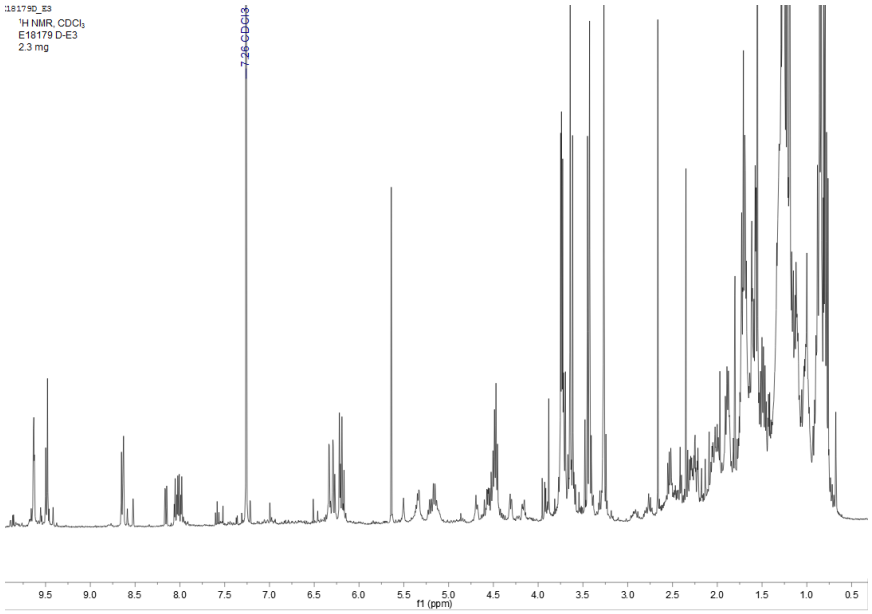

Figure II.2.5 - ^{1}H NMR spectrum for E18179 D-E3 in $CDCl_3$ (recorded at 400 MHz).

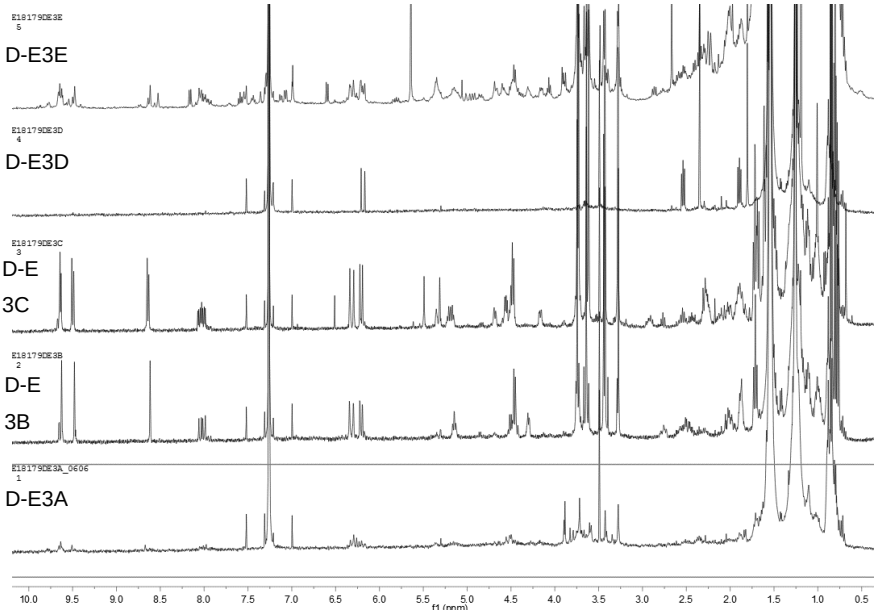

Figure II.2.6 - ^{1}H NMR spectra with comparison of proton profile between sub-fractions E18179 D-E3A to D-E3E in $CDCl_3$ (recorded at 400 MHz).

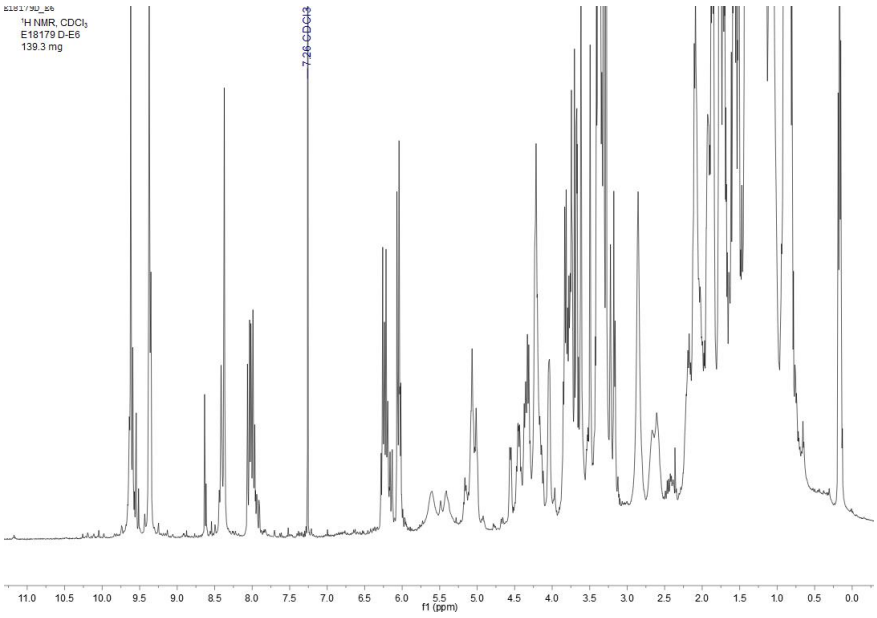

Figure II.2.7 - ^{1}H NMR spectrum for E18179 D-E6 in $CDCl_3$ (recorded at 400 MHz).

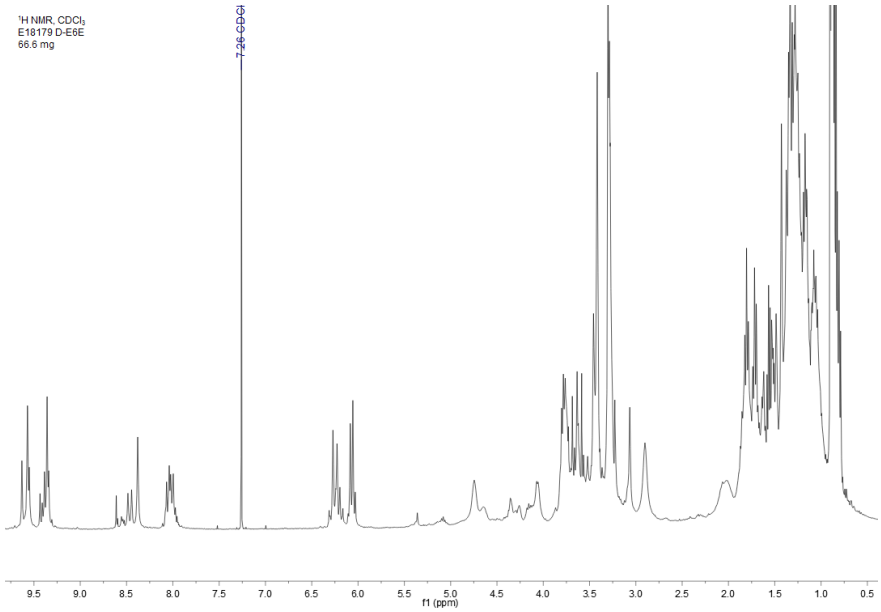

Figure II.2.8 - ^{1}H NMR spectrum for E18179 D-E6E in $CDCl_3$ (recorded at 400 MHz).

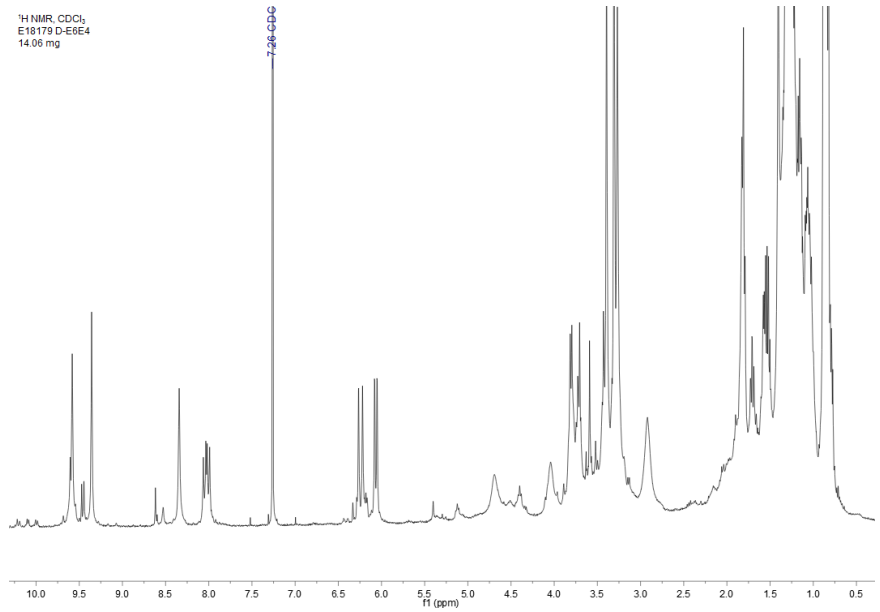

Figure II.2.9 - ^{1}H NMR spectrum for E18179 D-E6E4 in $CDCl_3$ (recorded at 400 MHz).

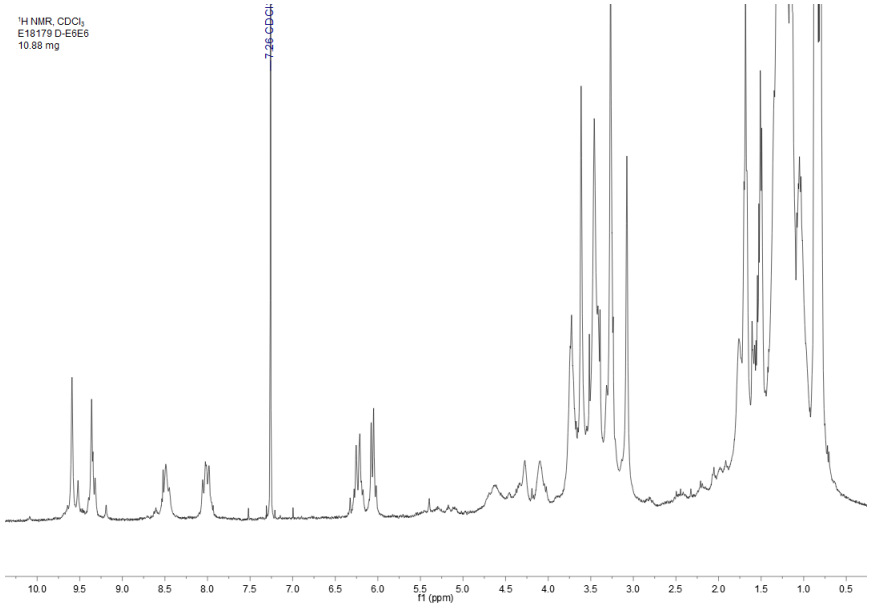

Figure II.2.10 - ^{1}H NMR spectrum for E18179 D-E6E6 in $CDCl_3$ (recorded at 400 MHz).

Appendix III – Data of chemical structural elucidation through 1D and 2D NMR experiments of compound (1), derived from study of E17161 originated in strain *Nodosilinea* sp. LEGE 06001.

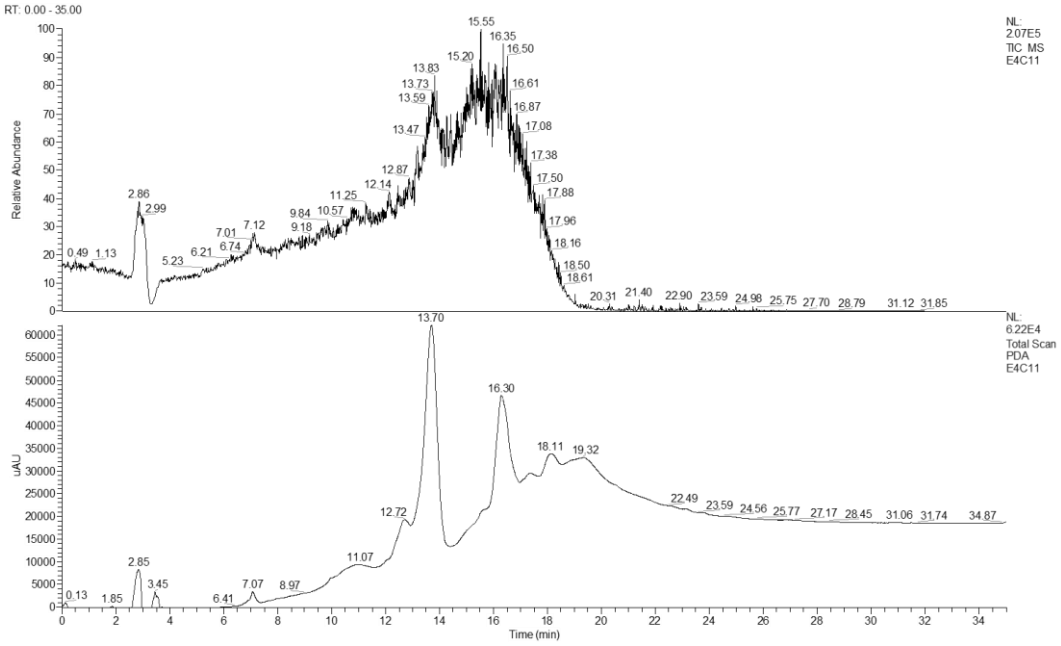

Figure III.1 – Full scan of low resolution LC-MS chromatogram of sub-fraction E4C11. The chromatographic column used was Luna 5 µm C18 100 Å (250 x 4.6 mm) analytical column (Phenomenex). The elution was done with acidified solvents with 0.1% formic acid in a flow of 0.8 ml/min^{-1} for 30 min with the following gradient: 15 minutes 1:1 to 0:1 H_2O/MeCN and 15 minutes 0:1 H_2O/MeCN. The injection volume was 20 µl. The MS data were collected in negative mode. Peak of interest with a retention time of 13.70 min (UV detection at 238 nm).

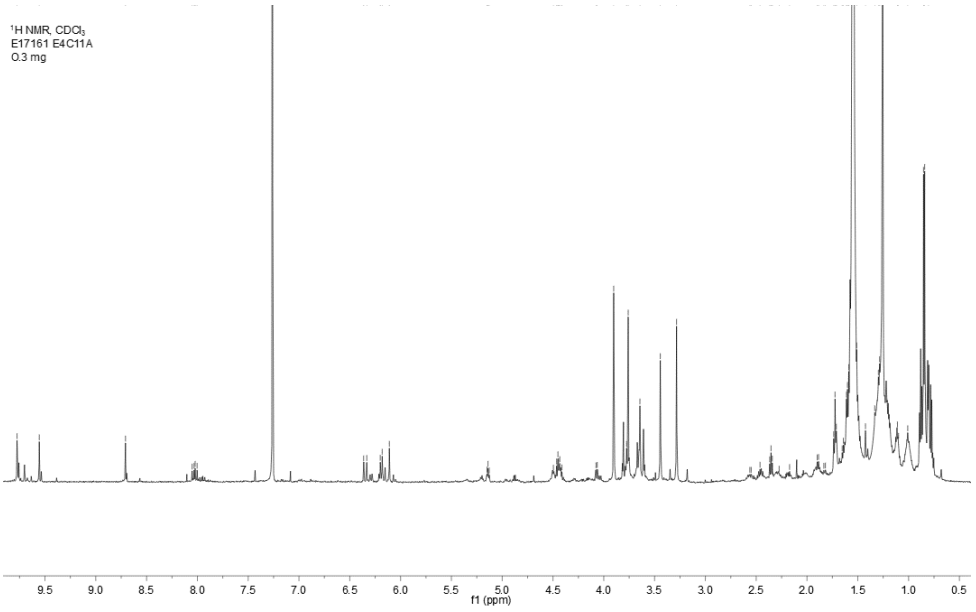

*Figure III.2 - ^{1}H NMR spectrum for compound **(1)** in $CDCl_3$, with relevant chemical shifts peaks marked (recorded at 600 MHz).*

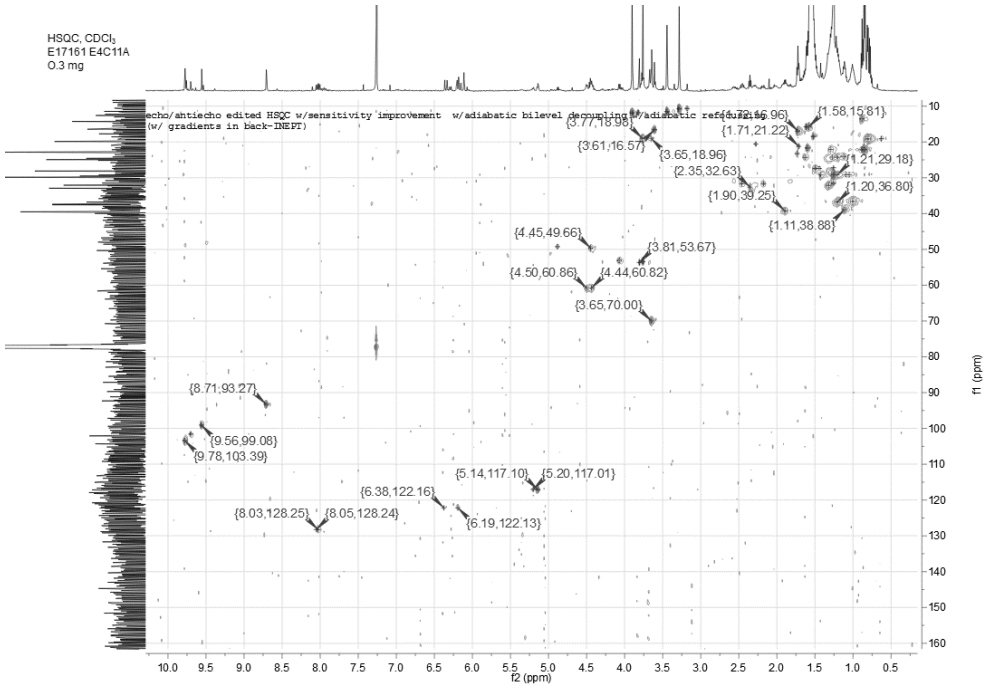

*Figure III.3 – HSQC spectrum for compound **(1)** in $CDCl_3$, with relevant one bond C-^{1}H correlation signals marked (recorded at 600 MHz).*